APR 29
1957

Journal of Research

of the

National Bureau of Standards

UNIVERSITY OF MICHIGAN
APR 26 1957
PHYSICS LIBRARY

APRIL 1957

VOLUME 58 NUMBER 4

U. S. DEPARTMENT OF COMMERCE
Sinclair Weeks, Secretary
NATIONAL BUREAU OF STANDARDS
A. V. Astin, Director

APRIL • 1957
VOLUME • 58
NUMBER • 4

JOURNAL OF RESEARCH
of the
NATIONAL BUREAU OF STANDARDS

PERIODICALS OF THE NATIONAL BUREAU OF STANDARDS
(Published monthly)

The National Bureau of Standards is engaged in fundamental and applied research in physics, chemistry, mathematics, and engineering. Projects are conducted in fifteen fields: electricity and electronics, optics and metrology, heat and power, atomic and radiation physics, chemistry, mechanics, organic and fibrous materials, metallurgy, mineral products, building technology, applied mathematics, data processing systems, cryogenic engineering, radio propagation, and radio standards. The Bureau has custody of the national standards of measurement and conducts research leading to the improvement of scientific and engineering standards and of techniques and methods of measurement. Testing methods and instruments are developed, physical constants and properties of materials are determined, and technical processes are investigated.

JOURNAL OF RESEARCH

The Journal presents research papers by authorities in the specialized fields of physics, mathematics, chemistry, and engineering. Complete details of the work are presented, including laboratory data, experimental procedures, and theoretical and mathematical analyses. Annual subscription: domestic, $4.00; $1.25 additional for foreign mailing.

TECHNICAL NEWS BULLETIN

Summaries of current research at the National Bureau of Standards are published each month in the Technical News Bulletin. The articles are brief, with emphasis on the results of research, chosen on the basis of their scientific or technologic importance. Lists of all Bureau publications during the preceding month are given, including Research Papers, Handbooks, Applied Mathematics Series, Building Materials and Structures Reports, Miscellaneous Publications, and Circulars. Each issue contains 12 or more two-column pages; illustrated. Annual subscription: domestic, $1.00; 35 cents additional for foreign mailing.

BASIC RADIO PROPAGATION PREDICTIONS

The Predictions provide the information necessary for calculating the best frequencies for communication between any two points in the world at any time during the given month. The data are important to all users of long-range radio communications and navigation, including broadcasting, airline, steamship, and wireless services, as well as to investigators of radio propagation and ionosphere. Each issue, covering a period of one month, is released three months in advance and contains 16 large pages, including pertinent charts, drawings, and tables. Annual subscription: domestic, $1.00; 25 cents additional for foreign mailing.

Order all publications from the Superintendent of Documents
U. S. Government Printing Office, Washington 25, D. C.

Use of funds for printing this publication approved by the Director of the Bureau of the Budget (May 14, 1956)

Journal of Research of the National Bureau of Standards Vol. 58, No. 4, April 1957 Research Paper 2749

Comparisons of National Radium Standards

T. P. Loftus, W. B. Mann, L. F. Paolella, L. L. Stockmann, and W. J. Youden

The national primary radium standards of the Federal Republic of Germany and the Dominion of Canada have recently been compared with the two United States national primary radium standards at the National Bureau of Standards. The comparisons were made using the standard electroscope and radiation balance, and the results obtained for these four Hönigschmid standards have been compared with those obtained in an earlier comparison of the United States primary radium standards with that of the United Kingdom, which is also a Hönigschmid standard. In every case, agreement with Hönigschmid's values to within 0.2 percent has been obtained.

1. Introduction

During January and February 1954 the British primary radium standard and the Canadian national radium standard were compared with the United States primary radium standards at the National Bureau of Standards [1,2].[1] The British and United States standards were Hönigschmid standards, whereas the Canadian standard consisted of radium chloride sealed in a glass tube of considerably smaller dimensions than those of the Hönigschmid standards and therefore considerably more closely packed [1]. In any gamma-ray comparison between this Canadian standard and a Hönigschmid standard, it is therefore necessary to apply corrections for self-absorption of the source [3]. In 1955 the National Research Council of Canada procured a Hönigschmid standard (No. 5425), to replace the older preparation, as the primary radium standard of Canada [4]. This new Hönigschmid standard was compared during the summer of 1955 with the German (No. 5426) and British (No. 5432) Hönigschmid standards in Braunschweig and Teddington, respectively, and was then brought, in early December 1955, to Washington, D. C., for comparison with the United States Hönigschmid standards (Nos. 5437 and 5440) at the Bureau.

In November 1955 the Hönigschmid standard of the Physikalisch-Technische Bundesanstalt was also compared with the two United States standards.

The results of the measurements carried out on the Canadian, German, and United States Hönigschmid standards are given in this paper, together with a reassessment of the measurements previously carried out at the Bureau on the British and United States Hönigschmid standards [1,2].

2. Methods of Measurement

For the comparisons of the Canadian and the German standards with the United States standards, only the NBS standard electroscope [5] and Peltier-effect microcalorimeter, or radiation balance [6,7], were used. These have already been demonstrated to give precise and reproducible results and consequently the counting methods, previously utilized [1], were not again employed to supplement the measurements of the electroscope and microcalorimeter. The procedures of the earlier comparison for both these methods have already been fully described [1] and were again followed precisely.

A new and very careful determination of the thermoelectric power (dE/dT) of the Peltier couples of the radiation balance was carried out, using a pair of copper-sheathed heating and compensating resistance coils whose difference in resistance was precisely measured. The results of a great many measurements gave a new average value at 25° C of dE/dT equal to 58.71 μv/deg, as compared with 58.78 μv/deg used in the earlier work [2]. This new value will not affect the ratios of the standards as then determined, but will give a different value for the absolute rates of energy emission for the different radium standards. For the purpose of comparison with the results obtained in the Canadian and German intercomparison, those for the British intercomparison have therefore

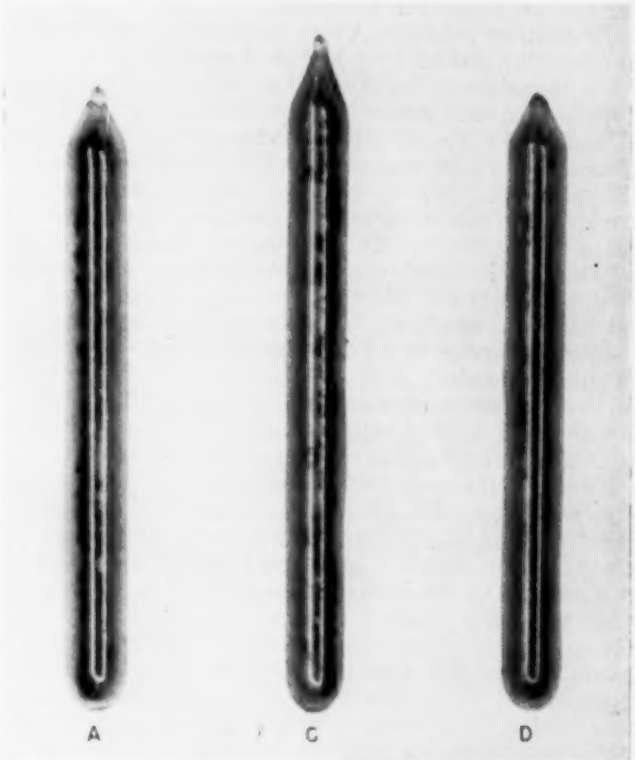

FIGURE 1. *Three Hönigschmid national radium standards with the grains of salt distributed along the length of the tubes.*

A, American; *C* Canadian *D*, American.

[1] Figures in brackets indicate the literature references at the end of this paper.

TABLE 1.—*Masses of five Hönigschmid radium standards, in Hönigschmid milligrams*

	A U. S. primary radium standard (5437, XIV)	*B* British primary radium standard (5432)	*C* Canadian primary radium standard (5425)	*D* U. S. primary radium standard (5440, XV)	*G* German primary radium standard (5426)
Mass of radium chloride as determined by Hönigschmid on June 2, 1934 [a]	50.22	20.50	31.73	26.86	19.19
Radium content, as of June 1934, as given by:					
1. Hönigschmid's weighings [a]	38.23	15.60	24.15	20.45	14.61
2. By comparison with Paris and Vienna 1911 standards [b]	38.12	.....	.....	20.37	.....

[a] Hönigschmid stated [8] that his weights were calibrated against each other but not in relation to the standard kilogram. He also found [8] that the calibration corrections for his weights were greatly in excess of the weighing errors. The masses of radium have therefore been designated throughout this paper in terms of "Hönigschmid milligrams." This practice should also have been adopted in the previous paper [1, 2].

[b] Corrected from "the end of 1936 or beginning of 1937", using a half-life of 1,620 years. It is uncertain what relation these masses in milligrams bear to Hönigschmid's later weighings [8].

been recalculated. Values for the rates of energy emission for all five standards (British, Canadian, German, and both United States) have also been corrected back to their date of sealing by Hönigschmid, namely, June 2, 1934, in order to eliminate the correction for the decay of radium and the considerably larger correction for the growth of radium E and polonium–210 between February 1954, when the British intercomparison was carried out, and November and December 1955, when the German and Canadian standards, respectively, were intercompared with the United States standards. In the recalculation of the British results the best estimates have been derived, incorporating the results obtained for the old Canadian standard.

In addition, the sensitivity of the radiation balance has been increased by a factor of some 6.7, to give a scale deflection of 2.8 mm/μw instead of 0.42 mm/μw. This was done primarily to calibrate a preparation of some 4.8 curies of tritium in the preparation of the Bureau's tritium standard. The radiation balance has also been placed in a temperature-attenuating enclosure to minimize the effects of fluctuations in the room temperature. This enclosure consists of a box of about ¾-in.-thick dural, with internal dimensions of approximately 10 by 10 by 10 in., surrounded by about a 2-in. thickness of balsa wood. The radiation balance is placed on a balsa-wood block in the middle of this enclosure. A small opening in the top surface of the enclosure provides for access to the balance. An over-all improvement in the operating characteristics of the radiation balance was obtained.

In the subsequent discussion of the results, the United States Hönigschmid standards will again be designated *A* and *D*, the British standard *B*, the new Canadian standard *C*, and the German standard *G*. A summary of their essential data is given in table 1, and the two United States standards with the Canadian and German standards are shown in figures 1 and 2. The tubes containing each of the four standards are of Thüringen glass of 3-mm internal diameter and 0.27-mm wall thickness, and their lengths vary from 36 to 40 mm.[2]

[2] *A* was described as 36 mm long and *D* as 37 mm long in table 1 of the earlier paper [1], and they are indeed thus described in the certificates issued by the International Radium Standards Commission. Measurement of the photographs of *A* and *D* reveal, however, that *A* is the longer standard, being about 36.7 mm long, whereas *D* is only some 36.3 mm in length.

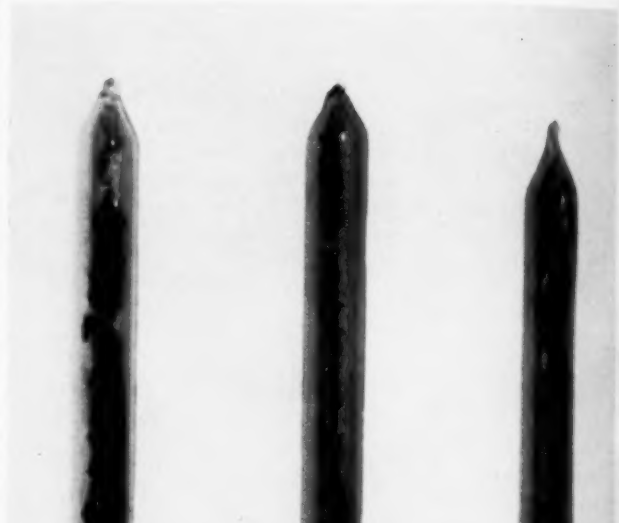

FIGURE 2. *Three Hönigschmid national radium standards, with the grains of salt distributed along the length of the tubes.*

A, American; *D*, American; *G*, German.

3. Results

In table 2 are summarized the results of all the measurements of energy-absorption rates for all five standards, both singly and balanced in pairs, at the different times of measurement, uncorrected for either the decay of radium or the growth of its daughter products.

The best estimates of the rates of energy absorption for *A*, *B*, *C*, *D*, and *G*, derived by the method previously described [2], are given in table 3, together with the values of these rates of energy absorption corrected to June 2, 1934. Two additional values of *A*

TABLE 2. *Rate of energy absorption, in microwatts*

Date	Source	Energy absorbed	Source	Energy absorbed
February 1954	*A*	6271.0	*A−D*	2930.9
Do	*B*	2566.3	*A−B*	3721.2
Do	*D*	3364.2	*D−B*	786.5
November 1955	*A*	6294.4	*A−D*	2925.3
Do	*G*	2416.6	*A−G*	3895.1
Do	*D*	3368.5	*D−G*	956.8
December 1955	*A*	6295.7	*A−D*	2942.8
Do	*C*	3981.2	*A−C*	2323.6
Do	*D*	3362.2	*C−D*	619.7

TABLE 3. *Best estimates of rates of energy absorption, in microwatts*

Date	Source	Energy absorbed	Energy absorbed as of June 2, 1934
February 1954	*A*	6280.6	5747.5
Do	*B*	2563.8	2346.2
Do	*D*	3353.0	3067.7
November 1955	*A*	6298.6	5729.3
Do	*G*	2411.1	2193.6
Do	*D*	3369.9	3065.4
December 1955	*A*	6300.3	5731.0
Do	*C*	3979.1	3619.4
Do	*D*	3359.7	3055.1
December 1955	*A*	6304.1	5734.9
February 1956	*A*	6304.4	5730.8
Do	*D*	3364.7	3057.8

and one additional value for *D*, obtained in the course of calibrating two other radium preparations for use at the Bureau, are also included.

In the comparisons carried out with the NBS standard electroscope, the method of adjustment of the ratios previously described [2] was again used. The results for the adjusted ratios obtained by the electroscope and also for the ratios obtained from the best estimates of the rates of energy absorption given by the radiation balance are summarized in table 4, together with the corresponding ratios obtained from Hönigschmid's weighings. Slight differences in the last figure from the ratios previously reported [1] are due mainly to the rounding off of the last figure in the calculations and are insignificant. In table 4 it will be noted that the electroscope ratios are almost always lower than those obtained by the radiation balance by an amount varying from about 0.1 to 0.4 percent. This would, however, be consistent with a slight gamma-ray source-self-absorption in the larger standard, which, in the ratios given, always appears in the numerator.

For complete internal consistency the ratios shown in columns 3, 4, and 5 of table 4 should be the same for any given pair of standards, apart from the effect of gamma-ray source-self-absorption just noted. It is interesting therefore to compare the percentage or fractional divergencies of these ratios one from another. This can best be done by dividing one ratio into another, whereupon any systematic error should immediately become apparent. The results of such a comparison are shown in columns 6, 7, and 8 of table 4, and the effect of gamma-ray source-self-absorption immediately becomes apparent from column 6 by the systematic trend of 2 or 3 parts in a thousand (except in the case of the ratio of *C* to *D*, which are of nearly the same mass).

Column 7 shows the divergence of the radiation-balance ratios relative to Hönigschmid-weighing ratios to be fairly random. Neither of these methods of measurement involves any gamma-ray effect.

Once again, however, a systematic trend of 3 or 4 parts in a thousand is apparent in column 8. This is consistent with the effect of gamma-ray source-self-absorption decreasing the electroscope readings for the larger standards. Here again the ratios for *C* to *D* would be expected to be higher due to their near equality in mass.

These trends are only slightly significantly greater, however, than the experimental errors involved, but a comparison of the figures of columns 7 and 8 does tend to confirm that the radiation balance is more nearly measuring the ratios as determined by Hönigschmid's own weighings.

As in the earlier intercomparison of the United States and British radium standards [1], it is of interest to compare the radioactive effect per milligram of radium element for each of the standards in order to check the combined internal precision of the electroscope or radiation-balance results, on the one hand, and of Hönigschmid's weighings, on the other.

TABLE 4. *Adjusted ratios for five international radium standards*

Date	Standards	Electroscope	Radiation balance	Hönigschmid	Ratio of radiation balance ratio to electroscope ratio	Ratio of radiation balance ratio to Hönigschmid ratio	Ratio of electroscope ratio to Hönigschmid ratio
February 1954	*A/B*	2.441	2.450	2.450	1.003	1.000	0.997
Do	*A/D*	1.870	1.873	1.870	-----	-----	-----
Do	*D/B*	1.305	1.308	1.310	1.002	0.998	.996
November 1955	*A/G*	2.608	2.612	2.617	1.002	.998	.996
Do	*A/D*	1.870	1.869	1.870	-----	-----	-----
Do	*D/G*	1.395	1.398	1.400	1.002	.999	.996
December 1955	*A/C*	1.578	1.583	1.583	1.003	1.000	.997
Do	*A/D*	1.870	1.875	1.870	-----	-----	-----
Do	*C/D*	1.185	1.184	1.181	1.000	1.003	1.003
February 1956	*A/D*	-----	1.874	1.870	-----	-----	-----
Average	*A/D*	1.870	1.873	1.870	[a] 1.002	[a] 1.002	[a] 1.000

[a] Ratio of averages.

The results of such an internal precision check are given in tables 5, 6, and 7, for the electroscope and for the radiation-balance measurements. As before, the radioactive effect per Hönigschmid milligram, namely, divisions per second for the electroscope and microwatts for the radiation balance, has been normalized to make the "best average" in each case equal to 100.00. This best average has again been determined by dividing the sum of Hönigschmid's masses into the sum of the radioactive effects for each series of three standards.

In table 8 are shown the values for B, C, and G that are obtained by assuming Hönigschmid's values for A and D and multiplying by the appropriate adjusted ratios, the values for which are given in table 4. In table 4 the results have been rounded off to four significant figures.

TABLE 5. *Radioactive effect per Hönigschmid milligram of radium element, normalized to make the best average equal to 100.00*

British intercomparison, February 1954

Method	A	B	D	Best average	Standard deviation (2 degrees of freedom)
Electroscope	99.93	100.31	99.88	100.00	0.24
Radiation balance	100.05	100.08	99.85	100.00	.13

TABLE 6. *Radioactive effect per Hönigschmid milligram of radium element, normalized to make the best average equal to 100.00*

German intercomparison, November 1955

Method	A	D	G	Best average	Standard deviation (2 degrees of freedom)
Electroscope	99.94	99.92	100.28	100.00	0.21
Radiation balance	99.96	99.98	100.13	100.00	.09

TABLE 7. *Radioactive effect per Hönigschmid milligram of radium element, normalized to make the best average equal to 100.00*

Canadian intercomparison, December 1955

Method	A	C	D	Best average	Standard deviation (2 degrees of freedom)
Electroscope	99.92	100.22	99.90	100.00	0.18
Radiation balance	100.08	100.06	99.72	100.00	.21

TABLE 8. *Values of B, C, and G, in Hönigschmid milligrams of radium element as of June 2, 1934, derived from A and D by means of radiation-balance and electroscope measurements*

Standard	Radiation balance through—		Electroscope through—		Average all values
	A	D	A	D	
B	15.60_8	15.63_7	15.65_8	15.66_7	15.64_2
C	24.14_3	24.22_9	24.22_3	24.22_8	24.20_4
G	14.63_4	14.63_2	14.66_1	14.66_4	14.64_8

4. Discussion of Results

4.1. Radiation-Balance Measurements

The radiation balance permits measurements for each standard separately or for a comparison of any pair of standards. The practice followed in these experiments has, as previously, been that of measuring each standard separately and of making all possible comparisons. There are $n(n-1)/2$ possible pairs that can be formed from n standards. These $n(n-1)/2$ measurements, together with the n measurements on the standards alone, give a total of $n(n+1)/2$ observations for the estimation of n quantities. Section 3 in the preceding study [2] lists the formulas from which the least-squares estimates for values of the radium standards have been derived. These estimates are the so-called "adjusted values," which have been used in all subsequent numerical calculations.

The differences between the adjusted values and the original observations provide an estimate of the standard deviation of the measurements. Table 9 shows a recalculation for the comparison of the United States standards with the British standard and the old Canadian standard. The calculations are also shown for the comparison with the German standard and with the new Canadian standard. The three estimates for the standard deviation of a single measurement are 7.2, 6.4, and 3.8 μw and are in

TABLE 9. *Calculation of standard deviation, in microwatts, for each comparison of the national radium standards*

Standard [a]	Observed	Adjusted	Difference	(Difference)^2
A	6271.0	6280.6	9.6	92.16
B	2566.3	2563.8	2.5	6.25
C*	4117.5	4121.7	4.2	17.64
D	3364.2	3353.0	11.2	125.44
A−B	3721.2	3716.8	4.4	19.36
A−C*	2160.9	2158.9	2.0	4.00
A−D	2930.9	2927.7	3.2	10.24
C*−B	1558.6	1557.9	0.7	0.49
D−B	786.5	789.2	2.7	7.29
C*−D	774.2	768.7	5.5	30.25
			Total	313.12
A	6294.4	6298.6	4.2	17.64
D	3368.5	3369.9	1.4	1.96
G	2416.6	2411.1	5.5	30.25
A−D	2925.3	2928.7	3.4	11.56
A−G	3895.1	3887.5	7.6	57.76
D−G	956.8	958.8	2.0	4.00
			Total	123.17
A	6295.7	6300.3	4.6	21.16
C	3981.2	3979.1	2.1	4.41
D	3362.2	3359.7	2.5	6.25
A−C	2323.6	2321.2	2.4	5.76
A−D	2942.8	2940.6	2.2	4.84
C−D	619.7	619.4	0.3	0.09
			Total	42.51

Comparison	Total of (Difference)^2	Degrees of freedom	Quotient	Standard deviation	
				Single measurement	Adjusted value
British	313.12	6	52.19	7.2	4.5
German	123.17	3	41.08	6.4	4.5
Canadian	42.51	3	14.17	3.8	2.7

[a] C* designates the former Canadian standard [1,2], which was not a Hönigschmid standard.

unusually close agreement, considering the limited number of degrees of freedom available for each estimate. In the course of calibrating another radium preparation against A and D at the Bureau, a fourth estimate of the standard deviation was also found to be 3.8 μw.

The standard deviation for the adjusted estimates is obtained by dividing the calculated standard deviation shown in table 9 by the square root of $(n+1)/2$, where n standards have furnished $n(n+1)/2$ measurements. In the present work, with three standards the divisor is $\sqrt{2}$, and with four standards the divisor is $\sqrt{2.5}$.

4.2. Electroscope Measurements

Comparison of two radium standards by the electroscope is best effected by alternating the two standards in a support at a fixed distance from the electroscope and taking the ratio of the times (corrected for background) for the electroscope leaf to fall through a specified angle. Three standards are intercompared by determining the ratios for all three possible pairs of standards, a complete set of readings being taken by each of two operators. These measurements were repeated twice, using two fixed distances from the electroscope for the new Canadian standard, whereas four different distances were used in the work with the German standards. In the earlier work [1] with the British standard and the old Canadian standard, three operators and two distances were used and a complete repetition made, so that 12 measurements were available.

Statistical examination of the results showed them independent of both distance and operator. The standard deviation for any particular ratio was determined from the 8, 6, or 12 individual determinations available. The standard deviations calculated for the various ratios are shown in table 10, both as calculated and when expressed as parts per thousand of the average value for the ratio. The standard deviation for a result obtained by one operator working at one distance is 2.1 parts per thousand. The standard deviation for the average ratio is obtained by dividing by the square root of the number of measurements, giving 0.75, 0.85, and 0.85 parts per thousand as the standard deviation for the average ratios for the German, Canadian, and British studies, respectively.

TABLE 10. *Standard deviations for electroscope measurements*

Radium standards compared [a]	Average ratio, unadjusted	Number of measurements [b]	Standard deviation	
			Absolute	Parts per thousand
A/D	1.8684	8	0.0043	2.3
A/G	2.6095	8	.0058	2.2
D/G	1.3936	8	.0033	2.6
A/D	1.8709	6	.0041	2.2
A/C	1.5771	6	.0026	1.7
D/C	0.84454	6	.0013	1.6
A/C	1.8703	12	.0043	2.3
A/B	2.4438	12	.0083	3.4
A/C^*	1.5675	12	.0048	3.1
B/C^*	0.64246	12	.0022	3.4
B/D	0.76650	12	.0024	3.1
C^*/D	1.1918	12	.0027	2.3

[a] C^* designates the former Canadian standard [1, 2], which was not a Hönigschmid standard.
[b] Degrees of freedom equals number of measurements minus 1.

5. Best Estimates for the Hönigschmid Standards

The data tabulated in table 4 have been used to fit straight lines to points that have been plotted using the radiation-balance ratio as ordinate and the weight ratio as abscissa. Only the ratios using D as the denominator are used. The three points plotted for the February 1954 data have the coordinates (1.869, 1.873), (0.7628, 0.7648), (1.000, 1.000). The point (1.000, 1.000) establishes a unit scale where one unit is set equal to 20.45 Hönigschmid milligrams. The line is determined by minimizing the sum of the squares of the perpendicular distances from the plotted points to the fitted line. The formulas are given in [2]. A perpendicular from each plotted point to the fitted line determines the coordinates of matching points on the line. The abscissa for each point is then converted back to Hönigschmid milligrams by multiplying by 20.45. The weights corresponding to the points on the line are compared with Hönigschmid's masses in table 11.

TABLE 11. *Estimates, in Hönigschmid milligrams, of the masses of the Hönigschmid radium standards as of June 2, 1934*

Standard	A	B	C	D	G
Hönigschmid's mass	38.23	15.60	24.15	20.45	14.61
Mass derived from radiation balance and Hönigschmid	38.23_7	15.60_3	------	20.43_1	------
	38.24_2	------	24.15_4	20.42_1	------
	38.22_5	------	------	20.45_9	14.62_9
Mass derived from electroscope and Hönigschmid	[a] 38.21_6	[a] 15.62_8	------	[a] 20.44_2	------
	38.21_6	------	24.17_7	20.44_1	------
	38.22_3	------	------	20.44_5	14.63_3

[a] These results differ slightly from those given in table 5 of reference [1], the computations having been repeated giving greater weight (k=1) to the electroscope ratios than in that paper (k=2).

Three similar lines were calculated for the ratios obtained with the electroscope. In every instance the derived masses in Hönigschmid milligrams agree with Hönigschmid's masses within his stated weighing errors. In order to be assured that no preference was given to D, in taking it as unity in the estimates of the best values, the calculation was run again in the BAD and GAD series, respectively, taking B and G, the smallest standards, as unity. No greater differences than 2 or 3 parts in the third decimal place were, however, observed.

It should be emphasized that these derived masses are the best estimates of the values of the Hönigschmid standards so far as the National Bureau of Standards results are concerned. Internationally recommended values must await the correlation of the results from all other laboratories.

We gratefully acknowledge the courtesy of the President of the National Research Council of Canada and of the President of the Physikalisch-Technische Bundesanstalt of the Federal Republic of Germany for making their respective Hönigschmid radium standards available to us for measurement; and we express our thanks to K. W. Geiger and G. v. Droste, respectively, for bringing the standards personally to Washington, D. C. We also extend grateful acknowledgments to W. E. Perry of the National Physical Laboratory for many helpful discussions and especially for drawing our attention to Hönigschmid's statement that his weights were not compared with the standard kilogram.

We also express our thanks to Mary G. Natrella of the NBS Statistical Engineering Laboratory, for assistance with the computing; and one of us (W. B. M.) is very grateful to M. Waxman, of the NBS Temperature Measurements Section, for his kind advice on the temperature-attenuating enclosure for the radiation balance that was installed some time prior to the investigations here described.

6. References

[1] T. I. Davenport, W. B. Mann, C. C. McCraven, and C. C. Smith, J. Research NBS **53,** 267 (1954), RP2544 part 1.
[2] W. S. Connor and W. J. Youden, J. Research NBS **53,** 273 (1954), RP2544, part 2.
[3] W. S. Michel and G. N. Whyte, Can. J. Phys. **33,** 521–52 (1955).
[4] C. Garrett and K. W. Geiger, Can. J. Phys. **34,** 107 (1956).
[5] L. F. Curtiss, Rev. Sci. Instr. **16,** 363 (1928).
[6] W. B. Mann, J. Research NBS **52,** 177 (1954), RP2486
[7] W. B. Mann, J. Research NBS **53,** 277 (1954), RP2545
[8] O. Hönigschmid, Anz. Akad. Wiss. Wien **82,** 30 (1945)

Washington, May 11, 1956.

Journal of Research of the National Bureau of Standards Vol. 58, No. 4, April 1957 Research Paper 2750

Temper Brittleness of Boron-Treated Steels

Samuel J. Rosenberg

Two series of steels, melted to the base composition of 8140, were studied to ascertain whether titanium and zirconium (present in many commercial boron addition agents) had any adverse effect upon the impact properties of the base steels, particularly with reference to temper brittleness.

The results obtained indicate that with fully hardened steels tempered at 1,200° F, the presence of relatively small amounts of titanium as introduced into the test steels by the boron addition agents is sufficient to cause an impairment in the Charpy V-notch impact properties of the steels or an increased susceptibility to temper brittleness, or both. This was confirmed by the addition of titanium without boron. Similar effects, previously thought possibly due to the presence of zirconium, were not observed.

1. Introduction

A study of the impact properties of boron-treated steels, conducted at the National Bureau of Standards,[1] indicated that boron itself had no effect upon the phenomenon of temper brittleness. The increased susceptibility to temper brittleness of some of the boron-treated steels was ascribed to other elements present in the steels in small quantities (from the addition agents) and, by the process of elimination, it appeared that titanium and zirconium may have been responsible for the effects observed. The purpose of this study was to establish whether or not these elements are responsible for increasing the susceptibility to temper brittleness of boron-treated steel.

The steels tested previously were from a commercial open-hearth heat of 0.4 percent C, 1.6 percent Mn base composition; the steels melted for the present study were electric- and induction-furnace heats of the 8140 type.

2. Steels Investigated

One series of steels was melted at the U. S. Bureau of Mines, Pittsburgh, Pa., in a 500-lb basic electric-arc furnace. In order to control variations in base composition, only one heat was used. The melt was deoxidized with aluminum (2 lb/ton) and then split seven ways. All additions of boron were made in the ladle, and the compositions of the addition agents are given in table 1. Addition agents X, Y, and Z were commercial agents selected so that X contained neither titanium nor zirconium; Y contained titanium but not zirconium; and Z contained both titanium and zirconium. The steels were poured in the following order:

Steel	M731	No addition (base).
	M732	FeB.
	M733	Addition agent X.
	M734	FeB plus FeTi.
	M735	Addition agent Y.
	M736	Addition agent Z.
	M737	FeB plus FeZr.

[1] Samuel J. Rosenberg and John D. Grimsley, A study of the impact properties of boron-treated steels, J. Iron Steel Inst. **182**, 278 (March 1956).

TABLE 1. *Composition of the addition agents*

Addition	Percentage by weight [a]						
	B	Ti	Si	C	Mn	Zr	Al
Ferroboron	10.84	-----	-----	----	----	-----	-----
Ferrotitanium	-----	15.12	-----	7.2	----	-----	-----
Ferrozirconium	-----	-----	----	----	----	39.43	-----
Agent X	3.75	-----	45.00	----	----	-----	-----
Agent Y	2.40	18.15	3.50	5.42	----	-----	-----
Agent Z	0.49	18.96	3.03	0.16	8.28	3.20	12.70

[a] Analyses were made only for the elements indicated.

All steels were poured into split steel molds, 2¾ in. square at the bottom, 3¾ in. square at the top, and 15 in. tall, equipped with hot tops. After discarding the hot tops, the yield was about 35 lb of usable metal.

A second series of 8140 steels was melted in an induction furnace at NBS. This also was a split heat deoxidized with aluminum (2 lb/ton), and, as before, the additions noted were made in the ladle. The order of pouring was as follows:

Steel	M744	No addition (base).
	M745	FeTi.
	M746	FeZr.
	M747	FeB.
	M748	FeB plus FeTi.

The sixth steel, designed to have an addition of FeB plus FeZr, unfortunately was lost. Analyses of the two series of steels are given in table 2. It will be noted that the boron contents of the Bureau of Mines steels were higher than those normally obtained in boron-treated steels; those of the NBS steels were within the normal range.

The ingots were cleaned by shot-blasting or grinding, forged to 2½ in. square, and then rolled to 1¼-in.-thick plate. A 5-in. length was sheared from the bottom of the slabs for Jominy specimens, and the remainder of the slabs were rolled to ⅝-in.-thick plate. Hot-working was started at 2,150° to 2,200° F and continued to 1,600° to 1,700° F; each slab was reheated once during fabrication. The hot-rolled plates were cut into lengths of 14 in. prior to

TABLE 2. *Compositions of the test steels*

Steel	Addition	Percentage by weight[a]											
		C	Mn	P	S	Si	Ni	Cr	Mo	Ti	Zr	B	N
M731	None	0.43	0.85	0.022	0.018	0.22	0.30	0.52	0.12	(b)	(b)	(b)	0.006
M732	FeB	------	------	------	------	------	------	------	------	(b)	(b)	0.0035	.005
M733	Agent X	------	------	------	------	------	------	------	------	(b)	(b)	.0025	.005
M734	FeB+FeTi	------	------	------	------	------	------	------	------	0.015	(b)	.0036	.006
M735	Agent Y	------	------	------	------	------	------	------	------	.016	(b)	.0047	.007
M736	Agent Z	------	------	------	------	------	------	------	------	.033	0.004	.0024	.007
M737	FeB+FeZr	.43	.91	.028	.014	.25	.31	.50	.12	(b)	<.005	.0038	.006
M744	None	.40	.77	.010	.012	.32	.31	.49	.11	(b)	(b)	(b)	.006
M745	FeTi	.39	------	------	------	------	------	------	------	.025	(b)	(b)	.005
M746	FeZr	.39	------	------	------	------	------	------	------	(b)	.003	(b)	.005
M747	FeB	.39	------	------	------	------	------	------	------	(b)	(b)	.0018	.005
M748	FeB+FeTi	.38	.83	------	------	.32	.30	.49	.11	.021	(b)	.0016	.006

[a] For steels M731 to 737, inclusive, analyses for C, Mn, P, S, Si, Ni, Cr, and Mo were made on drillings from the first and last ingots by the Bureau of Mines. All other analyses were made at NBS. All analyses were made on samples taken from the tops of the ingots after discarding the hot tops.
[b] Not added to these particular steels and presumed not present, hence no analyses were made.

normalizing. The schedule of heat treating and machining operations was as follows:

Normalize—1½ hr at 1,650° F, air-cool.

Rough machine specimens to 2.165 in. long by 0.415 in. square.

Harden—½ hr at 1,600° F, oil-quench.

Temper—1 hr at 1,200° F, cool at three different rates: (1) water-quench, (2) air-cool, (3) furnace-cool at 30° F/hr.

One group of specimens water-quenched from the tempering temperature was stress-relieved 1 hr at 600° F; another group of water-quenched specimens was isothermally treated by holding for 48 hr at 930° F. Some of these treatments were omitted on some of the steels, as indicated in the discussion.

Following heat treatment, all specimens were ground to size (0.394 in. square) and notched (Charpy standard V-notch). The hardnesses resulting from these various treatments are given in table 3.

TABLE 3. *Hardness of the Charpy impact specimens after tempering at 1,200° F*

Steel	Addition agent	Rockwell C[a], after indicated treatment[b]				
		Water-quenched	Water-quenched plus 1 hr at 600° F	Air-cooled	Furnace-cooled	Water-quenched plus 48 hr at 930° F
M731	None	27.1	26.1	25.7	25.7	27.4
M732	FeB	27.0	25.3	25.4	25.7	27.2
M733	Agent X	27.2	26.6	26.0	26.2	27.7
M734	FeB+FeTi	27.6	27.1	26.5	26.7	
M735	Agent Y	27.5	27.0	26.4	26.5	28.0
M736	Agent Z	27.8	27.5	26.9	27.2	
M737	FeB+FeZr	26.4	25.7	25.7	25.8	27.6
M744	None	24.5	------	------	22.6	23.5
M745	FeTi	24.2	------	------	23.6	23.6
M746	FeZr	23.6	------	------	21.8	22.7
M747	FeB	23.3	------	------	21.9	22.5
M748	FeB+FeTi	24.8	------	------	22.9	23.7

[a] Each hardness value represents the average of all determinations made on all of the specimens given the indicated treatment.
[b] These treatments followed the 1-hr temper at 1,200° F.

3. Results and Discussion

End-quench (Jominy) hardenability tests were made on specimens of all of the steels; the results are shown in figures 1 and 2. The effectiveness of the boron addition in increasing the hardenability of all the boron-treated steels melted at the Bureau of Mines is apparent (fig. 1); the boron-treated steel M747 melted at NBS did not, however, show any increase in hardenability (fig. 2). It has been shown [2] that only the portion of boron that is in solid solution at the time of quenching contributes toward an increase in hardenability. Boron that is undissolved or in the form of compounds is ineffective.

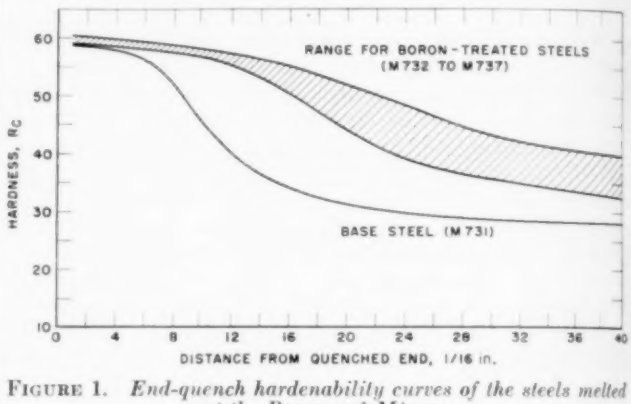

FIGURE 1. *End-quench hardenability curves of the steels melted at the Bureau of Mines.*

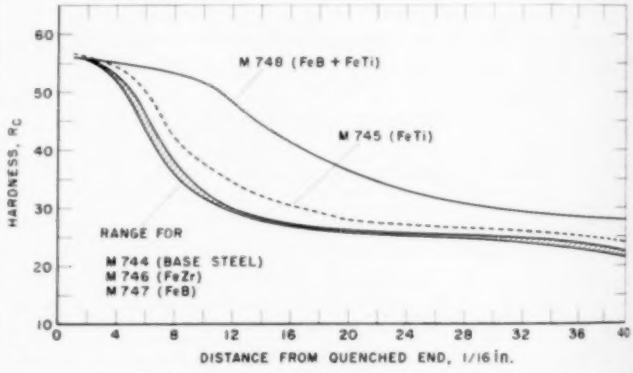

FIGURE 2. *End-quench hardenability curves of the steels melted at the National Bureau of Standards.*

[2] Thomas G. Digges, Carolyn R. Irish, and Nesbit L. Carwile, Effect of boron on the hardenability of high-purity alloys and commercial steels, J. Research NBS **41**, 545 (1948) RP1938.

Although steel M747 was treated with aluminum, it is possible that all of the nitrogen was not fixed as aluminum nitride and that nitrogen combined with the boron to form a boron nitride. That the boron was not lost from the steel during hot-working was confirmed by a check spectrochemical determination made on the Jominy specimen itself; the value of 0.0017 percent of boron obtained was a close check of the original value of 0.0018 percent (table 2).

Charpy impact tests were made over a range of temperatures from ambient to −320° F; generally 12 specimens were required for establishing the curve of impact energy versus test temperature. Because of a shortage of material, the curves of some of the isothermally embrittled Bureau of Mines steels were defined by fewer specimens. Usually one specimen was broken at each temperature, although in some cases duplicate specimens were used. All impact tests were made in a machine of 240-ft-lb capacity; specimens were cooled in suitable liquid baths for at least 30 min prior to breaking. After fracture, the relative proportion of brittle and fibrous fracture was determined for each specimen. Results of the impact tests are presented graphically in figures 3 to 14.

Examination of the curves summarizing the data obtained on the Bureau of Mines steels (figs. 3 to 9), using the water-quenched steels as a base, showed that air-cooling from the tempering temperature had a generally minor effect upon the impact properties. A stress relief at 600°F after water-quenching from the tempering temperature also had a minor effect upon the impact properties. Furnace-cooling from the tempering temperature had a definite embrittling effect on all of the steels, as did the 48-hr treatment at 930°F following water-quenching from the tempering temperature. This last treatment was not used for steels M734 and M736 because of insufficient material.

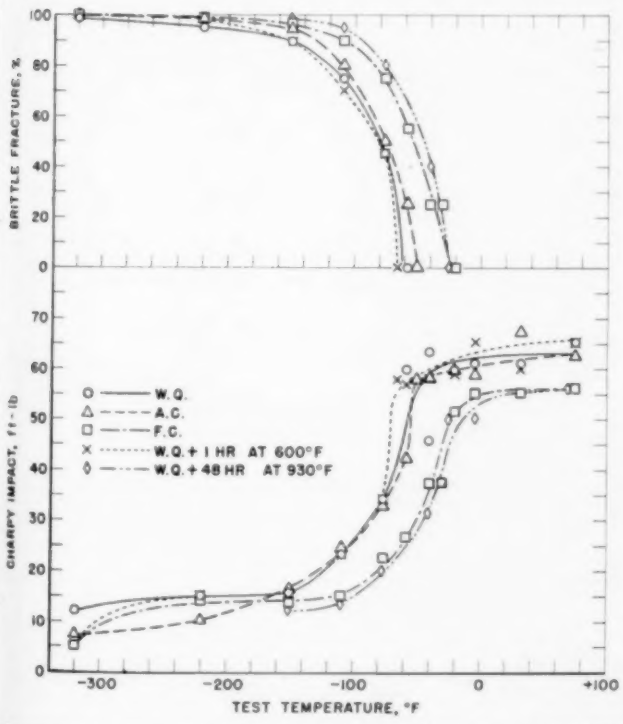

FIGURE 3. *Impact curves for Bureau of Mines steel M731 (base steel).*

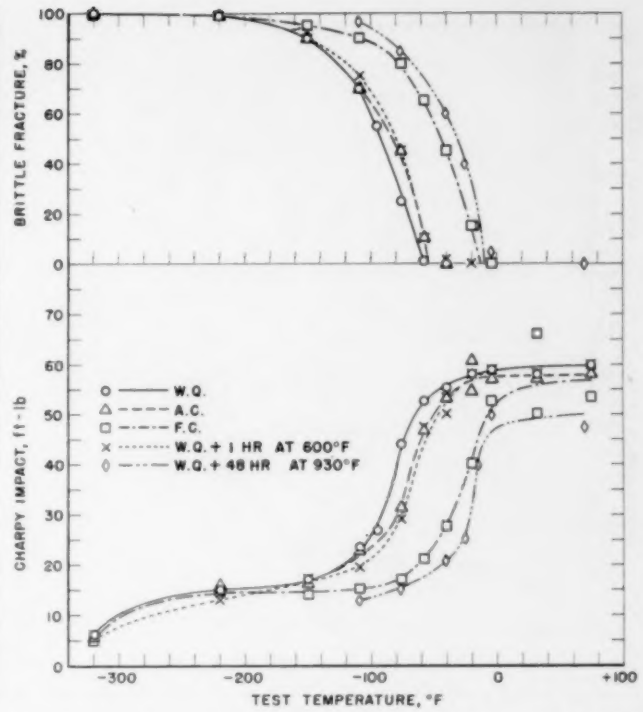

FIGURE 4. *Impact curves for Bureau of Mines steel M732 (FeB).*

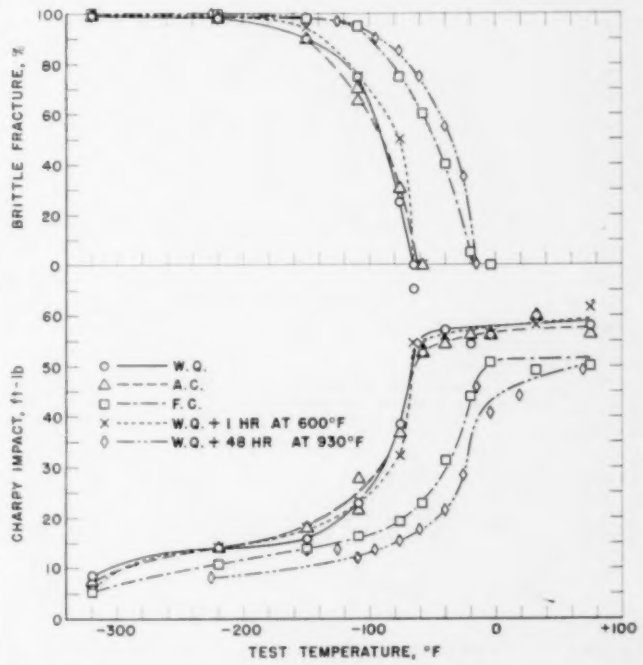

FIGURE 5. *Impact curves for Bureau of Mines steel M733 (agent X).*

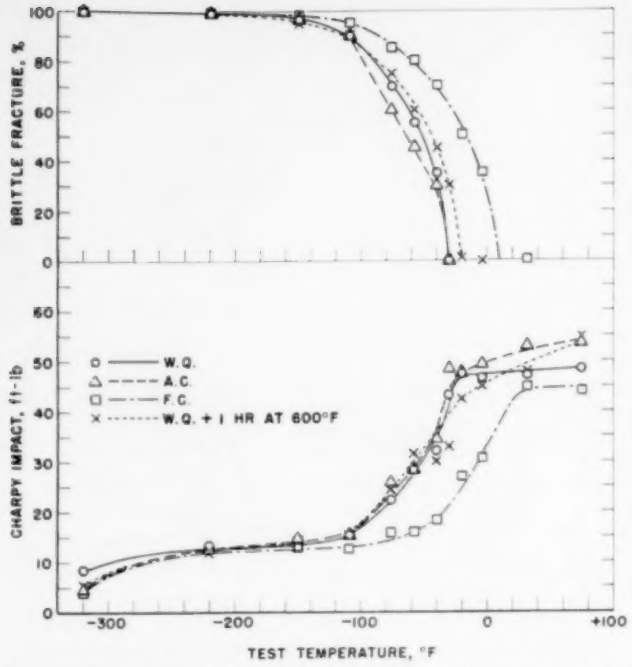

FIGURE 6. *Impact curves for Bureau of Mines steel M734 (FeB plus FeTi).*

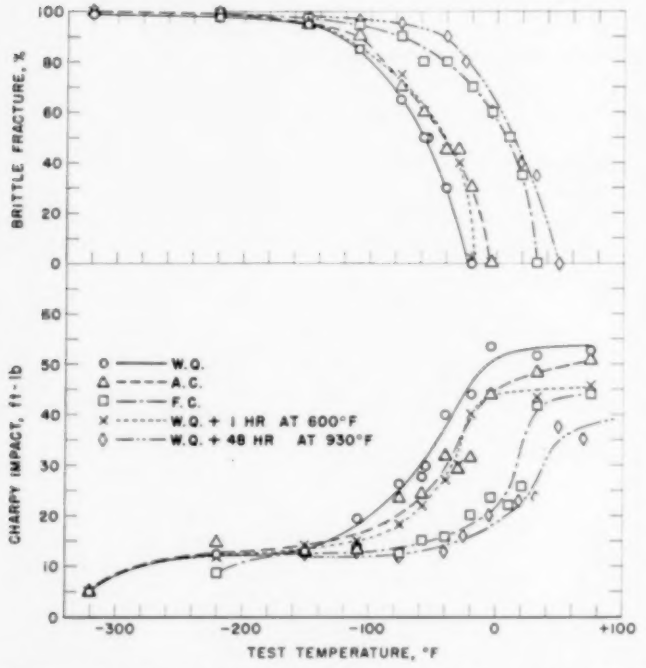

FIGURE 7. *Impact curves for Bureau of Mines steel M735 (agent Y).*

In view of the trends shown by the Bureau of Mines steels, no tests were made on the NBS steels as air-cooled from the tempering temperature, nor as water-quenched followed by the stress-relief treatment. Only steel M747 (FeB, fig. 13) showed no temper embrittlement. Because base steel M744 (fig. 10) showed some temper embrittlement, it would seem as if the addition of boron alone were a curative; that this is not so may be seen by comparing the corresponding Bureau of Mines steels (figs. 3 and 4) and from the results of a previous study (see footnote 1). However, the Bureau of Mines steel M732 contained 0.0035 percent of B, and the hardenability was increased over that of the base steel; the

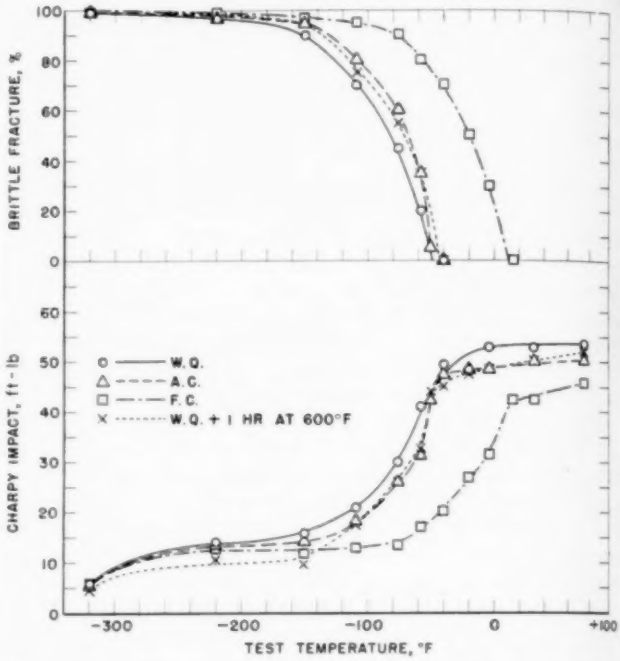

FIGURE 8. *Impact curves for Bureau of Mines steel M736 (agent Z).*

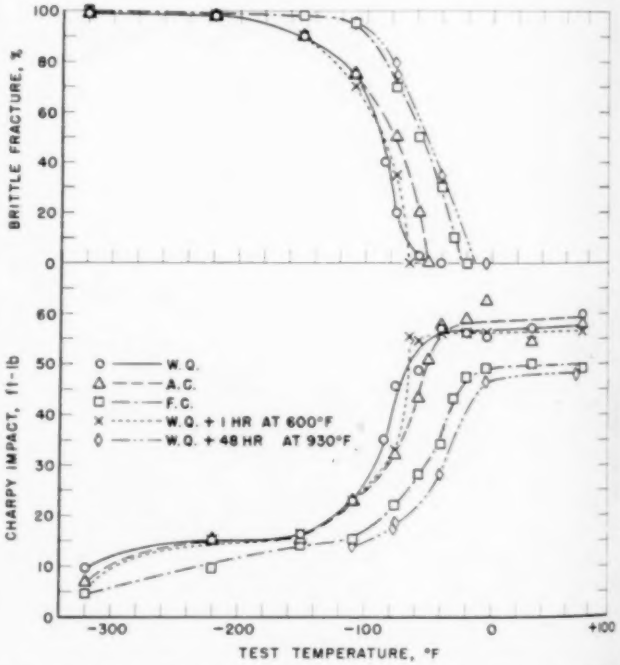

FIGURE 9. *Impact curves for Bureau of Mines steel M737 (FeB plus FeZr).*

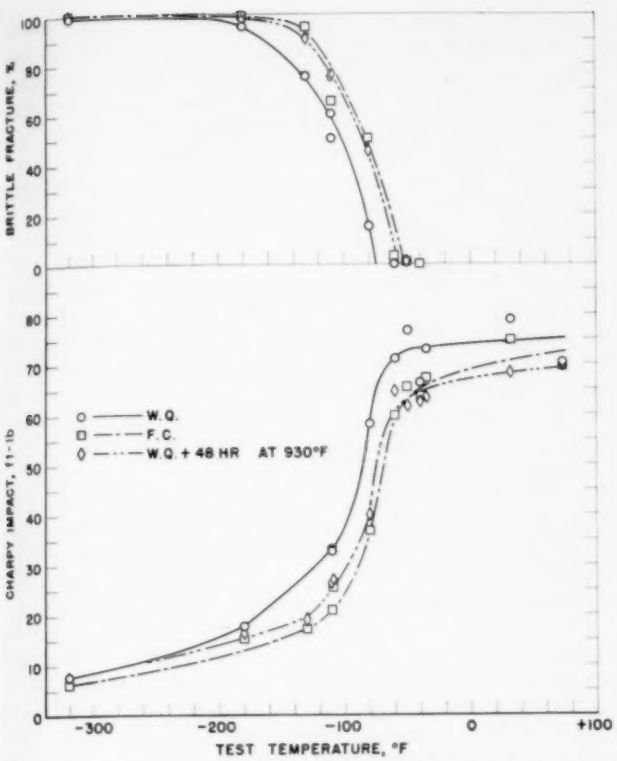

FIGURE 10. *Impact curves for the National Bureau of Standards steel M744 (base).*

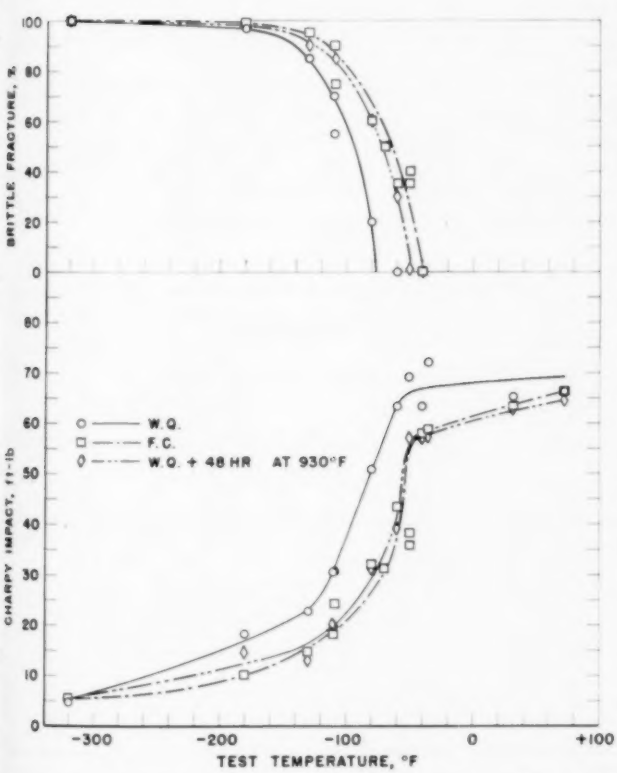

FIGURE 11. *Impact curves for the National Bureau of Standards steel M745* (FeTi).

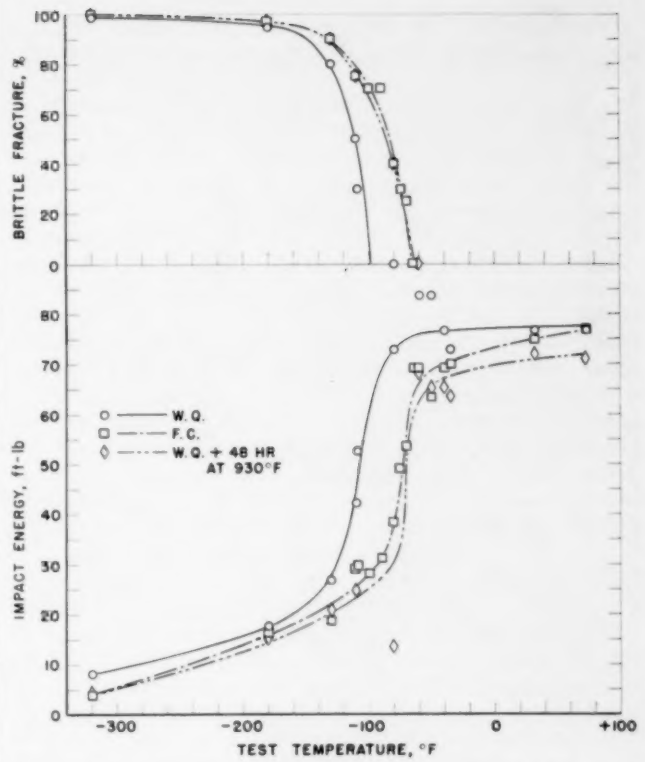

FIGURE 12. *Impact curves for the National Bureau of Standards steel M746* (FeZr).

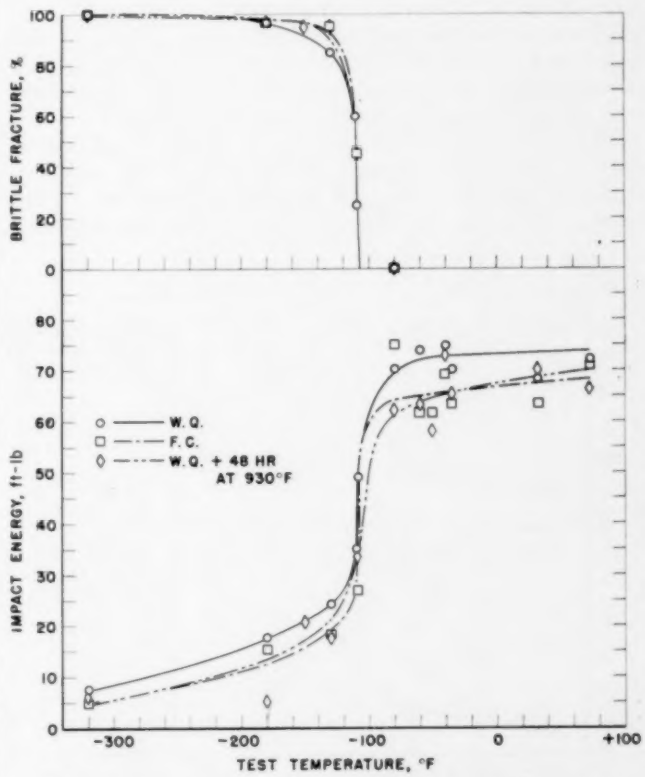

FIGURE 13. *Impact curves for the National Bureau of Standards steel M747* (FeB).

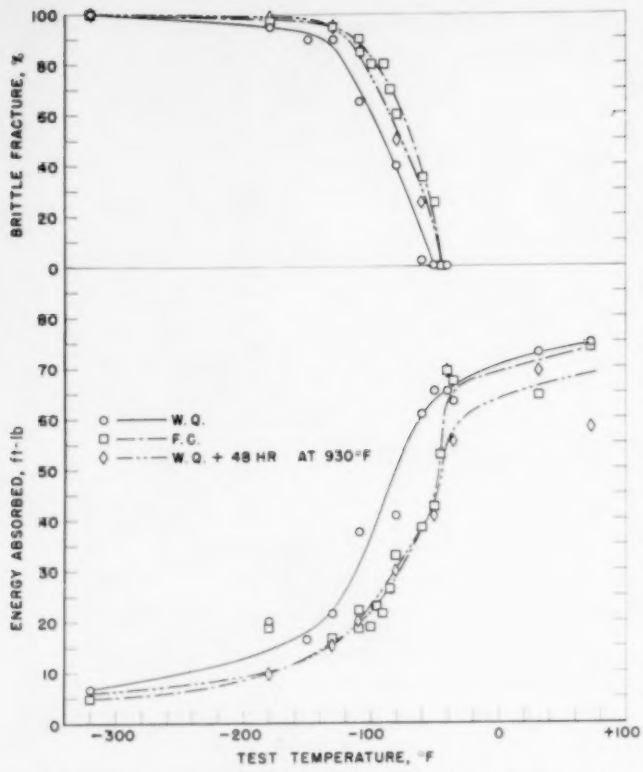

FIGURE 14. *Impact curves for the National Bureau of Standards steel M748* (FeB *plus* FeTi).

NBS steel M747 contained 0.0018 percent of B, and hardenability was not increased over that of the base steel. The actual reason for the differences in susceptibility to temper brittleness of the two steels treated with ferroboron alone is not known.

The summary curves presented in figures 15 and 16 may be used to compare the effects of the various addition agents upon the impact properties of the steels. For the Bureau of Mines steels in all conditions of treatment investigated (fig. 15), steels M734, M735, and M736 (curves 4, 5, and 6, respectively) compare unfavorably with the base steel (curve 1). These three steels were treated either with addition agents or ferroalloys that contained titanium. The additions incorporated in steels M732, M733, and M737 (curves 2, 3, and 7, respectively) had but negligible effect upon the impact properties as compared with those of the base steel, and none of these additions contained titanium, although they contained boron or zirconium or both. For the NBS steels (fig. 16), the deleterious effect of the titanium additions, alone or with boron (curves B and E), was not evident in the water-quenched steels. However, when isothermally treated at 930°F or when furnace-cooled from the tempering temperature, a slight deleterious effect was observed. The steel treated with ferroboron (M747, curve D) actually showed somewhat better impact properties than the base steel in each of the three conditions; the steel treated with ferrozirconium (M746, curve C) showed slightly better impact properties than the base steel in the water-quenched condition only.

Considering both series of steels (figs. 15 and 16), it may be concluded that, qualitatively, titanium has an adverse effect upon the impact properties of the steels as fully hardened and tempered at 1,200°F and that boron and zirconium do not.

The transition temperatures of the various steels were determined, using seven different criteria, as follows:

(1) The minimum temperature corresponding to 0-percent-brittle fracture.

(2) The temperature corresponding to 50-percent-brittle fracture.

(3) The temperature corresponding to the average energy level. The average energy level was obtained by taking the arithmetic mean of the average value of the upper (maximum average) and lower (minimum average) flat portions of the curve of impact energy versus test temperature.

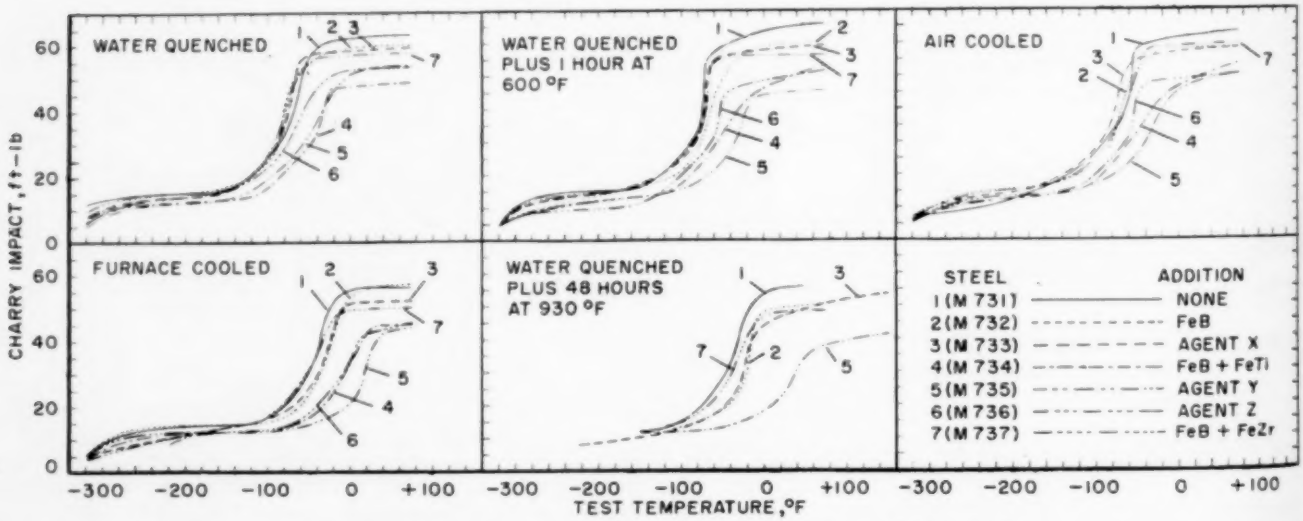
WATER QUENCHED
WATER QUENCHED PLUS 1 HOUR AT 600 °F
AIR COOLED
FURNACE COOLED
WATER QUENCHED PLUS 48 HOURS AT 930 °F
CHARRY IMPACT, ft-lb
TEST TEMPERATURE, °F
STEEL ADDITION
1 (M 731) NONE
2 (M 732) FeB
3 (M 733) AGENT X
4 (M 734) FeB + FeTi
5 (M 735) AGENT Y
6 (M 736) AGENT Z
7 (M 737) FeB + FeZr

FIGURE 15. *Summary of impact curves for the Bureau of Mines steels.*

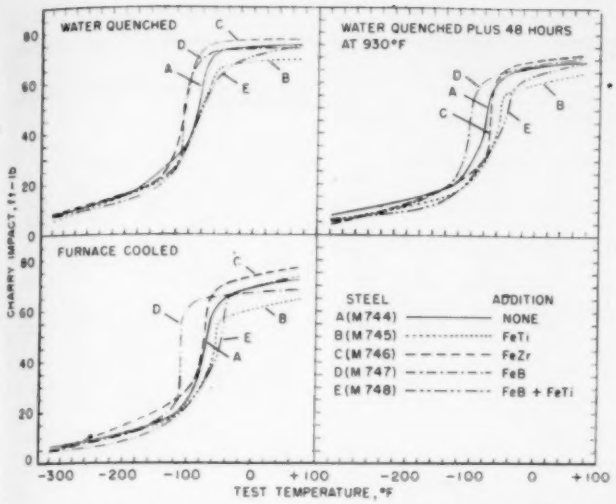

FIGURE 16. *Summary of impact curves for the National Bureau of Standards steels.*

(4) The temperature corresponding to 80 percent of the maximum average energy.
(5) The temperature corresponding to 40 ft-lb.
(6) The temperature corresponding to 30 ft-lb.
(7) The temperature corresponding to 20 ft-lb.

The transition temperatures so derived, together with other pertinent data, are given in tables 4 and 5. For more ready comparison, the various transition temperatures are plotted as bar graphs in figures 17 to 23, inclusive.

Obviously, the transition temperatures and the relative ratings of any two steels could be influenced by the transition criterion used. In spite of these variables, however, it is significant that, with all seven of the criteria utilized, the steels containing titanium (M734, M735, M736, M745, and M748) generally have higher transition temperatures than the corresponding base steels. A few exceptions to this generalization may be observed for the unembrittled conditions (water-quenched, water-quenched plus 1 hr at 600° F, and air-cooled); however, even in these cases the embrittling treatment caused a greater increase in the transition temperature of the steels containing titanium than was observed with the base steels. Although none of the steels contained as much zirconium as was desired, it was apparent that the zirconium present had no significant effect upon the impact properties.

Although several criteria for transition temperature have been used, it is believed that the criterion of 50-percent-brittle fracture possibly has the greatest significance. Using this criterion, figure 24 has been prepared so as to give a quick comparison of the shift in transition temperature caused by furnace-cooling from the tempering temperature as compared with the corresponding water-quenched steel. In

TABLE 4. *Transition temperatures—Bureau of Mines steels*

Steel	Tempering treatment [a] 1 hr at 1,200°F	0%-brittle fracture		50%-brittle fracture		Average energy level				80% maximum average energy		40 ft-lb	30 ft-lb	20 ft-lb
						Max	Min	Avg	Temp					
		°F	ft-lb	°F	ft-lb	ft-lb	ft-lb	ft-lb	°F	ft-lb	°F	°F	°F	°F
M731 (base)	W.Q.	−62	44	−79	33	62	15	38	−69	50	−58	−67	−87	−123
	W.Q.+1 hr at 600°F	−65	56	−80	32	65	15	40	−73	52	−70	−73	−85	−124
	A.C	−50	57	−76	33	61	11	36	−69	49	−55	−62	−85	−129
	F.C	−23	50	−54	28	56	14	35	−40	45	−31	−35	−50	−81
	W.Q.+48 hr at 930°F	−25	44	−45	30	51	12	32	−40	41	−29	−29	−44	−74
M732 (FeB)	W.Q.	−57	52	−92	27	59	15	37	−82	47	−71	−80	−86	−123
	W.Q.+1 hr at 600°F	−54	46	−80	28	59	13	36	−68	47	−53	−63	−76	−108
	A.C	−54	48	−83	28	57	15	36	−72	46	−59	−68	−79	−119
	F.C	−13	47	−44	26	55	15	35	−28	44	−17	−21	−36	−62
	W.Q.+48 hr at 930°F	−9	46	−31	23	54	13	34	−18	43	−11	−15	−21	−43
M733 (agent X)	W.Q.	−65	52	−89	30	58	14	36	−79	46	−69	−75	−89	−122
	W.Q.+1 hr at 600°F	−65	54	−76	33	58	14	36	−73	46	−68	−71	−83	−127
	A.C	−62	52	−90	30	57	14	36	−80	46	−68	−75	−91	−138
	F.C	−17	46	−48	26	51	11	31	−36	41	−23	−24	−38	−73
	W.Q.+48 hr at 930°F	−15	40	−36	22	50	10	30	−24	40	−13	−13	−24	−45
M734 (FeB+FeTi)	W.Q.	−30	41	−52	29	48	13	30	−46	38	−34	−32	−48	−85
	W.Q.+1 hr at 600° F	−20	42	−44	34	49	12	30	−53	39	−31	−28	−54	−86
	A.C	−30	44	−64	27	52	13	32	−47	42	−32	−33	−54	−90
	F.C	+10	38	−16	26	44	12	28	−11	35	+5	+16	−6	−34
	W.Q.+48 hr at 930°F													
M735 (agent Y)	W.Q.	−23	45	−58	30	53	13	33	−50	42	−30	−34	−59	−99
	W.Q.+1 hr at 600°F	−18	41	−41	26	44	13	28	−37	35	−26	−20	−34	−66
	A.C	−6	43	−43	28	48	13	30	−37	38	−22	−17	−38	−77
	F.C	+32	40	+7	24	43	12	28	+14	34	+21	+30	+17	−7
	W.Q.+48 hr at 930°F	+49	34	+13	20	40	12	26	+31	32	+42	+115	+38	+11
M736 (agent Z)	W.Q.	−49	44	−83	28	53	14	34	−69	43	−51	−58	−76	−116
	W.Q.+1 hr at 600°F	−43	45	−71	27	49	10	30	−65	39	−53	−52	−63	−98
	A.C	−49	44	−68	28	49	13	31	−61	39	−52	−51	−62	−97
	F.C	+11	40	−20	26	44	12	28	−14	35	+2	+10	−9	−42
	W.Q.+48 hr at 930°F													
M737 (FeB+FeZr)	W.Q.	−50	54	−87	33	57	15	36	−83	46	−72	−78	−92	−123
	W.Q.+1 hr at 600°F	−65	53	−87	28	56	15	36	−73	45	−66	−68	−84	−120
	A.C	−50	50	−77	32	58	15	36	−67	46	−55	−62	−81	−123
	F.C	−24	46	−55	29	49	10	30	−53	39	−34	−32	−52	−84
	W.Q.+48 hr at 930°F	−13	44	−52	24	47	14	30	−37	38	−25	−21	−37	−65

[a] W.Q.=Water-quenched from tempering temperature. A.C.=Air-cooled from tempering temperature. F.C.=Furnace-cooled from tempering temperature (30°F/hr).

TABLE 5. *Transition temperatures—NBS steels*

Steel	Tempering treatment [a] 1 hr at 1,200°F	0%-brittle fracture		50%-brittle fracture		Average energy level				80% maximum average energy		40 ft-lb	30 ft-lb	20 ft-lb
						Max	Min	Avg	Temp					
		°F	ft-lb	°F	ft-lb	ft-lb	ft-lb	ft-lb	°F	ft-lb	°F	°F	°F	°F
M744 (base)	W.Q.	−74	66	−101	37	74	13	43	−92	59	−79	−96	−122	−169
	F.C.	−52	62	−82	34	68	10	39	−78	54	−65	−77	−88	−113
	W.Q.+48 hr at 930°F	−57	62	−85	36	67	12	40	−81	54	−72	−80	−98	−128
M745 (FeTi)	W.Q.	−77	52	−95	40	68	14	41	−94	54	−73	−96	−111	−151
	F.C.	−40	58	−65	33	62	9	36	−62	49	−53	−57	−70	−104
	W.Q.+48 hr at 930°F	−48	56	−72	33	59	10	34	−69	47	−56	−61	−78	−109
M746 (FeZr)	W.Q.	−98	62	−110	45	77	13	45	−110	61	−99	−114	−126	−156
	F.C.	−65	63	−83	35	73	12	42	−77	58	−69	−78	−93	−144
	W.Q.+48 hr at 930°F	−64	60	−86	28	70	14	42	−71	56	−68	−72	−81	−132
M747 (FeB)	W.Q.	−106	55	−110	42	73	14	43	−110	58	−103	−110	−115	−158
	F.C.	−106	57	−110	30	66	10	38	−108	54	−108	−108	−109	−113
	W.Q.+48 hr at 930°F	−106	38	−110	33	67	10	38	−106	54	−97	−105	−113	−134
M748 (FeB+FeTi)	W.Q.	−51	63	−90	43	70	12	41	−93	56	−69	−95	−111	−139
	F.C.	−44	60	−67	34	70	8	39	−58	56	−42	−56	−77	−106
	W.Q.+48 hr at 930°F	−43	52	−76	32	65	9	37	−63	52	−43	−56	−80	−110

[a] W.Q. = Water-quenched from tempering temperature. A.C. = Air-cooled from tempering temperature. F.C. = Furnace-cooled from tempering temperature (30°F/hr).

assessing the magnitude of these shifts, which are a direct measure of temper embrittlement, consideration must also be given to the effects the addition agents have upon the transition temperature of the water-quenched steels. For instance, in figure 24, the transition temperature of steel M734 (FeB+FeTi) has been raised 36 deg F by furnace-cooling as compared with water-quenching from the tempering temperature and the corresponding shift in steel M737 (FeB+FeZr) was only 32 deg F—certainly an insignificant difference. However, the transition temperature of the titanium-treated steel M734 as water-quenched was −52°F—a value considerably higher than that for the zirconium-treated steel M737 (−87°F). Apparently the titanium addition was sufficient to raise the transition temperature of the water-quenched steel so much that the additional shift caused by furnace-cooling appeared innocuous. Indeed, the transition temperature of the titanium-treated steel M734 as *water-quenched* was actually higher than that of the zirconium-treated steel M737 as *furnace-cooled* (−52° and −55°F, respectively).

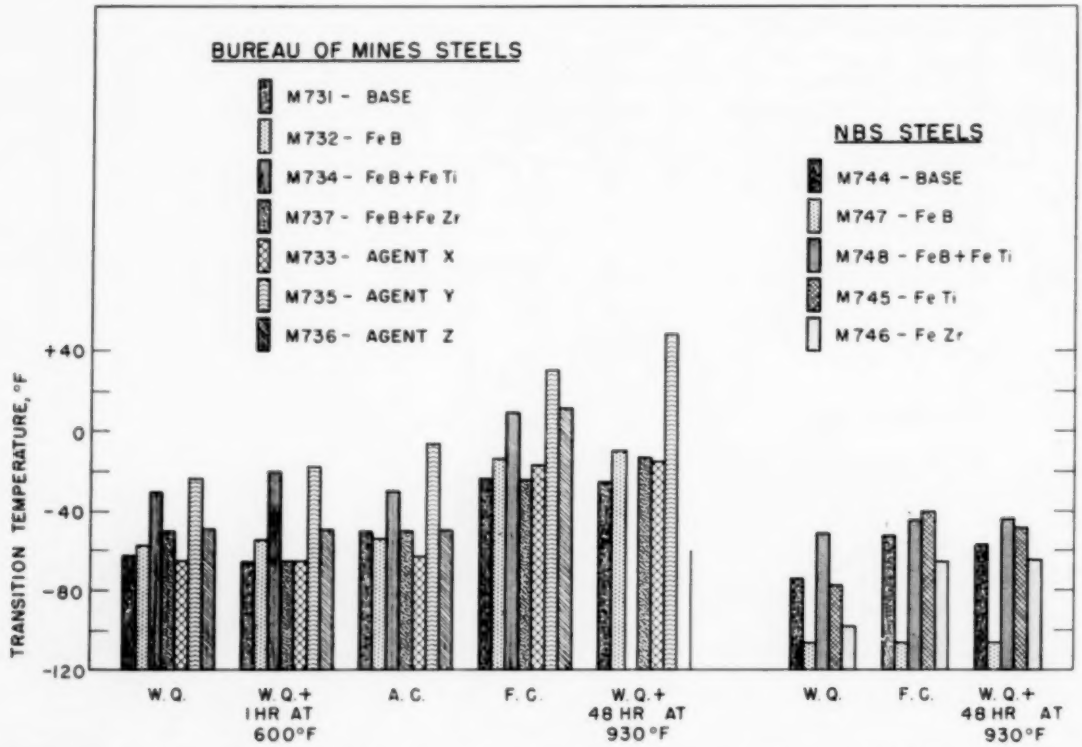

FIGURE 17. *Transition temperatures of the various steels (transition criterion, 0%-brittle fracture).*

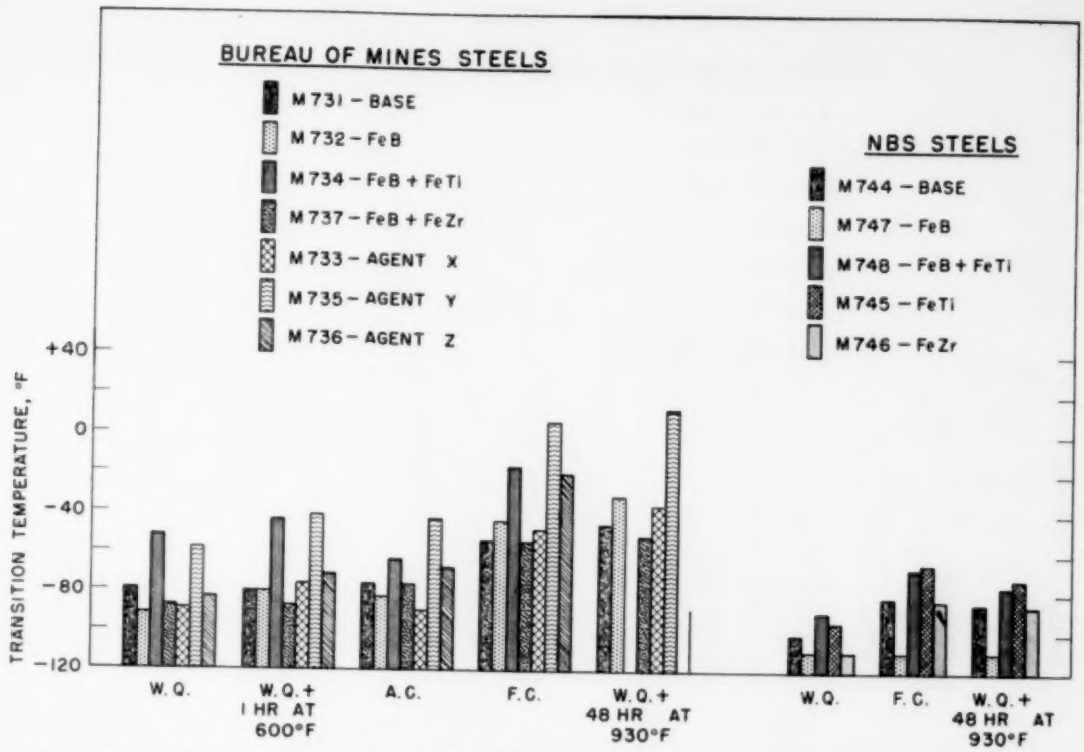

FIGURE 18. *Transition temperatures of the various steels (transition criterion, 50%-brittle fracture).*

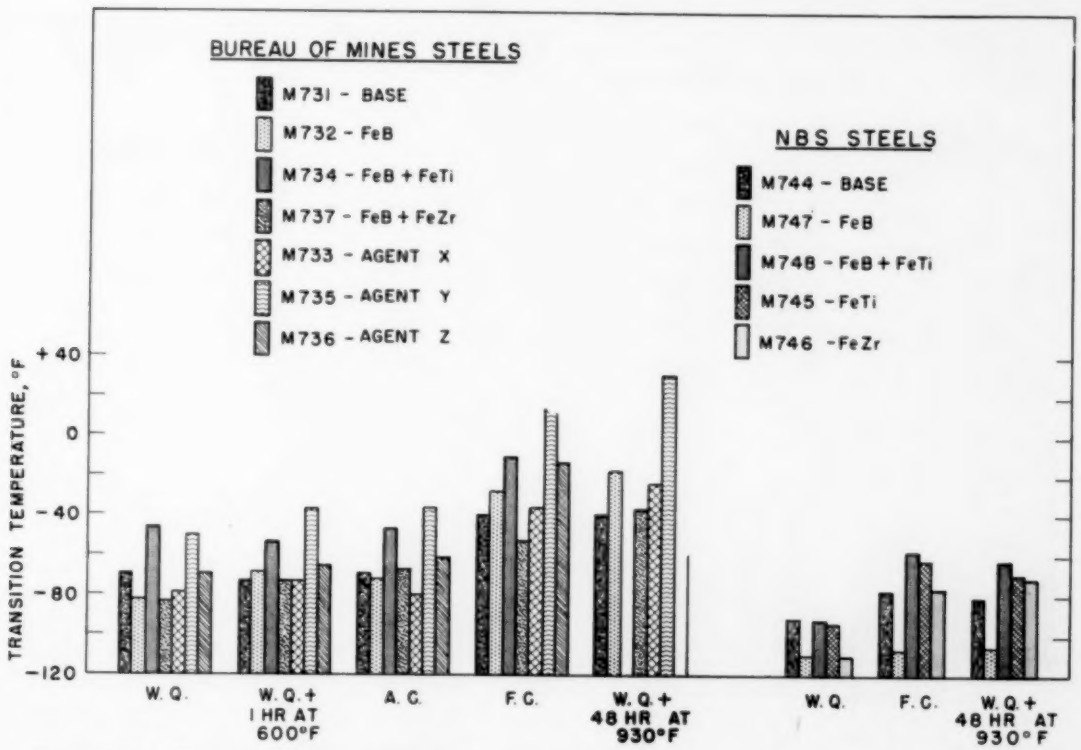

FIGURE 19. *Transition temperatures of the various steels (transition criterion, average energy level).*

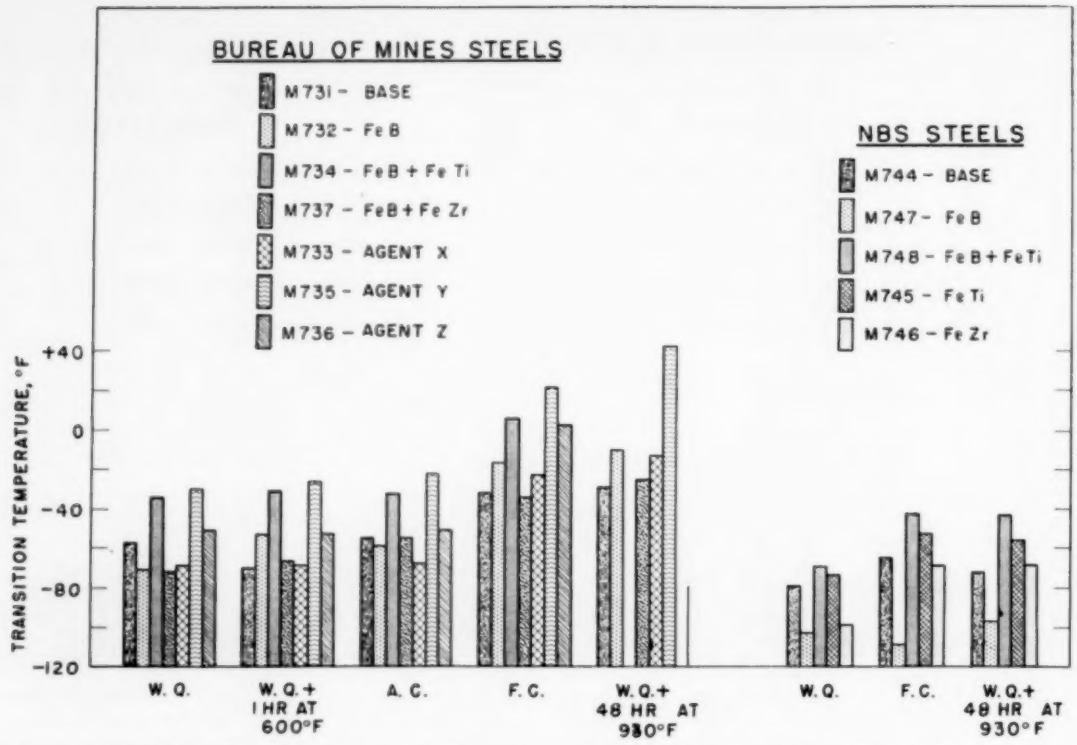

FIGURE 20. *Transition temperatures of the various steels (transition criterion, 80% of the maximum average energy).*

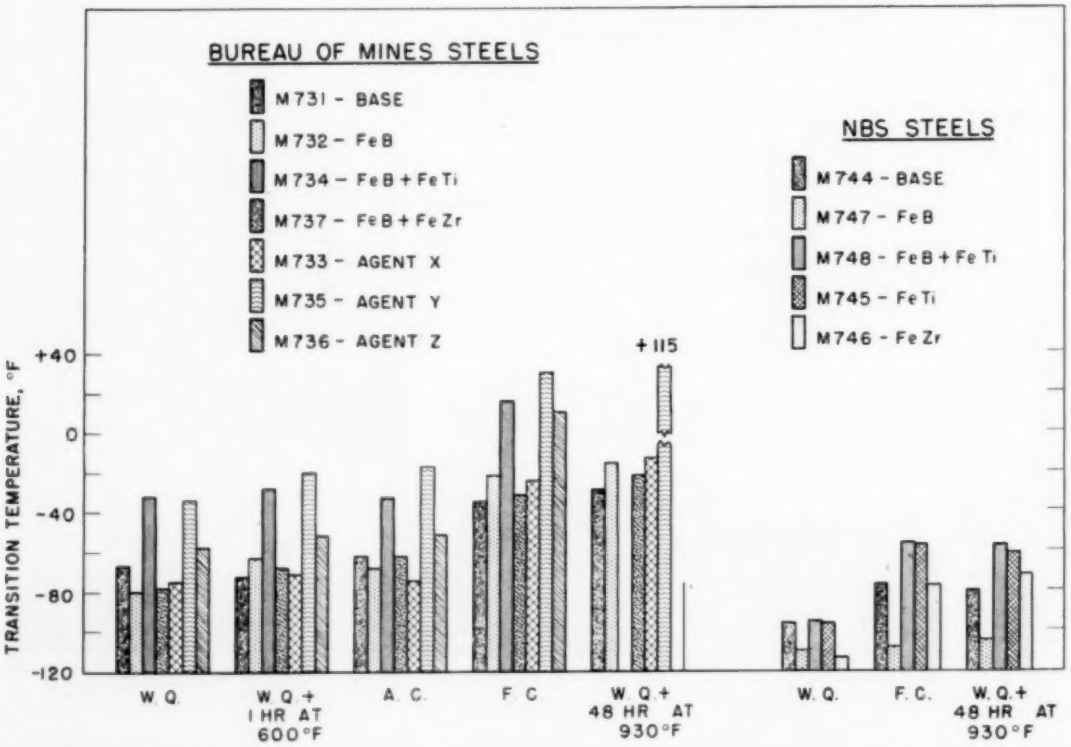

FIGURE 21. *Transition temperatures of the various steels (transition criterion, 40 ft-lb).*

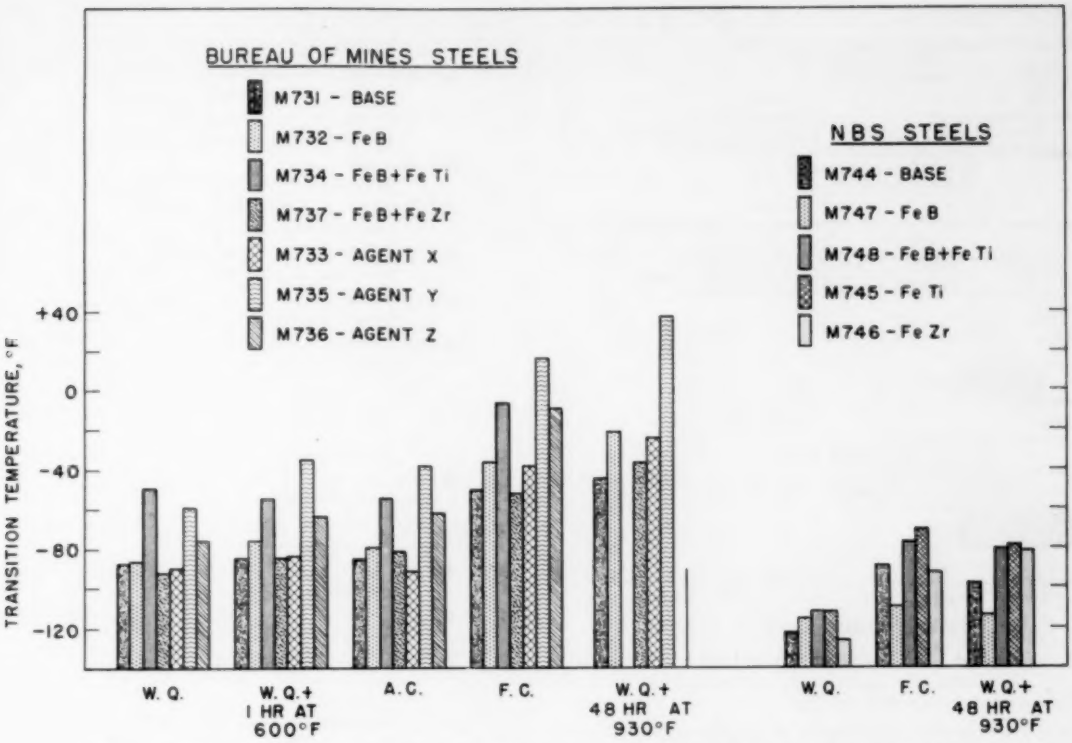

FIGURE 22. *Transition temperatures of the various steels (transition criterion, 30 ft-lb).*

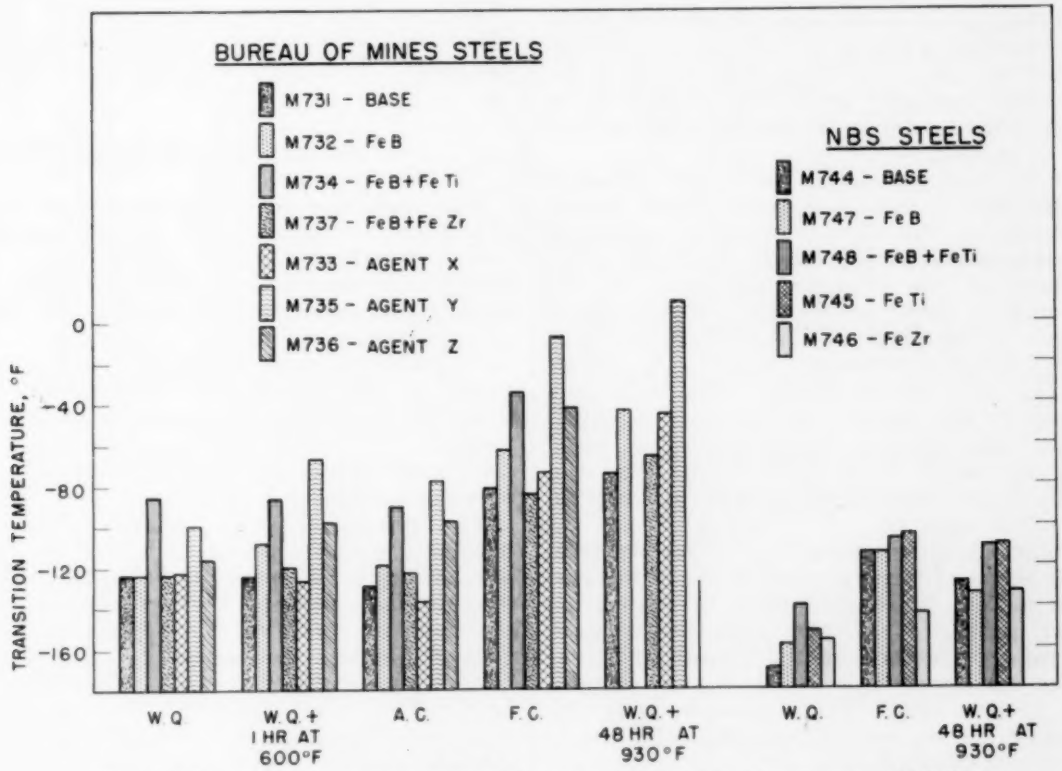

FIGURE 23. *Transition temperatures of the various steels (transition criterion, 20 ft-lb).*

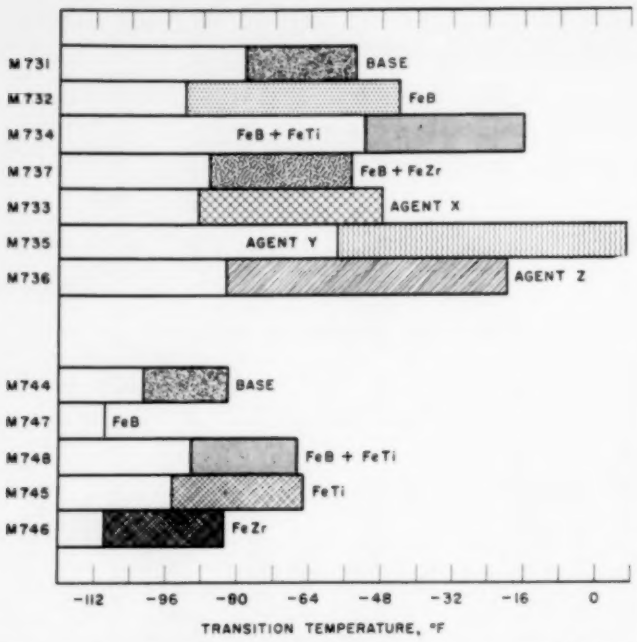

FIGURE 24. *Increase in transition temperature (50%-brittle fracture) of the furnace-cooled steels as compared with the corresponding water-quenched steels.*

Open bars give the transition temperatures of the water-quenched steels; shaded bars those of the furnace-cooled steels. The lengths of the shaded bars, therefore, indicate the increase in transition temperatures. Steel M747 had the same transition temperature in both conditions of treatment.

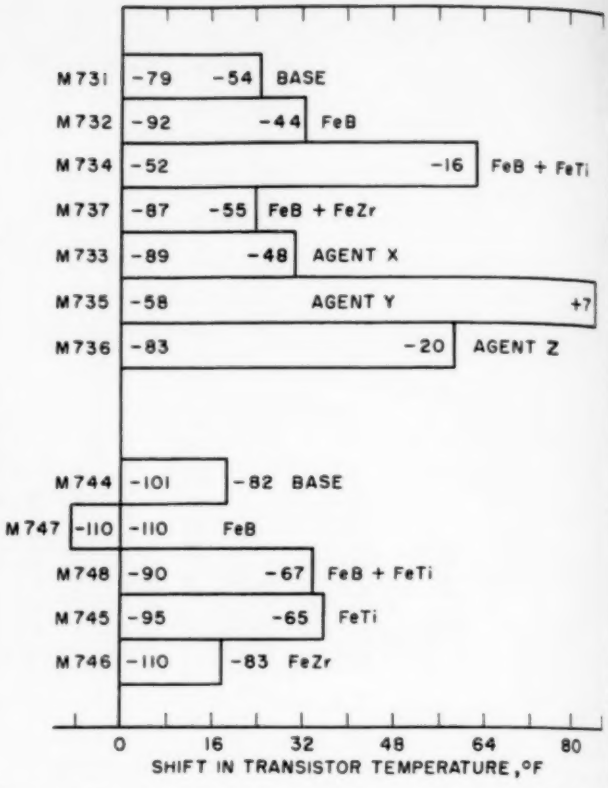

FIGURE 25. *Increase in transition temperature (50%-brittle fracture) of the furnace-cooled steels as compared with the water-quenched base steel.*

Figures in bars indicate the actual transition temperatures of the various steels both as water-quenched (lower temperature) and as furnace-cooled (higher temperature).

It is obvious that any attempt to measure the effect of the addition agents in causing temper brittleness merely by calculating the shift in transition temperature caused by the embrittling treatment on the individual steels can give erroneous conclusions as to the effect of these addition agents upon the impact properties in general.

In figure 25 these same data have been replotted to show the shift in transition temperature caused by furnace-cooling the various steels as compared with the *water-quenched base steel.* Here the deleterious effects of the titanium additions on the impact properties stand out clearly. The steels so treated were M734 (FeB+FeTi), M735 (addition agent Y), M736 (addition agent Z), M748 (FeB+FeTi), and M745 (FeTi). The additions incorporated in the other steels had a negligible effect upon the impact properties. The same general picture would have been evident had the isothermally treated steels been compared with the water-quenched steels.

Even though the same general trends were observed both in the series of steels melted at the Bureau of Mines and at the National Bureau of Standards, the impact properties of the NBS steels were markedly superior to those of the Bureau of Mines steels. The cause of this difference in impact properties is not clear. It is possible that the slightly lower carbon content of the NBS steels may be partly responsible.

4. Summary and Conclusions

Two series of steels, melted to the base composition of 8140, were studied to ascertain whether titanium and zirconium (present in many commercial boron addition agents) had any adverse effect upon the impact properties of the base steels, particularly with reference to temper brittleness. All steels were given the same hardening treatment (½ hr at 1,600° F, oil quench) and were tempered 1 hr at 1,200° F. The rate of cooling from the tempering temperature was varied so as to develop temper brittleness and an isothermal embrittling treatment also was employed.

The results obtained indicate that with fully hardened steels tempered at 1,200° F the presence of relatively small amounts of titanium as introduced into the test steels by the boron addition agents is sufficient to cause an impairment in the Charpy V-notch impact properties of the steels or an increased susceptibility to temper brittleness, or both. This was confirmed by the addition of titanium without boron. Similar effects, previously thought possibly due to the presence of zirconium,

were not observed. The zirconium additions, however, were very small, although within the range of residual amounts usually found in steels treated with addition agents containing zirconium.

The author is indebted to R. J. Leary of the Bureau of Mines, Pittsburgh, Pa., and to R. H. Harwell of NBS for their invaluable cooperation in melting the experimental steels, and to T. P. Royston and C. R. Irish of NBS for their conscientious assistance during the course of the investigation. The study was sponsored by Wright Air Development Center, with Howard Zoeller acting as project engineer.

WASHINGTON, October 26, 1956.

Journal of Research of the National Bureau of Standards Vol. 58, No. 4, April 1957 Research Paper 2751

Optical and Volumetric Relaxation Effects in Glass Following Removal of High Hydrostatic Pressures

C. Weir, S. Spinner, I. Malitson, and W. Rodney

Optical and volumetric relaxations in glass were studied after compressing specimens 4 hours at 9,000 atmospheres and 21° C. Following release of pressure the refractive index was higher than the original value and decreased with time, recovering its initial value within 12 hours. Optical-relaxation curves for lead and borosilicate glasses were complex, the detailed behavior depending on composition and thermal history. No corresponding effects were observed in fused silica after exposure to even higher pressures. Volumetric changes associated with index changes were determined interferometrically and found to be less than corresponding changes known to accompany annealing. Possible implications of the results are discussed.

1. Introduction

The delayed volumetric reaction of glass subjected to pressure was reported initially by Bridgman [1].[1] The first detailed study of the phenomenon was made by Bridgman and Simon [2], and was followed by experiments in which tensile stresses were combined with hydrostatic pressure [3]. The foregoing experiments indicated a threshold pressure below which compaction did not occur in most glasses [2]. Weir and Shartsis [4] measured the compressibility of binary alkali borate and silicate glasses up to 10,000 atm. They observed a nearly constant total decrease in volume of about 0.2 percent following compression. The maximum pressure was considerably below the reported thresholds for compaction of the alkali silicates [2], and the changes in volume were independent of composition. It was concluded that the effects observed were caused by loss of fragments of glass or penetration of the confining liquid into small crevices under pressure [4]. Anderson [5] studied the change in density at room temperature of glasses subjected to pressure at elevated temperatures for periods as long as 1 week. He found the process of density change at constant pressure to be complex and to consist of an initial reversible increase in density that approached a constant value after about 4 hr and a subsequent irreversible increase in density that continued unabated for periods as long as 1 week. Bridgman, in a recent report [6], considers that no irreversible change in density should occur under purely hydrostatic compression and attributes his previous results [2] to the complex stress applied. He studied [6] a soda-silica glass under approximately hydrostatic conditions to 100,000 kg/cm^2 (about 97,000 atm) and detected no change in dimensions on removal of pressure. Under the experimental conditions, however, very small changes could not have been detected.

Because evaluation of compressibility data on glasses requires some knowledge of the properties of a delayed volumetric response, it was considered desirable to ascertain the magnitude of this effect in glasses subjected to pressures of the order of 10,000 atm at room temperature. It was decided to measure aftereffects of hydrostatic pressure, using the index of refraction as the indicating property, because it is known, on theoretical as well as experimental grounds, that the index is related to the density. The advantage of using the index lies in the fact that it can be measured with high precision, permitting the detection of small internal changes in the glass.

The data obtained by several workers [7, 8, 9] show that the index changes linearly with density for the same glass on annealing. Analysis of the data of these workers [10], for a borosilicate glass (BSC 517) that was similar in composition to the ones used in the present study, shows the following empirical relationship between relative changes in index, $\Delta n/n$, and relative changes in density, $\Delta\rho/\rho$:

$$\Delta\rho/\rho = 3.5\ \Delta n/n. \quad (1)$$

It can be shown from theoretical relationships between density and index [11, 12] that the numerical constant in eq (1) should have approximately the observed value, if the index is measured in a region of low dispersion. Such an analysis is given subsequently. Tool, Tilton, and Saunders [7] studied six glasses of widely different compositions, but the value of the numerical constant of eq (1) derived from their data was found to range only between 3.2 and 3.5.

This report describes the optical relaxation observed in the index of refraction of glasses subjected to hydrostatic pressures of 9,000 atm at room temperature. Observations on other properties of interest, such as dimensions and absorption characteristics, were also conducted.

2. Experimental Materials and Methods

2.1. Glasses

Most of the studies were made by using a borosilicate glass designated as BSC 517/645. The weight percentages of the component oxides of the glass calculated from the batch composition were

[1] Figures in brackets indicate the literature references at the end of this paper.

SiO_2, 66.4 percent; B_2O_3, 12.4 percent; Na_2O, 8.4 percent; K_2O, 11.8 percent; ZnO, 0.5 percent; and As_2O_3, 0.5 percent. Two specimens were cut from the same large sample. Different refractive indices (and densities) were obtained by applying different annealing procedures to each specimen. The higher index resulted from annealing at 585° C for 12 hr and cooling at a rate of 4 deg C/hr, whereas the lower index resulted from annealing at 590° C for 12 hr and cooling at a rate of 50 deg C/hr. These annealing procedures are in general agreement with the procedures described by Lillie and Ritland [13] for obtaining relatively strain-free specimens having a uniform index.

Additional experiments were performed on an experimental lead silicate glass consisting of 30 percent of SiO_2 and 70 percent of PbO by weight as well as a specimen of fused silica of extremely high purity [14].

2.2. Pressure Apparatus

The apparatus and techniques used for obtaining high hydrostatic pressure have been described in detail [15]. Briefly, the glass specimens were immersed in a light petroleum distillate in the smooth bore of a heavy-walled pressure vessel. A leakproof piston, forced into the bore of the vessel by means of a hydraulic press, generated hydrostatic pressure by compressing the liquid. This pressure was measured with a manganin pressure gage mounted inside the vessel. A pressure of 9,000 atm was used in all experiments except one, which used 11,000 atm.

Pressure was applied at the rate of 1,000 atm/min until the maximum pressure was attained. This pressure was maintained for 4 hr ± 1 min and released very rapidly. The pressure was dropped rapidly to 1,000 atm, with a subsequent drop to 1 atm on disassembly of the pressure vessel. The entire operation of release of pressure and removal of the specimen required approximately 2 min.

The specimens were chilled by the rapid decompression of the confining liquid and were transferred immediately to vacuum bottles containing water or petroleum distillate for transport to the laboratories in which the index and length measurements were made. The bottles and liquids were thermally equilibrated in the respective laboratories for at least 12 hr prior to use. It was observed experimentally that a 4- to 5-min immersion was sufficient to provide thermal equilibrium between the specimen and the excess liquid in the container. The pressure equipment itself was contained in a temperature controlled room at 21 ± 1° C.

2.3. Refractive-Index Measurements

The refractive indices of each prismatic sample of glass used in these experiments were measured on a precision spectrometer. The collimator and telescope have achromatic objective lenses of 250-mm focal length and a 27-mm clear aperture. The collimator is equipped with a bilateral variable slit, and the telescope has an Abbe-type autocollimating eyepiece. The telescope rotates on a cylindro-conical bearing.

The divided circle, approximately 3 in. in radius, is made of glass and graduated in intervals of 4 min of arc. The circle-reading microscope employs an optical coincidence micrometer with the eyepiece conveniently located below the telescope. Two diametrically opposite parts of the circle are simultaneously observed, and the optical micrometer permits direct readings to 0.1 sec of arc free of any error of eccentricity. The prism table, equipped with tangent screw and clamp, rotates on a vertical axis completely independent of the axis of rotation of the telescope. A removable table consisting of two slides that travel in superimposed ways at right angles to each other was constructed and mounted on the prism table to facilitate the proper centering of the prism with respect to the collimator and telescope [16, 17].

Standard technique for high-precision refractive-index measurements was carefully followed in these experiments. Measurements before and after compression showed no change in the refracting angles. Repetitive measurements were made at intervals over a period of 12 hr, with shorter intervals between measurements when the slope was greater. The indices were determined for two wavelengths, the 5461–A line of mercury and the 6438–A line of cadmium. All index measurements were carried out in a temperature-controlled laboratory, the temperature of which varied not more than ± 0.5 deg C during the course of the measurements.

With a prism of refracting angle near 60° and index near 1.5, it has been calculated that an error of ± 1 sec of arc in measuring the double-deviation angle leads to an error of $\pm 1.7 \times 10^{-6}$ in index. Any error in measurement of this prism angle does not affect the results, as long as the angle remains constant, because the main concern is the *change* in index.

It is estimated that the errors in measured angles do not exceed ± 0.75 sec of arc or $\pm 1.2 \times 10^{-6}$ in index. This estimate is based on comparative measurements between the instruments used and another high-precision spectrometer and on measurements of the angles of standard prisms and stainless-steel wedges whose angles are estimated to be accurate to ± 0.3 sec of arc.

2.4. Dimensional Measurements

The dimensional studies were made by using Saunders' [18] refinement of the interferometer method described by Peters and Cragoe [19]. The optical flats were separated by two specimens of the same glass, only one of which had been subjected to pressure. Each specimen was ground manually to contain three bosses for contact on the bottom flat, whereas the test specimen had a single boss and the comparison specimen two bosses for support of the upper plate. Monochromatic helium 5876–A light was used for illumination. The specimens used were 3 cm in height, and the flats were silvered to produce a sharpened fringe system. The lower flat was very close to the bottom surface of the upper flat and

produced a true Fabry-Perot fringe system. This arrangement permitted counting of fractional fringes with a precision of about ± 0.1 fringe.

It will be noted that a relaxation of the compressed specimen involves a tilting of the upper flat, and therefore requires a knowledge only of the total number of fringes. A variation in the ambient temperature produces only a translation of the entire fringe system.

2.5. Transmission Measurements

Absorption characteristics of the glasses were measured in transmission by using a manually operated commercial spectrophotometer. The specimens used were taken from samples of the glasses used for the index measurements.

3. Results and Discussion

3.1. Optical Relaxation

The measurements of index of refraction for different intervals following hydrostatic compression are shown graphically in figures 1 to 3. Each figure shows data at wavelengths of 5461–A and 6438–A. The index of refraction prior to compression is represented by the point in each figure at zero time. Duplicate measurements were made on the two borosilicate glasses, and both sets of data are shown in figures 1 and 2. These duplicates represent data obtained at different times on the same specimen. The dimensions of each point in the figures represent the estimated precision in index and time measurements.

Examination of the graphical results permits the following general conclusions:

a. A small but measurable relaxation in index of refraction follows the release of hydrostatic pressure on these glasses under the conditions of the experiments.

b. No permanent change in the index of refraction is observed, the value after about 12 hr agreeing with the initial value within the experimental error.

c. The reproducibility of the data was generally within the experimental error in one case (fig. 2), whereas in the other (fig. 1), it was just outside the experimental error. Even in the latter case, however, curves obtained from either run retain their essential characteristics, so that any subsequent conclusions are unaffected by the differences.

d. The relaxation process is complex, consisting of two or more consecutive processes.

All curves show a rather rapid decay of index occurring in the first ½ hr, which is followed by at least one additional relaxation occurring after a considerably longer interval. The second relaxation, occurring at approximately 400 min, is larger than the experimental error of the index determination only by a factor of about two. In addition, there is some uncertainty in the time base. It is conceivable then that the second relaxation may not be real if some unrecognized systematic error exists.

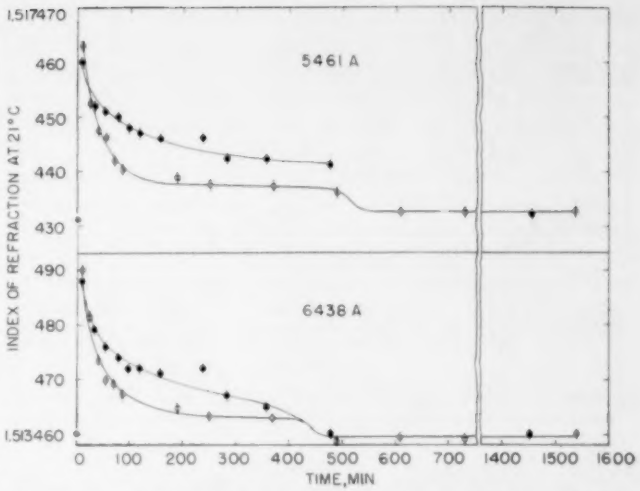

FIGURE 1. *Isothermal relaxation in index at 1 atmosphere of specimen of borosilicate glass subjected to hydrostatic pressure of 9,000 atmospheres for 4 hours.*

Initial density of glass, 2.513 g/cm.³

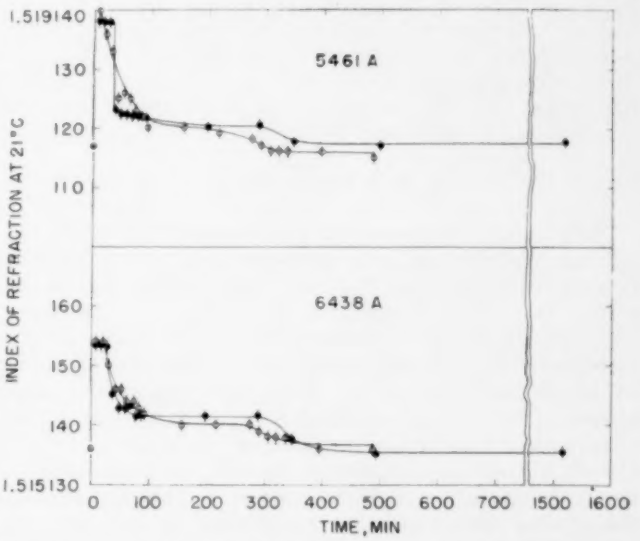

FIGURE 2. *Isothermal relaxation in index at 1 atmosphere of specimen of borosilicate glass subjected to hydrostatic pressure of 9,000 atmospheres for 4 hours.*

Initial density of glass, 2.530 g/cm.³

Consideration of the precision of the measurements, as well as the fact that the phenomenon appears in each case, requires the conclusion that the second relaxation is probably real.

In the lead silicate glass, there appears to be a third relaxation process occurring, although the magnitude of the slowest of these is not appreciably beyond the experimental error. It is also interesting to note that only in this glass is there any substantial evidence that the relaxation processes occur at different times for the two wavelengths. This point is discussed later.

Because the two specimens of borosilicate glass studied were identical in composition, varying only

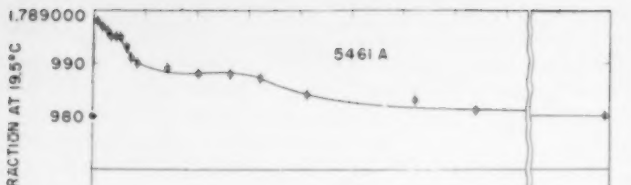

FIGURE 3. *Isothermal relaxation in index at 1 atmosphere of specimen of lead silicate glass subjected to hydrostatic pressure of 9,000 atmospheres for 4 hours.*

in their densities, it was expected that the less-dense specimen would show the greater effect after compression. This was actually observed, as shown in figures 1 and 2. The less-dense (lower-index) glass (fig. 1) shows a greater relaxation than the more-dense (higher-index) glass shown in figure 2. It will also be observed that the over-all rate of relaxation appears to be related to the density. Both of these observations apply specifically to the initial relaxation, as the second effect is so small that no reliable conclusion may be drawn.

3.2. Fused Silica

Following the initial measurements on the borosilicate glasses, an attempt was made to observe relaxation in fused silica. Measurements made under the same conditions as those for the borosilicates showed no change in index. An additional experiment was performed by using a pressure of 11,000 atm for 6 hr. No change in index was observed under these conditions. It is concluded that within the experimental error of these measurements no optical relaxation occurs in fused silica in the time-pressure regions studied. This conclusion does not eliminate the possibility of relaxations occurring in less than the approximate 7 min required to obtain the initial measurement after release of pressure. With this reservation, the negative finding corroborates the report of Bridgman and Simon [2] of the marked threshold for the compaction of fused silica. The effect found for the borosilicates, coupled with the negative result for fused silica, pointed to the possibility that B_2O_3 was involved directly in the phenomenon because no threshold appears to exist for vitreous B_2O_3 [2]. To test this possibility the lead silicate glass that contained no B_2O_3 was tested; the relaxation observed eliminates the necessity of the direct involvement of B_2O_3.

3.3. Effect of Ambient Temperature

The precautions taken to maintain constant temperature during compression, index, and dimensional measurements, as well as during the transfer of the specimens, have already been mentioned. It is interesting to consider the effect of variations in temperature on the index and dimensional data.

The index of refraction of most glasses, including the types studied here, rises with increasing temperature in the vicinity of room temperature [20]. The value of the index-temperature coefficient is on the order of 2×10^{-6}/°C. This means that in order to produce the observed initial index increase it would be necessary to assume a temperature rise of about 15 deg C. This was impossible in view of the experimental precautions exercised.

The actual effect of rapid decompression is to chill the specimens. Therefore, any difference between the specimen temperature and the ambient temperature at the start of the index measurements would be in a direction to counteract the observed index effect. There is, indeed, a possibility that the horizontal portion of the curve observed at the onset in some of the figures could arise from these opposing tendencies.

In the case of the dimensional measurements, on the other hand, the effect of any initial cooling would be to augment the observed dimensional increase through the usual thermal expansion of the material occurring in the first few minutes of the observations. No such thermal effects were noted under the experimental conditions.

3.4. General Considerations of Optical Relaxation

All previous studies of glasses have resulted in reports of permanent increases in density [2, 3, 5]. Under the conditions of the present experiments, which used index as a measure of the condition of the glass, permanent changes were not observed. The permanent changes reported by Bridgman and Simon [2] may be attributed to the much higher pressures used or to the fact that the pressures used were not purely hydrostatic [6]. In Anderson's work [5], temperature was an added variable, but the pressures were somewhat lower than the 9,000 atm used here.

The index of refraction is related to both the density and the characteristic frequencies of the constituents of the glass [11, 12]. The observed relaxation in index might arise from a relaxation in volume or in the change of characteristic frequencies or more probably a combination of both effects. The absorption properties of the glasses are of importance in considerations of optical relaxation.

3.5. Optical Adsorption in the Glasses

It has recently been reported that the ultraviolet absorption spectrum of benzene broadens and shifts to longer wavelengths on compression [21] and that a similar effect occurs in the infrared spectrum of deformed alkali halide crystals [22]. In the present experiments displacement of the electronic ultraviolet absorption region toward the measured wavelengths under pressure and a relaxation of the shift on removing the pressure would produce a result of type the observed.

An experiment was conducted to detect a shift in the absorption edge of the lead silicate glass. No change in the position or shape of the absorption edge could be detected at 1 atm following compression at 9,000 atm for 4 hr. The precision of the absorption measurements was only of the order of a few parts in a thousand, and in view of the small change in index, the negative finding is not unexpected.

The absorption edge of the lead silicate glass is located at approximately 3500 A. The glass was chosen for study for this reason, as well as the fact that it contained no B_2O_3, because wavelength dependence of the relaxation curves might be expected to be in evidence. The data of figure 3 indicate a difference in behavior at 6438 A and 5461 A. From the previous considerations these differences may be indicative of absorption-band relaxation, although additional studies to corroborate the observation are required.

3.6. Volume Relaxation

Volume relaxation in gases and condensed phases is of considerable interest at the present time, with attention being concentrated on the subject principally by researches involving ultrasonics [23, 24, 25]. The relaxation in index observed here is doubtless accompanied by a related relaxation in volume, although in view of the foregoing discussion the two effects are not necessarily related linearly. As the glasses used here are considered to be isotropic and all changes are small, the relaxation in length may be considered to be one-third of the corresponding volume effect.

Studies of length changes were made only on the borosilicate glass of lesser density, as it would be expected to exhibit the largest effects. Using the ordinary interferometer system [19], any relaxation in length of the compressed specimen was so small as to be doubtful. From repeated experiments, however, it was concluded that a real relaxation occurred, which gave a value of $\Delta l/l$ of the order of 1×10^{-5}; On using a refined interferometer [18], a value of $1.2\pm0.3\times10^{-5}$ was obtained for $\Delta l/l$. Although the precision of the measurement was not adequate to determine reliable rate curves, it was observed that the general shape of the relaxation curve followed the index-time curve, with an initially rapid relaxation rate that decreased with time. From figure 1 the value of $\Delta n/n$ for this glass is observed to be -2.0×10^{-5}; if eq (1) were valid for this process, a corresponding value for $\Delta l/l$ would be 2.3×10^{-5}. Thus the value of 1.2×10^{-5} obtained experimentally for $\Delta l/l$ is approximately half that predicted by eq (1). It would appear that most of the probable systematic experimental errors (mainly arising from temperature) would tend to produce too low a value of $\Delta n/n$ and too large a value for $\Delta l/l$ because the thermal coefficients of index and length are positive [20] (sec. 3.3). It is concluded, therefore, that eq (1), which describes the index-density relationship on annealing, does not describe the processes occurring on volume relaxation in the glass studied.

The previous observations that the relative volume relaxation does not agree with that to be expected from the annealing relationship (eq 1) indicate that the relaxation effect involves shifts in the absorption frequencies in addition to the compaction (sec. 3.5). This concept may be developed in the following way: It may be assumed that the ordinary dispersion equations [11,12] apply to these glasses. For the purposes of this discussion, similar results will be obtained from any of these equations and the Sellmeier equation is chosen for convenience. This relates the index, n, to the absorption wavelengths, λ_i, and the measured wavelength, λ, by the equation

$$n^2=1+\sum_i \frac{A_i\lambda^2}{\lambda^2-\lambda_i^2}, \tag{2}$$

where A_i is proportional to the number of oscillators per unit volume. We are concerned with electronic absorption principally, and in the case of a glass the λ_i will most probably consist of an average value of a distribution of individual λ_i for each type of oscillator. Irrespective of the specific nature of the λ_i, on differentiation of eq (2), the following equation may be obtained:

$$\frac{dn}{n}=\frac{1}{2n^2}\left[\sum_i\left(\frac{A_i\lambda^2}{\lambda^2-\lambda_i^2}\frac{dA_i}{A_i}+\frac{2A_i\lambda^2\lambda_i d\lambda_i}{(\lambda_2-\lambda_i^2)^2}\right)\right]. \tag{3}$$

Prorided $dA_i/A_i=-dV/V$, and in view of eq (2) eo (3) becomes

$$\frac{dn}{n}=\frac{1}{2n^2}\left[(1-n^2)dV/V+\sum_i\frac{2A_i\lambda^2}{(\lambda^2-\lambda_i^2)^2}\lambda_i d\lambda_i\right]. \tag{4}$$

The first term in brackets reflects the change arising from dimensional changes alone, whereas the second reflects that caused by shift in the λ_i. For glasses of index approximately 1.5, the numerical coefficients of dV/V reduce to 0.28, which is approximately the reciprocal of the numerical coefficient of eq (1). If $\lambda_i d\lambda_i/\lambda^2-\lambda_i^2\ll1$, the second term can be neglected, and eq (1) results from substituting $-d\rho/\rho$ for dV/V and rearranging. If the present values of dl/l and dn/n obtained on relaxation are substituted in eq (4), it is not satisfied unless the absorption-shift term is retained. For these experiments it appears that the absorption-shift term and the volume-change term contribute about equally to the change in index. Conversely, it seems that on annealing, the change in index is almost fully accounted for by volumetric changes.

It is also of interest to note that increasing the density by lowering the temperature generally results in a decrease in index, indicating that the second term of eq (4) predominates [20].

4. References

[1] P. W. Bridgman, Proc. Am. Acad. Arts Sci. **81,** 165 (1952)
[2] P. W. Bridgman add I. Simon, J. Appl. Phys **24,** 405 (1953).
[3] P. W. Bridgman, J. Appl. Phys. **24,** 560 (1953).

[4] C. E. Weir and L. Shartsis, J. Am. Ceram. Soc. **38,** 299 (1955).
[5] O. L. Anderson, J. Appl. Phys. **27,** 943 (1956).
[6] P. W. Bridgman, Proc. Am. Acad. Arts Sci. **84,** 111 (1955)
[7] A. Q. Tool, L. W. Tilton, and J. B. Saunders, J. Research NBS **38,** 519 (1947) RP1793.
[8] N. J. Kreidl and R. A. Weidel, J. Am. Ceram. Soc. **35,** 198 (1952).
[9] H. N. Ritland, J. Am. Ceram. Soc. **38** 86 (1955).
[10] S. Spinner and A. Napolitano, J. Am. Ceram. **39,** 390 (1956).
[11] F. A. Jenkins and H. E. White, Fundamentals of optics, 2d ed. (McGraw-Hill Book Co., Inc., New York, N. Y., 1950).
[12] F. Seitz, The modern theory of solids (McGraw-Hill Book Co., Inc., New York, N. Y., 1940).
[13] H. R. Lillie and H. N. Ritland, J. Am. Ceram. Soc. **37,** 466 (1954).
[14] W. S. Rodney and R. J. Spindler, J. Research NBS **53,** 185 (1954) RP2531; J. Opt. Soc. **44,** 677 (1954).
[15] C. E. Weir, J. Research NBS **45,** 468 (1950) RP2160.
[16] L. W. Tilton, BS J. Research **2,** 909 (1929) RP64.
[17] R. J. Spindler and W. S. Rodney, J. Research NBS **43** 253 (1949) RP2361.
[18] J. B. Saunders, J. Research NBS **28,** 51 (1942) RP1445
[19] C. G. Peters and C. H. Cragoe, BS Sci. Pap. **16,** 449 (1920).
[20] G. W. Morey, The properties of glass, 2d ed., p. 43 (Reinhold Publishing Corp., New York, N. Y., 1954)
[21] W. Robertson, S. Babb, and F. Matsen, J. Chem. Phys **26,** 367 (1957).
[22] H. P. Lipson, E. Burnstein, and P. Smith, Phys. Rev. **99,** 444 (1955).
[23] J. J. Markham, R. T. Beyer, and R. B. Lindsay, Rev. Mod. Phys. **23,** 353 (1951).
[24] E. G. Richardson, Rev. Mod. Phys. **27,** 15 (1955).
[25] S. Kavim and L. Rosenhead, Rev. Mod. Phys. **24,** 108 (1952).

WASHINGTON, November 2, 1956.

Journal of Research of the National Bureau of Standards Vol. 58, No. 4, April 1957 Research Paper 2752

Reference Wavelengths for Calibrating Prism Spectrometers

Earle K. Plyler, L. R. Blaine, and Matthew Nowak

Standard wavelengths for calibrating infrared-prism instruments have been measured from the absorption bands of polystyrene, 1,2,4-trichlorobenzene, and toluene. Several bands of didymium glass have been calibrated for the near-infrared region, and 27 rotational lines of the 3.3-micron band of methane have been measured.

The wavelengths fall in the region from 0.6 to 24 microns, but the greatest number are in the 3- to 6-micron region. A few bands of several other materials are also given in the wavelength tables, and 11 figures of the spectra marked with the calibrating values are included for identification.

1. Introduction

Two reports [1][1] have been issued by the Bureau on calibrating wavelengths for prism spectrometers. The present report incorporates the data of the earlier reports and gives the results of recent calibrations that have been made. Other papers have been published by several laboratories [2] and their results are of value for additional calibration points. All of the standard wavelengths that have been supplied are not sufficient for calibrations needed for the range of the infrared region from 0.8 to 150μ or for the wide variety of instruments used in this region, especially with the differences in resolution obtained with different prism materials. For example, the CO and CO_2 absorption bands between 4 and 5μ, are well suited for calibration but cannot be resolved into their rotational structure by a rock-salt prism. The requirements for the calibration of a spectrometer using a rock-salt prism are much different from those of an instrument using prisms of lithium fluoride and of calcium fluoride. When the thermocouple of an instrument is replaced by a PbS detector, more bands that contain the rotational structure of gases can be used for calibration. Still higher resolution can be obtained by replacing the prism in the spectrometer with a grating. This usually allows the use of many bands for calibration, and if too high a precision is not required, many bands that have been measured on large grating instruments can be used.

This report does not include methods of calibration of high-resolution grating spectrometers. The use of the fringe system of a Fabry-Perot interferometer for accurate measurement of line positions observed with grating spectrometers has been previously described [3].

The calibration points listed in the present paper are primarily suited for low-resolution instruments.

2. Method of Measurement

A large grating spectrometer can easily measure sharp spectral lines with an error not greater than 1 part in 100,000. This accuracy can be obtained by using standard lines of neon, argon, krypton, or xenon, in higher orders that overlap the band being measured. The standard spectral lines or the fringe system of a Fabry-Perot interferometer are recorded simultaneously with the absorption band being studied. The grating spectrometer and the method of calibration are described in reference [3].

The measurement of the absorption bands of liquids and solids under high resolution often reveals side bands or complex structure. The way in which the components add up to produce a seemingly sharp band on a prism instrument must be approximated by the intensity and the positions of the various components. Any band in the range 1 to 10 μ that is found to have an uncertainty of more than ± 0.003 μ is not listed as a wavelength for calibration.

Another approach in the calibration of bands is to open the slit of the grating spectrometer so that resolution equal to that of a prism spectrometer is obtained. This method reduces the high precision of measurement with the grating spectrometer, but with the wide range of resolution of different spectrometers, the band shapes could not be matched for all instruments. In order to avoid the difficulties of the low-resolution method, all the bands reported in this work have been calibrated with high-resolution spectrometers.

In the measurement of *Q*-branches of bands, considerable fine structure is observed. The *Q*-branch of the NH_3 band at 2.999 μ is shown in figure 1. There are 30 or more separate lines and the band extends from 2.996 to 3.002 μ; the center on low resolution is estimated to be 2.9990 ± 0.0005 μ. All of the bands measured on the grating instrument appear to be broad, and the estimate of the center for low resolution accounts for the uncertainty given with the results listed in the tables.

2.1. Region From 0.6 to 2.6 Microns

Although the intense infrared bands of molecules are observed at wavelengths greater than 2 μ, it is sometimes necessary to measure the transmission of filters and the absorption of combination bands in the near-infrared region. The atomic spectral lines are well suited for calibration in this region. The

[1] Figures in brackets indicate the literature references at the end of this paper.

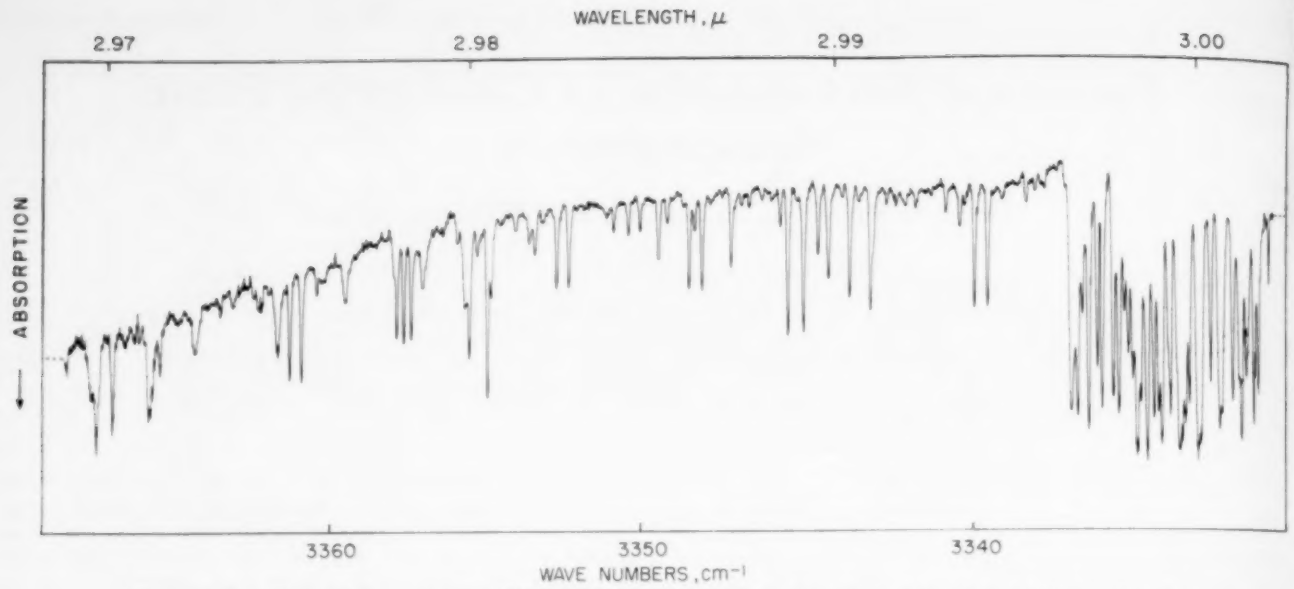

FIGURE 1. *Absorption spectrum of* NH_3 *in the Q-branch of the 2.999-micron band with high resolution.*

The spectrum was observed with a meter cell at 5 mm (Hg) pressure.

spectra of mercury, neon, argon, krypton, and xenon are rich in near-infrared lines, some of which have been measured and listed in another publication [3].

The atomic spectral lines are observed in emission, but it is usually easier to use calibrating wavelengths in absorption on most infrared spectrometers.

Several bands of polystyrene, 1,2,4-trichlorobenzene, didymium glass, and carbon disulfide have been measured from 0.6 to 2.6 μ, and the wavelengths are listed in table 1. In addition to wavelengths, the wave numbers in vacuum, the state, the thickness, and the material are tabulated. For spectrometers that are able to resolve the rotational structure of the CO band at 2.34 μ, there are provided about 50 lines from 2.3 to 2.5 μ that are known to a high accuracy [4]. Table 1 is essentially the same as that given previously [1].

The observed spectrum of didymium glass, 1,2,4-trichlorobenzene, and polystyrene with low resolution are shown in figures 2, 3, and 4.

TABLE 1. *Calibration wavelengths for prism instruments from 0.6 to 2.6 μ*

Wavelength μ (air)	Wave number (vacuum)	State	Thickness	Substance
	cm^{-1}		*mm*	
0.684 ±0.001	14616	Solid	6	Didymium glass.
.740 ±.001	13510	do	6	Do.
[a].743 ±.002	13455	do	6	Do.
.748 ±.001	13365	do	6	Do.
.808 ±.001	12373	do	6	Do.
.880 ±.001	11361	do	6	Do.
1.067 ±.002	9369	do	6	Do.
1.220 ±.002	8195	do	6	Do.
1.517 ±.003	6590	do	6	Do.
1.681 ±.002	5947	Film	0.6	Polystyrene.
1.918 ±.003	5212	Solid	6	Didymium glass.
2.144 ±.001	4663	Film	0.6	Polystyrene.
[b]2.170 ±.002	4607	do	.6	Do.
2.187 ±.001	4571	do	.6	Do.
2.222 ±.002	4499	Liquid	5	Carbon disulfide.
1.6606 ±.0002	6020.3	do	0.5	1,2,4-Trichlorobenzene.
2.1526 ±.0002	4644.3	do	.5	Do.
2.3126 ±.0002	4322.9	do	.5	Do.
2.4030 ±.0002	4160.3	do	.5	Do.
2.4374 ±.0002	4101.6	do	.5	Do.
2.494 ±.002	4009	do	.5	Do.
2.543 ±.002	3931	do	.5	Do.

[a] Average value of the maxima for 0.740 and 0.748 μ.
[b] Principal band observed with prism spectrometer.

2.2. Region From 2.6 to 22 Microns

The region from 2.6 to 15 μ is employed for analysis of many compounds. As there are many automatic instruments in use that give the wavelength readings directly, it is important to have a

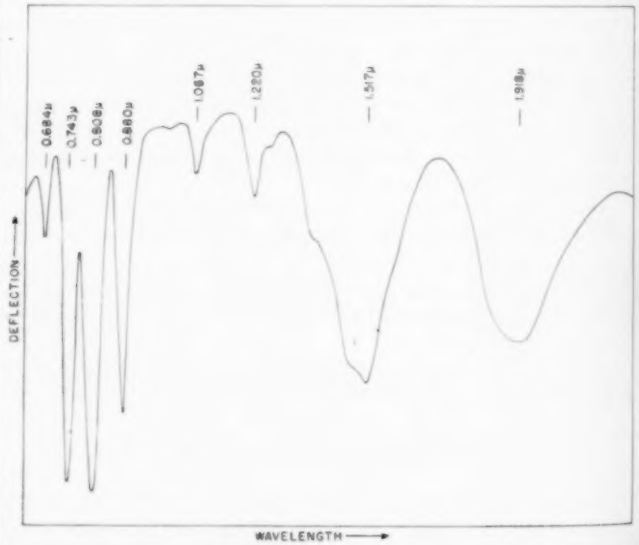

FIGURE 2. *Absorption spectrum of didymium glass, 6 millimeters thick, in the region from 0.6 to 2 microns.*

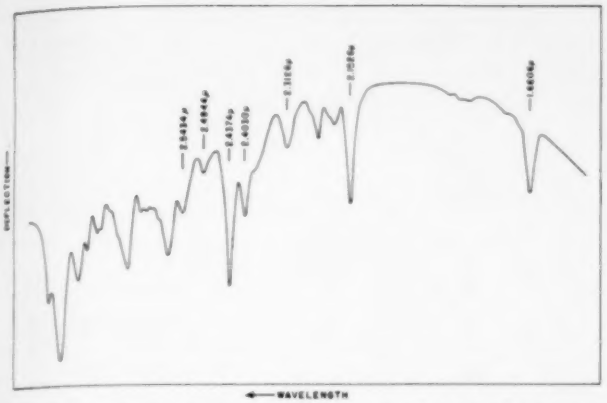

FIGURE 3. *Near-infrared spectrum of 1,2,4-trichlorobenzene for a cell thickness of 0.5 millimeter.*

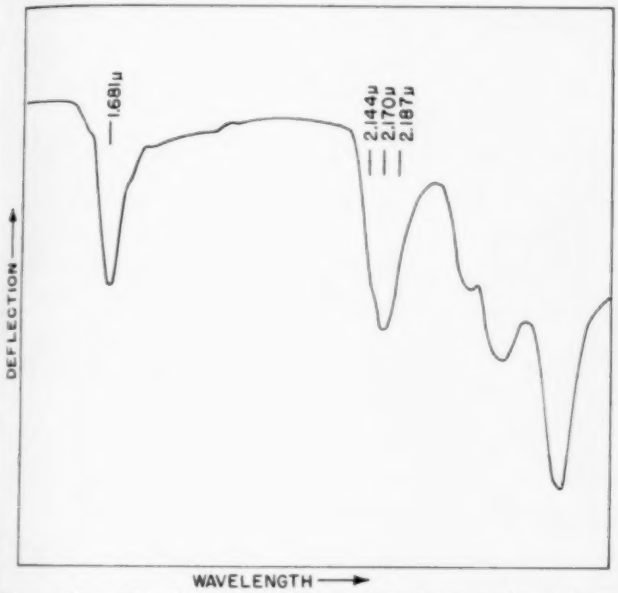

FIGURE 4. *Near-infrared spectrum of polystyrene for a thickness of 0.6 millimeter.*

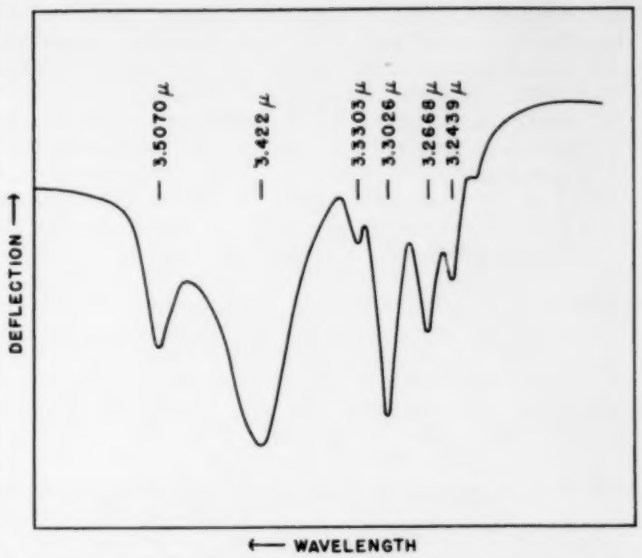

FIGURE 5. *Infrared absorption bands of polystyrene in the region of 3.4 microns for a film about 25 microns thick, as observed with a lithium fluoride prism.*

few substances that can be used to check the calibration of the instrument. A number of absorption bands have been measured for this region. The largest number of bands have been selected from the spectrum of polystyrene, toluene, and 1,2,4-trichlorobenzene.

Polystyrene films are easily made, and the spectrum is suitable for a check of the instrument. Several of the bands have been remeasured, and the wavelengths check closely with the previous values [1], and an estimate of the accuracy of the wavelengths has been given.

Figure 5 shows the bands in the 3.4-μ region of polystyrene as measured with a LiF prism.

Figure 6 is a record of the spectrum from 2 to 15 μ, measured with a rock-salt prism. When the

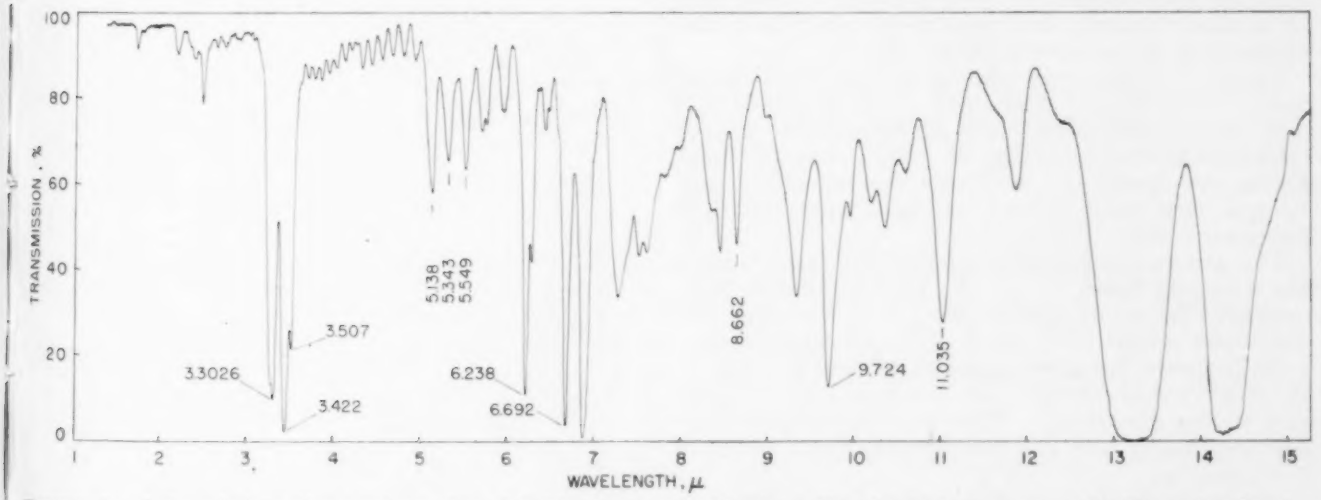

FIGURE 6. *Infrared absorption spectrum, from 2 to 15 microns, of a 50-micron film of polystyrene measured with a rock-salt prism instrument.*

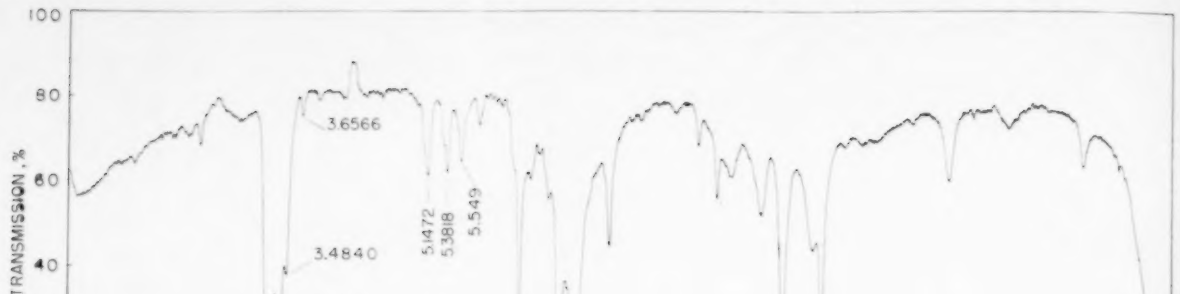

FIGURE 7. *Infrared spectrum of toluene from 2 to 15 microns, as observed with a rock-salt prism.*

Cell thickness was 0.05 mm.

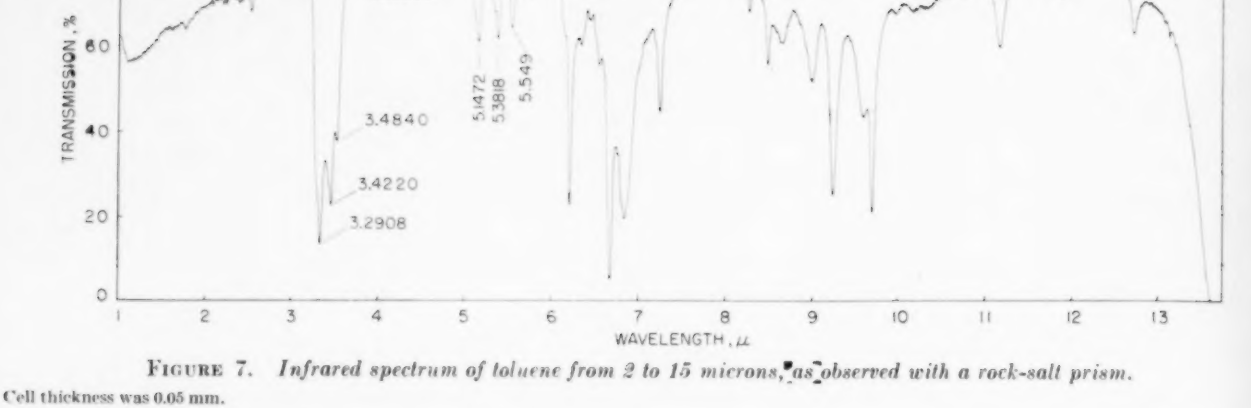

FIGURE 8. *Spectrum of 1,2,4-trichlorobenzene from 2 to 15 microns, as observed with a rock-salt prism.*

Cell was 0.025 mm, and the insert spectrum from 3.5 to 5 μ was measured with a cell of 0.2 mm.

surfaces of the film are parallel a number of interference fringes appear in the spectrum. The fringes are of low intensity and usually do not change the wavelength of the absorption bands.

Figure 7 represents the spectrum of toluene. Some of the bands that have been measured fall close to the calibrated bands of polystyrene and of 1,2,4-trichlorobenzene (fig. 8). Any one of these substances would be sufficient for checking any changes that may occur in a spectrometer with a wavelength scale.

The absorption spectrum of Corning fused quartz has a strong band at 2.7 μ. This band has been measured for a calibration point in this region, and the center occurs at 2.735 μ. The absorption spectrum is shown for a thickness of 0.7 mm in figure 9. With a thinner sample the band is not as broad and is less absorbing. This band is produced by occluded water and it is not present in all types of fused quartz.

Other materials with absorption bands, listed in table 2, are carbon dioxide, carbon disulfide, methyl-

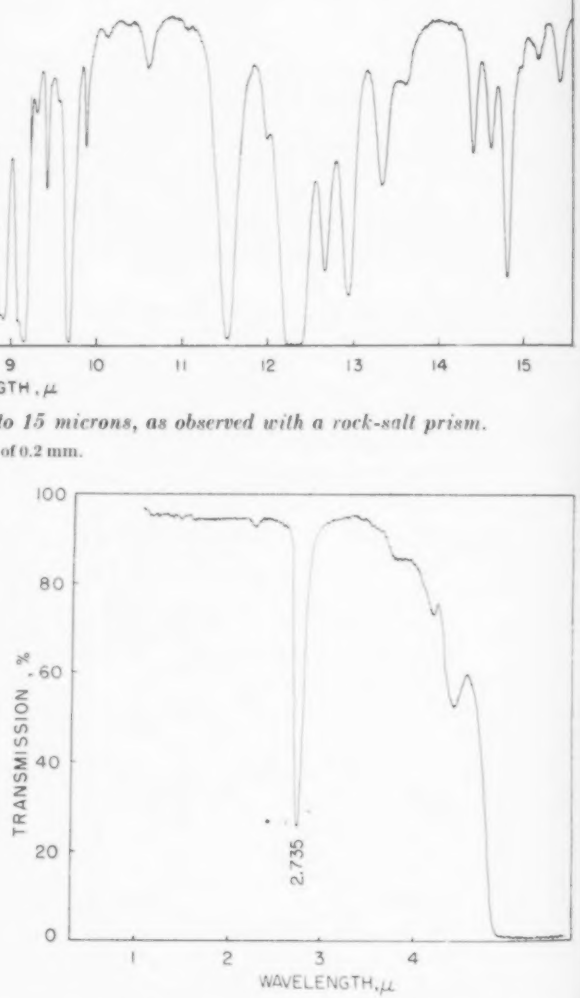

FIGURE 9. *Band at 2.735 microns in Corning fused silica f 0.7-millimeter thickness.*

TABLE 2. *Calibrating wavelengths from 3 to 24 μ*

Wavelength (air)	Wave number (vacuum)	State	Description	Substance
μ	cm^{-1}			
2.735 ±0.0002	3655.3	Solid	0.7 mm thick	Quartz.
2.9990 ±.0005	3333.5	Gas	1-m cell, 5 mm (Hg).	NH_3.
3.3101	3020.2	do	5.0-cm cell, 10 cm (Hg).	Methane.
3.2204	3104.4	Solid	25-μ film	Polystyrene.
3.2439 ±.0002	3081.9	do	do	Do.
3.2668 ±.0002	3060.3	do	do	Do.
3.3026 ±.0001	3027.1	do	do	Do.
3.3303 ±.0001	3001.9	do	do	Do.
3.422 ±.001	2921.5	do	do	Do.
3.5070 ±.0005	2850.7	do	do	Do.
5.138 ±.005	1945.8	do	50-μ film	Do.
5.343 ±.003	1871.1	do	do	Do.
5.549 ±.002	1801.6	do	do	Do.
6.238	1602.7	do	do	Do.
6.692	1493.9	do	do	Do.
8.662	1154.2	do	do	Do.
9.724	1028.1	do	do	Do.
11.035	906.0	do	do	Do.
3.2393 ±.0006	3086.2	Liquid	0.05-mm cell	Toluene.
3.2908 ±.0003	3038.0	do	do	Do.
3.4220 ±.0009	2921.5	do	do	Do.
3.4840 ±.0004	2869.5	do	do	Do.
3.6566 ±.0002	2734.0	do	do	Do.
5.1472 ±.0007	1942.3	do	do	Do.
5.3818 ±.0006	1857.6	do	do	Do.
5.549 ±.002	1801.6	do	do	Do.
21.52	464.6	do	do	Do.
3.2434 ±.0003	3082.4	do	0.025-mm cell	1,2,4-Trichlorobenzene.
3.5564 ±.0002	2811.1	do	do	Do.
3.7067 ±.0002	2697.1	do	do	Do.
5.3034 ±.0025	1885.1	do	do	Do.
17.40	574.6	do	do	Do.
18.16	550.5	do	do	Do.
21.80	458.6	do	do	Do.
22.76	439.3	do	do	Do.
20.56	486.3	do	0.05-mm cell(sat. soln. in CS_2).	1,2,3-Trichlorobenzene.
2.7144	3683.0	Vapor	5.0-cm cell	Methanol.
4.866	2054.5	do	do	Do.
9.672	1033.6	do	do	Do.
4.258	2347.9	Gas	Atmospheric	Carbon dioxide.
13.883	720.1	do	do	Do.
14.98	667.4	do	do	Do.
7.268	1375.5	Liquid	0.05-mm cell	Methylcyclohexane.
11.475	871.2	do	do	Do.
11.862	842.8	do	do	Do.
23.85	419.2	Vapor	Atmospheric	Water.

cyclohexane, and methanol. The wavelengths of the bands of methanol have not been remeasured but are taken from the work of Borden and Barker [5].

The spectrum of 1,2,4-trichlorobenzene has been measured in the region from 14 to 24 μ, figure 10. The absorption bands at 17.40, 18.16, and 21.80 μ were measured on a grating spectrometer. The broad band at 22.76 μ was measured on a prism spectrometer and is probably accurate to ±0.02 μ.

The absorption spectra of many gases have been measured and would be useful for calibration. If the prism spectrometer cannot resolve the spectra into the rotational lines, they should not be used. The atmospheric-water-vapor lines in the vibrational rotational band are not properly resolved with prism instruments, but the pure rotation spectrum from 20 to 150 μ is well suited for calibration. These lines have been measured by Randall, Dennison, Ginsburg, and Weber [6], and their article lists the observed wavelengths.

The spectrum of methane at 3.3 μ contains many rotational lines of the *P*- and *R*-branches, which are spaced at intervals of about 10 cm^{-1}. This band was recently measured with high resolution, and many of the lines were found to have several components. The spectrum was then recorded with a resolution of 0.3 cm^{-1}, and the center of the components of a line was estimated by comparing the results with the high-resolution measurements. A photograph of the low-resolution trace is shown in figure 11, and the positions of lines are given in table 3. Where partial resolution is obtained in some lines of the *P*-branch, the wavelength and wave number are listed as applying to the strongest component.

The absorption lines observed between the methane lines are part of the $2\nu_2$ band of atmospheric water vapor. The values of the wave numbers of the lines reported in this table are probably accurate to ±0.05 cm^{-1}, but a more precise table of wave numbers, including all the components of the lines, will be listed in another paper.

Hydrogen chloride and hydrogen bromide also have many rotational lines in their spectra that fall

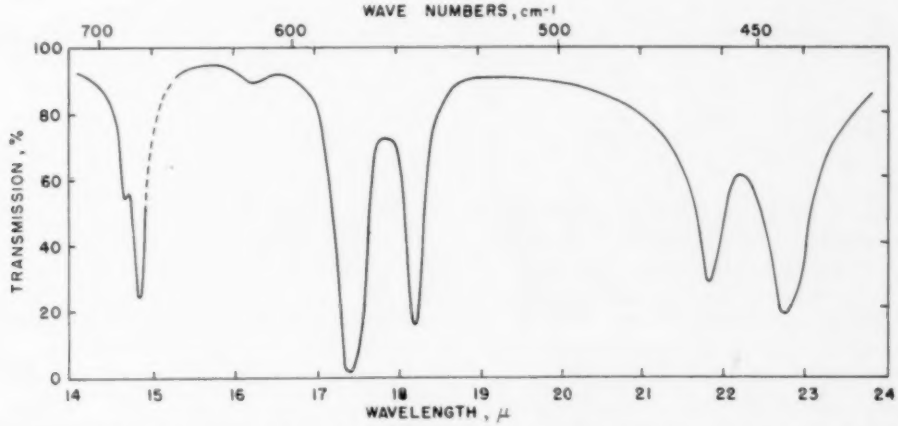

FIGURE 10. *Spectrum of 1,2,4-trichlorobenzene from 14 to 24 microns, as observed with a* KBr *prism.*

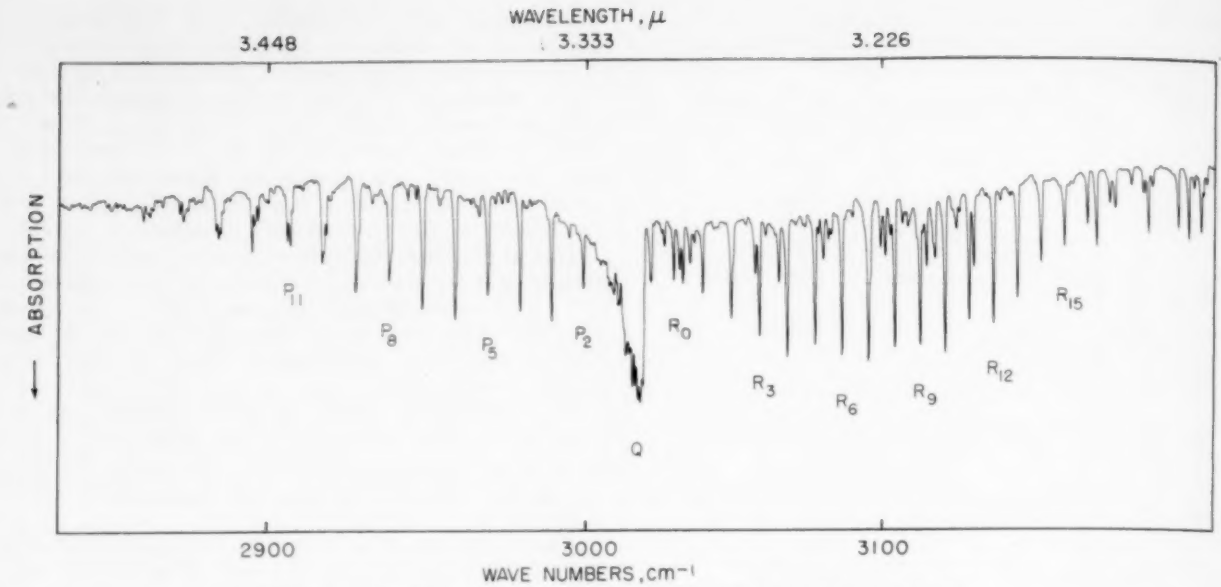

FIGURE 11. *The 3.3-micron band of methane with medium resolution.*

Cell length, 5 cm; pressure, 10 cm (Hg).

TABLE 3. *Rotational lines of methane in the 3.3-μ band*

Line	Wavelength (air)	Wave number (vacuum)
	μ	cm^{-1}
P_{12}	3.45309	2895.18
P_{11}	3.43937	2906.72
P_{10}	3.42801	2916.36
P_9	3.41571	2926.86
P_8	3.40352	2937.34
P_7	3.39131	2947.92
P_6	3.37952	2958.20
P_5	3.36760	2968.67
P_4	3.35592	2979.00
P_3	3.34552	2988.27
P_2	3.33343	2999.10
R_0	3.30070	3028.84
R_1	3.29012	3038.58
R_2	3.27969	3048.25
R_3	3.26945	3057.79
R_4	3.25932	3067.30
R_5	3.24932	3076.74
R_6	3.23955	3086.02
R_7	3.22992	3095.22
R_8	3.22041	3104.36
R_9	3.21103	3113.42
R_{10}	3.20174	3122.46
R_{11}	3.19261	3131.39
R_{12}	3.18365	3140.20
R_{13}	3.17480	3148.95
R_{14}	3.16610	3157.61
R_{15}	3.15751	3166.20

in the region from 3 to 5 μ. These gases have recently been measured by Thompson and his co-workers [7] on a grating spectrometer, and the positions of the lines are listed in his papers.

The absorption bands listed in tables 1 and 2 are selected for the calibration of spectrometers of low or medium resolution. The calibration of high-resolution instruments would require atomic-spectral lines or the rotational lines of the bands of gases.

Additional calibrating wavelengths can be obtained by using the bands of methane and ammonia, which almost completely cover the range from 6 to 12 μ. The wavelengths for these lines have not been listed because no high-precision measurements of these spectra are available, but the current measurements in the literature are sufficiently accurate for the calibration of prism spectrometers.

3. References

[1] Earle K. Plyler and C. Wilber Peters, J. Research NBS **45,** 462 (1950) RP2159. Nicolo Acquista and Earle K. Plyler, J. Research NBS **49,** 13 (1952) RP2338.

[2] R. A. Oetjen, Chao-Lou Kao, add H. M. Randall, Rev. Sci. Instr. **13,** 515 (1942). A. R. Downie, M. C. Magoon, Thomas Purcell, and Bryce Crawford, Jr., J. Opt. Soc. Am. **43,** 941 (1953). L. H. Jones, J. Chem. Phys. **24,** 1250 (1956).

[3] Earle K. Plyler, L. R. Blaine, and Eugene D. Tidwell, J. Research NBS **55,** 279 (1955) RP2630.

[4] Earle K. Plyler, W. S. Benedict, and Shirleigh Silverman, J. Chem. Phys. **20,** 175 (1952).

[5] Avis Borden and E. F. Barker, J. Chem. Phys. **6,** 553 (1938).

[6] H. M. Randall, D. M. Dennison, N. Ginsburg, and L. R. Weber, Phys. Rev. **52,** 160 (1937).

[7] H. W. Thompson, R. L. Williams, and H. J. Callomon, Spectrochim Acta **5,** 313 (1952). I. M. Mills, H. W. Thompson, and R. L. Williams, Proc. Roy. Soc. [A] **218,** 29 (1953).

WASHINGTON, November 15, 1956.

Journal of Research of the National Bureau of Standards Vol. 58, No. 4, April 1957 Research Paper 2753

Tensile Properties of Copper, Nickel, and 70-Percent-Copper–30-Percent-Nickel and 30-Percent-Copper–70-Percent-Nickel Alloys at High Temperatures

William D. Jenkins, Thomas G. Digges, and Carl R. Johnson

Short-time tensile tests were made at temperatures ranging from 75° to 1,700° F on high-purity nickel, copper, a 70-percent-nickel–30-percent-copper alloy, and a 70-percent-copper–30-percent-nickel alloy. The high-purity component metals and the two alloys were investigated in the initial conditions, as annealed for a uniform grain size, and as cold-drawn 40-percent reduction in area. The results were affected markedly by variations in the nickel content, temperature, and degree of cold-working. However, the effects of cold-drawing at room temperature were obliterated at temperatures above that of recrystallization.

The effects of cold-drawing the 30%-Ni–70%-Cu alloy different amounts and of variations in grain size of the copper on the tensile properties are evaluated. Results on the tensile properties of the same annealed materials at low temperatures are included for completeness.

1. Introduction

During the past several years, an investigation has been in progress in the Metallurgy Division, National Bureau of Standards, to evaluate the rheological behavior at subzero and elevated temperatures of high-purity nickel, copper, and certain alloys of these two elements. Some of the results obtained in this study have been presented in previous publications [1 to 7].[1] The present paper is concerned with the influence of temperature on the short-time tensile properties of the nickel, copper, and 70%-Ni–30%-Cu and 30%-Ni–70%-Cu alloys.

Tensile tests were made at temperatures ranging from 70° to 1,500° or 1,700° F on each of the four materials (table 1) in the conditions as annealed and as cold-drawn 40% reduction in area. In addition, the present program was extended to include tensile tests at various temperatures on the 30%-Ni–70%-Cu alloy as cold-drawn 25- and 70-percent reduction in area, and on the copper after annealing to produce a relatively large grain size.

TABLE 1. *Chemical composition (percentage by weight) of the metals and alloys used as determined by chemical, spectrochemical, and vacuum fusion analyses*

Metal	C	Cu	Ni	Co	Fe	Mn	Si	S	Zn	O_2	N_2	H_2	Average [c] grain diameter
													mm
Copper [a] (OFHC)	.....	99.99+	.....	.....	.....	.....	.....	.....	.....	.....	.....	.....	0.025
30%-Ni–70%-Cu	0.023	68.84	29.89	0.04	0.50	0.65	0.003	0.004	0.09	0.001	0.001	0.0002	.040
70%-Ni–30%-Cu	.017	29.71	70.08	[b]	.01	.01	.12	.002	.....	.001	.0015	.0003	.025
Nickel	.007	0.009	99.85	[b]	.04	.03	.11	.002	.....	.002	.001	.0002	.045

[a] The arc spectrum of the copper was examined for the sensitive lines of Ag, Al, B, Be, Co, Fe, In, Ir, Mg, Mo, Na, Ni, Pb, Sb, Si, Sn, Ti, V, and Zn. The lines for Ag, Al, Mg, and Si were identified and there was some indication of the presence of Fe, Ni, and Pb.
[b] Not detected.
[c] Values obtained on specimens prepared from the annealed bars.

2. Materials and Procedures

The chemical compositions of the four materials used are given in table 1. All the bars of each material were processed from a single heat and they were supplied in the form of ⅞- or $^{13}/_{16}$-in. rounds in the conditions as annealed or as cold-drawn. The annealing treatments produced the average grain sizes listed in table 1, and these annealing treatments were also used just prior to the final cold-drawing operations.

Tensile specimens, 0.505 in. in diameter and with a 2.0-in. reduced section, were machined from one bar of each material as initially annealed and from another bar as cold-drawn. Each specimen tested at 300° F, or higher, was heated in air in an automatically controlled electric furnace and held at the reported temperature for approximately 1 hour before testing. The specimen was maintained within ±3 deg F of the reported temperature during testing. The deformation was determined by following the change in minimum diameter of the specimen during testing in tension at room temperature, and by measuring the movement of the head of the hydraulic-type machine with a Templin stress-strain

[1] Figures in brackets indicate the literature references at the end of this paper.

TABLE 2. *Results of tensile tests on high-purity nickel*

Initial condition	Temperature [a]	Yield strength (0.2% offset)	Maximum load					True stress at complete fracture	Elongation in 2 in.	Reduction of area	True strain at complete fracture
			Tensile strength	True stress	Strain in 2 in.	Reduction in area [b]	True strain				
	° *F*	*lb/in* ²	*lb/in* ²	*lb/in* ²	%	%		*lb/in* ²	%	%	
Annealed	−320	17,000	82,000	127,500	55.5	35.5	0.44	244,700	72	78.5	1.543
Do	−220	16,700	69,000	104,400	51.5	34	.41	235,500	63.5	82.5	1.737
Do	−108	15,000	60,600	89,300	47.5	32	.39	215,100	60.5	83.5	1.813
Do	−22	15,000	56,200	81,900	46	31.5	.38	250,700	59	87	2.073
Do	75	11,100	51,800	74,200	43	31	.37	222,900	----------	87	2.034
Do	75	12,500	52,700	76,700	45	31	.39	278,600	56	89	2.27
Do	88	12,500	51,600	72,300	41	29	.34	222,800	56	87	2.076
Do	212	12,000	48,300	68,500	42	30	.36	224,200	57	88	2.11
Do	212	12,500	48,400	69,200	43	31	.37	210,600	57	87	2.054
Do	300	12,900	46,400	63,600	37	27	.32	194,100	52	87	2.053
Do	500	11,300	43,300	58,900	36	26	.31	208,500	51	89	2.263
Do	600	9,900	41,300	55,800	35	26	.30	243,200	53	90	2.515
Do	700	9,400	36,200	46,700	29	23	.26	215,200	56	90	2.555
Do	800	8,900	31,900	42,100	32	24	.28	189,100	62	91	2.586
Do	900	8,700	28,200	37,500	33	25	.29	216,500	68	91	2.991
Do	1,000	8,000	23,200	30,400	31	24	.27	200,500	77	96	3.307
Do	1,200	5,600	15,400	19,400	26	21	.23	40,600	61	99.7	5.787
Do	1,500	3,750	5,250	5,800	11	10	.10	-------	78	99.99+	9.269
Cold-drawn 40% reduction in area	75	80,100	81,600	82,200	1	1	.01	242,900	19	81.5	1.685
Do	300	75,100	76,100	76,900	1	1	.01	229,100	17	80.5	1.702
Do	500	65,600	69,800	70,500	1	1	.01	207,500	18	82	1.716
Do	700	58,000	60,800	61,400	1	1	.01	175,200	17	83.5	1.798
Do	800	53,400	56,800	57,400	1	1	.01	174,800	19	85	1.878
Do	900	44,900	47,700	48,700	2	1.96	.02	168,600	21.5	88	2.133
Do	1,000	39,400	42,000	43,300	3	2.5	.03	150,100	21	91	2.375
Do	1,200	6,000	16,700	22,000	31.5	24	.274	24,700	56	99.5	5.291
Do	1,500	2,700	7,450	8,600	15	13	.140	-------	67	99.99+	>10
Do	1,700	1,400	4,450	4,900	11	10	.104	-------	92	99.99+	>10

[a] Values at subzero temperatures obtained from data of Geil and Carwile [7]. [b] Reduction in area $(\%) = 100[(A_0 - A)/A_0] = 100[(L - L_0)/L_0]$.

TABLE 3. *Results of tensile tests on high-purity* 70%-Ni–30%-Cu *alloy*

Initial condition	Temperature [a]	Yield strength (0.2% offset)	Maximum Load					True stress at complete fracture	Elongation in 2 in.	Reduction of area	True strain at complete fracture
			Tensile strength	True stress	Strain in 2 in.	Reduction in area [b]	True strain				
	° *F*	*lb/in* ²	*lb/in* ²	*lb/in* ²	%	%		*lb/in* ²	%	%	
Annealed	−320	38,000	101,900	159,900	57	36.5	0.450	282,300	63.5	78	1.509
Do	−220	34,600	88,400	130,800	48	32.5	.392	244,800	56	79	1.561
Do	−108	32,100	79,600	114,700	45.5	31	.365	235,300	56	81	1.671
Do	−22	30,200	73,100	104,300	43	30	.356	261,200	52.5	84.5	1.875
Do	75	26,500	67,350	94,550	40.4	28.8	.339	304,900	59.1	88.4	2.150
Do	212	25,250	63,050	85,200	35.1	26	.301	321,500	51	89.3	2.235
Do	300	24,050	61,850	85,300	37.9	27.5	.321	277,900	52	88	2.113
Do	500	23,600	60,800	83,500	37.3	27.2	.317	247,400	48.3	85.5	1.929
Do	600	21,600	61,850	84,300	36.3	26.6	.309	221,500	51	85	1.894
Do	700	23,400	59,950	81,250	35.5	26.2	.304	227,800	49.2	84.1	1.840
Do	800	22,150	55,300	73,650	33.1	24.9	.286	190,300	45.2	81.7	1.698
Do	900	19,950	50,050	65,800	31.4	23.9	.273	153,500	46.8	78.7	1.546
Do	1,000	17,500	42,050	53,400	27	21.3	.239	98,300	47	71.6	1.257
Do	1,100	16,700	31,400	38,450	22.5	17.9	.203	53,100	42	66.5	1.098
Do	1,200	13,500	24,300	27,550	13.3	11.7	.125	26,800	37.5	58.1	0.869
Do	1,350	9,700	15,800	17,700	12.1	10.8	.114	19,200	35	49.4	.681
Do	1,500	5,750	10,300	11,250	9.2	8.4	.087	9,800	47	49	.671
Do	1,700	4,500	5,850	6,600	13.4	11.8	.127	6,400	47.5	45	.598
Cold-drawn 40% reduction in area	75	97,600	100,800	102,000	1	1	.01	290,200	17	81.4	1.680
Do	300	93,400	94,600	95,600	1	1	.01	258,700	15.5	80.2	1.620
Do	500	90,800	92,900	94,000	1	1	.01	228,400	16	76.8	1.463
Do	700	83,200	86,300	87,200	1.5	1.4	.015	185,100	15	71.3	1.248
Do	800	73,900	77,600	79,900	3	2.9	.03	199,900	19	76.2	1.438
Do	900	65,300	70,600	72,700	3	2.9	.03	142,600	18	68.8	1.165
Do	1,000	51,800	58,200	60,500	4	3.9	.039	82,700	26	62.9	0.992
Do	1,200	18,900	31,600	34,600	9.5	8.6	.09	72,200	26	71.6	1.257
Do	1,500	7,750	12,450	14,100	13.5	12	.127	14,500	34	43.4	0.568
Do	1,700	4,700	6,750	6,850	1	1	.01	7,600	35	35.8	.442

[a] Values at subzero temperatures obtained from data of Geil and Carwile [7]. [b] Reduction in area $(\%) = 100[(A_0 - A)/A_0] = 100[(L - L_0)/L_0]$.

recorder for the specimens tested at elevated temperatures. The rate of strain was approximately 1 percent per minute.

3. Results and Discussion

The experimental results of the tension tests made at various temperatures are summarized in tables 2 to 5. Some of the data previously obtained on the annealed materials at low temperature [7] are also included in these tables for completeness; these results were obtained on specimens prepared from different bars than those used in the present tests. The results obtained at low temperatures were presented graphically and discussed in some detail in relation to other properties in the previous publication.

3.1. True-Stress–True-Strain Relations at Room Temperature

The true-stress–true-strain curves for the annealed materials tested at room temperature are curvilinear (fig. 1A), and their slopes decrease as the true strain increases up to the beginning of fracture. The resistance to flow of the copper was considerably less than that of the other materials; the resistance of the 70%-Ni–30%-Cu alloy was appreciably greater than that of the nickel or the 30%-Ni–70%-Cu alloy. The flow curves for the nickel and the 30%-Ni–70%-Cu alloy cross at a true strain within the range of 0.4 to 0.6. Thus, the difference in curvature of the flow curves of these two materials indicate that the rate of strain hardening in the higher range of true strains is somewhat greater for the nickel than for

TABLE 4. *Results of tensile tests on* 30%–Ni–70%–Cu *alloy*

Initial condition	Temperature [a]	Yield strength (0.2% offset)	Drop of beam			Maximum load					True stress at complete fracture	Elongation in 2 in.	Reduction of area	True strain at complete fracture
			Stress at first drop of beam	Maximum drop		Tensile strength	True stress	Strain in 2 in.	Reduction in area [b]	True strain				
				Stress at occurrence	Amount of drop									
	°F.	lb/in.²	lb/in.²	lb/in.²	lb/in.²	lb/in.²	lb/in.²	%	%		lb/in.²	%	%	
Annealed	−320	30,900				83,700	127,800	52.5	34.5	0.423	229,700	61.5	77.5	1.504
Do	−220	27,400				71,900	105,800	47	32	.386	195,300	57.5	77.5	1.491
Do	−108	24,000				64,300	91,100	41.5	29.5	.348	170,700	56	77.5	1.506
Do	−22	22,000				58,600	81,600	39.5	28	.331	163,700	49.5	79	1.567
Do	75	21,500				54,400	74,100	37	27	.309	157,500	52	80.5	1.622
Do	75	21,500				54,400	73,200	36	26.5	.296	157,900	54	80.5	1.625
Do	300	18,800				47,900	63,900	33.5	25	.288	152,500	47	81.5	1.694
Do	500	16,600				44,100	58,400	32.5	24.5	.281	125,900	43	77.5	1.498
Do	600	16,000	38,400	39,700	200	43,300	57,400	32.5	24.5	.281	115,100	43	74.5	1.362
Do	700	16,500	17,300	32,600	750	43,100	56,000	30	23	.262	101,700	43.5	68.5	1.155
Do	700	16,000	17,800	39,900	850	42,700	55,500	30	23	.262	106,600	44	70.5	1.218
Do	800	15,500	16,900	17,500	375	40,400	52,500	30	23	.262	70,700	37	52	0.729
Do	900	13,800	30,600	30,600	25	34,800	44,500	28	22	.247	56,900	38.5	53	.751
Do	1,000	12,500				28,000	34,900	24.5	19.5	.219	43,400	42	56.5	.833
Do	1,100	11,500				22,300	26,400	18.5	15.5	.169	36,600	37	53	.759
Do	1,200	9,200				16,700	19,000	14	12.5	.131	22,900	27.5	42	.547
Do	1,200	8,800				16,900	19,600	16	14	.148	22,200	28	41	.528
Do	1,350	5,500				10,800	11,700	8.0	7.5	.077	12,200	17.5	24	.277
Do	1,500	4,350				7,130	7,300	2.0	2	.02	7,600	17	21	.236
Do	1,700	1,550	1,550	1,550	125	4,240	4,300	1.0	1	.011	4,100	23	26.5	.307
Do	1,700	1,500	1,700	1,700	65	3,830	3,900	1.5	1.5	.015	3,500	21	24.5	.285
Cold-drawn, 25% reduction in area	75	72,400				74,500	75,300	1.0	1	.011	161,300	19	74	1.343
Do	300	65,000				68,600	69,600	1.5	1.5	.015	148,700	17	74	1.350
Do	700	55,500	57,500	56,000	250	57,600	58,200	1.0	1	.011	104,300	13	56.5	.829
Do	900	38,500	43,600	43,600	5	43,600	44,300	1.5	1.5	.015	54,900	11.5	32.5	.395
Do	1,200	9,700				16,900	19,300	14	12.5	.131	22,100	26	41.5	.534
Do	1,500	4,100				7,200	7,400	2.0	2	.020	7,200	16	22	.246
Do	1,700	1,650	1,700	1,700	100	4,110	4,200	1.5	1.5	.015	4,000	22	25.5	.293
Cold-drawn, 40% reduction in area	75	81,400				82,600	83,400	1.0	1	.011	165,600	17	72	1.265
Do	300	73,300				75,300	76,100	1.0	1	.011	154,000	15	72.5	1.286
Do	700	61,700	60,900	60,900	50	63,600	64,200	1.0	1	.011	100,800	11.5	50	0.693
Do	900	43,900				48,400	49,100	1.5	1.5	.015	60,100	11	32	.383
Do	1,200	9,900				17,300	19,100	10.5	9.5	.099	23,100	25	44	.576
Do	1,500	4,000				6,950	7,100	1.5	1.5	.015	7,200	18	22	.248
Do	1,700	1,700	1,850	1,850	50	3,800	3,900	1.5	1.5	.015	4,100	22.5	27	.316
Cold-drawn, 70% reduction in area	75	92,500				95,200	96,300	1.0	1	.011	180,100	16	71	1.242
Do	300	80,800				87,500	88,800	1.5	1.5	.015	194,700	16	76	1.430
Do	700	71,100	69,600	69,600	5	73,600	74,300	1.0	1	.011	135,800	11	61	0.940
Do	900	52,600				56,900	57,500	1.0	1	.011	72,400	14	47.5	.636
Do	1,200	9,800				16,900	19,800	17	14.5	.157	21,400	29	45	.594
Do	1,500	3,700				6,990	7,200	2.5	2.5	.025	7,900	19	22	.246
Do	1,700	1,600	1,700	1,700	50	3,680	3,700	0.5	0.5	.005	3,500	22.5	28	.329

[a] Values at subzero temperatures obtained from data of Geil and Carwile [7]. [b] Reduction in area $(\%)=100[A_0-A)/A_0]=100(L-L_0)/L_0]$.

TABLE 5. *Results of tensile tests on OFHC copper*

Initial condition	Temperature [a]	Yield strength (0.2% offset)	Maximum load					True stress at complete fracture	Elongation in 2 in.	Reduction of area	True strain at complete fracture
			Tensile strength	True stress	Strain in 2 in.	Reduction in area [b]	True strain				
	°F	lb/in.²	lb/in.²	lb/in.²	%	%		lb/in.²	%	%	
Annealed; 0.025-mm av grain diameter	−320	8,100	51,600	81,400	58	36.5	0.46	176,500	72	80.5	1.738
Do	−220	8,100	43,400	65,700	50	34	.41	170,200	67	84	1.844
Do	−108	8,000	38,700	56,800	47	32	.38	165,000	61.5	86.5	1.995
Do	−22	7,600	35,100	49,400	40.5	29	.34	142,300	61.5	86	1.973
Do	75	12,200	31,900	44,000	39	28	.33	139,000	51	88	2.114
Do	110	7,300	30,750	44,000	43	30	.36	144,700	62.5	89	2.221
Do	250	6,700	27,000	38,900	44	30.5	.37	128,600	65	89	2.224
Do	300	7,000	25,850	36,800	42.5	30	.35	110,900	62.5	87	2.067
Do	400	6,000	22,950	31,700	38	27.5	.32	55,900	54	70	1.189
Do	500	4,700	20,750	28,300	36.5	27	.31	42,000	50	60	0.917
Do	600	3,800	17,350	22,500	29.5	23	.26	26,300	40	43	.557
Do	700	4,200	15,050	19,000	26	20.5	.23	20,300	34	37	.458
Do	700	4,000	14,400	18,200	26	20.5	.23	19,050	33	32	.38
Do	800	3,750	11,850	14,500	22	18	.20	15,000	29	30	.357
Do	900	3,000	9,800	11,500	17	14.5	.16	11,900	31	43	.561
Do	1,000	700	7,050	7,950	13	11.5	.12	9,150	36	51	.709
Do	1,100	850	5,250	5,800	11	10	.10	5,700	39	49.5	.682
Do	1,200	600	3,850	4,150	7.5	7	.07	4,150	18	27	.315
Do	1,200	750	4,000	4,300	8	7.5	.075	----	----	----	----
Do	1,500	500	2,025	2,200	9	8.2	.085	1,900	24	19.5	.215
Annealed, 0.120-mm av grain diameter	75	6,000	32,300	43,900	36	27	.31	142,600	62	85	1.96
Do	300	3,750	26,350	38,000	44	30.5	.37	82,700	62.5	79.5	1.581
Do	700	2,500	14,300	17,300	21	17.5	.16	16,800	25	22	0.247
Do	900	1,100	8,400	9,600	14	12.5	.13	8,400	17.5	16	.175
Do	1,200	800	3,630	4,000	10.5	9.5	.10	3,200	20	20.5	.228
Do	1,500	600	1,770	1,900	7	6.5	.07	1,450	10	12	.128
Cold-drawn 40% reduction in area; 0.025-mm av grain diameter before cold-drawing	75	50,300	51,100	51,500	1.0	1.0	.01	137,500	11	80	1.608
Do	110	48,000	50,400	50,700	0.5	0.5	.005	144,000	16	82	1.622
Do	250	44,800	46,500	46,700	.5	.5	.005	115,800	15.5	79	1.557
Do	300	42,400	44,450	44,700	.5	.5	.005	90,500	14	71	1.230
Do	500	28,900	34,000	34,300	1.0	1.0	.01	36,800	8	28	0.331
Do	600	6,500	19,100	23,400	22.5	18.5	.20	33,100	35	52	.728
Do	700	3,000	15,400	20,000	30	23	.26	24,700	39.5	45	.604
Do	800	3,000	12,500	15,800	26.5	21	.24	17,800	36	46.5	.627
Do	900	1,000	9,700	11,800	22	18	.20	13,800	39.5	60	.875
Do	1,200	750	4,075	4,450	9.5	8.5	.09	4,800	30.5	42.5	.551
Do	1,500	400	2,040	2,200	9	8	.085	1,950	14.5	19	.205

[a] Values at subzero temperatures obtained from data of Geil and Carwile [7].

[b] Reduction in area $(\%) = 100[A_0 - A)/A_0] = 100[(L - L_0)/L_0]$.

the alloy. This relation is also shown by a comparison of the relative positions of the flow curves of the initially cold-drawn materials (fig. 1B); the curve for the nickel lies above that for the alloy.

The true-stress–true-strain curves obtained on the specimens prepared from the cold-drawn materials (fig. 1, B) were more nearly linear for the copper, nickel, and 70%-Ni–30%-Cu alloy than for the 30%-Ni–70%-Cu alloy. However, the slope of the three former curves depended somewhat on the chemical composition of the materials; the slopes of the curves for the nickel and the 70%-Ni–30%-Cu alloy were nearly alike, and these slopes were somewhat greater than that of the curve for the cold-drawn copper. As is illustrated by the relative positions of the flow curves, the resistance of the initially cold-drawn materials to further plastic flow in tension also varied with their copper and nickel content.

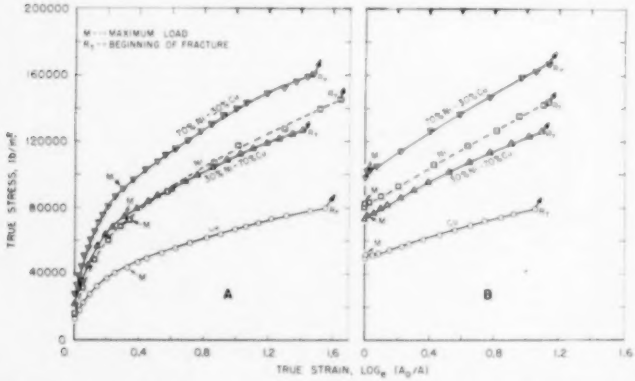

FIGURE 1. *Relation of true stress to true strain of the metals and alloys tested in tension at room temperature.*

A, Initially as annealed; B, initially as cold-drawn 40-percent reduction in area.

The effect of varying amounts of cold-drawing on the flow characteristics at room temperature of the 30%-Ni–70%-Cu alloy is shown by a comparison of the true-stress–true-strain curves of figure 2A. The resistance to flow in tension increased continuously with the amount of cold-drawing; this increase in resistance was accompanied by a decrease in amount of plasticity. The flow curves for all the cold-drawn specimens were curvilinear, with discontinuities exhibited in the region of maximum load. The relation between true stress and total true strain (due to cold-drawing and tension) is

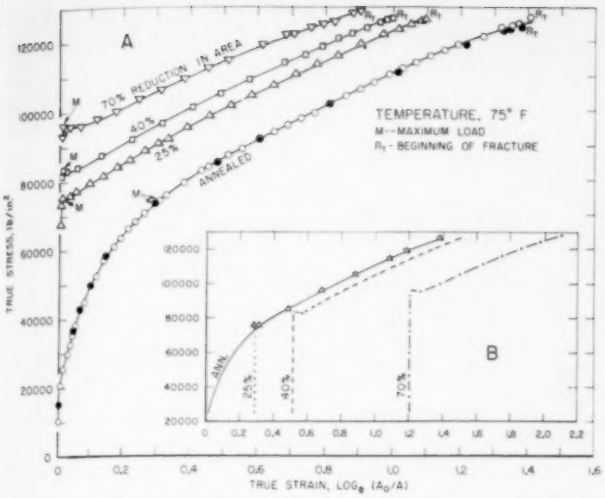

FIGURE 2. *Relation of true stress to true strain of the* 30%–Ni–70%–Cu *alloy tested in tension at room temperature.*

The alloy was initially annealed or cold-drawn different amounts as shown.

shown in figure 2B (insert). The curves for specimens as annealed or cold-drawn 25 percent coincide within the true-strain range of about 0.3 to 1.3. However, further cold-drawing either 40- or 70-percent reduction in area caused a lowering of these curves in the regions of true strains extending from the beginning of plastic deformation to fracture in tension. Thus, the positions of the true-stress–true-strain curves were affected by variations in the amount of cold-drawing and straining in tension.

3.2. Stress-Strain Relations at Elevated Temperatures

Selected autographic stress-strain curves that were obtained on some specimens of the annealed and cold-drawn 30%-Ni–70%-Cu alloy are reproduced in figure 3 as illustrative of the different types of flow observed in the tension tests at elevated temperatures. Discontinuous flow occurred in the initially annealed specimens of this alloy when extended in tension at 600°, 700°, or 800° F, as evidenced by serrations in the curve for the specimen

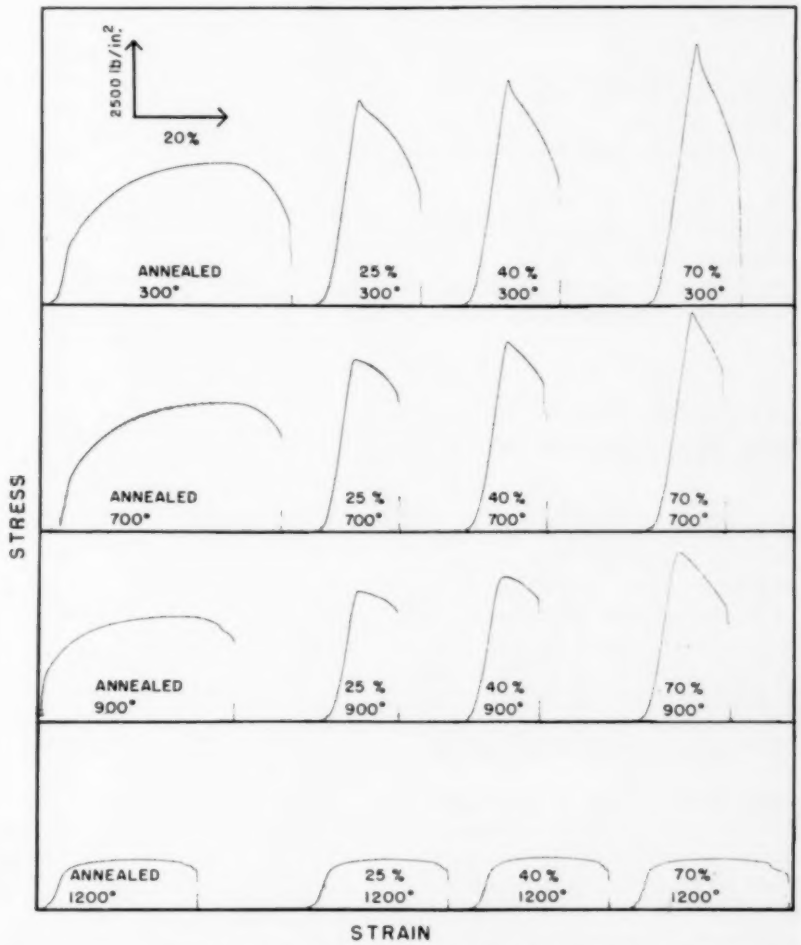

FIGURE 3. *Autographic stress-strain records of* 30%–Ni–70%–Cu *specimens tested in tension at different temperatures.*

The alloy was initially annealed or cold-drawn different amounts as shown.

at 700° F; the stress-strain curves are not shown for the specimens tested at 600° and 800° F. These serrations were more permanent in the curve for the specimen tested at 700° F than at either 600° or 800° F. However, cold-drawing this alloy 25 percent or more before testing in this temperature range reduced or entirely eliminated these serrations in the stress-strain curves. Similar serrations were observed in the curves for initially annealed specimens of the 70%-Ni–30%-Cu alloy extended in tension at temperatures ranging from 300° to 900° F, but they were not observed in the stress-strain curves for annealed specimens of the nickel or copper tested at temperatures below the start of recrystallization of these metals. The serrations that occurred in the stress-strain curves of specimens tested below the recrystallization temperature are believed to be associated with strain-aging and other atomic rearrangements. Cottrell [8] indicated the possible existence of such curves and presented experimentally an example of such a phenomenon in aluminum. Additional experimental evidence on the influence of rate of loading on the creep and aging characteristics of high-purity nickel and the effect of temperature on the aging characteristics of commercial and high-purity 70%-Ni–30%-Cu alloy has been presented by the present authors [5,6]. The breaks observed in some of the present stress-strain curves obtained on specimens at relatively high temperatures (1,200° to 1,700 ° F) are interpreted as being associated with recrystallization and grain growth in the specimens.

At temperatures below 1,200° F, the slope, height, width, and peaks in the vicinity of the maximum load of the stress-strain curves depended upon the nickel or copper content, test temperature, and initial structural condition (annealed or cold-drawn) of the material.

4. Influence of Solute Atoms and Temperature on the Tensile Properties of Nickel and Copper

A systematic analysis of the principles of solution hardening was presented recently by Parker and Hazlett [9]. They considered the mechanism of solution hardening in relation to the theories proposed by Cottrell [10], Suzuki [11], and Fisher [12]. Their interpretations were applied primarily to alloys of relatively low concentration of solute and analyzed for strength properties at small strain; the effect of solute content on ductility of the alloys was not considered in detail.

Geil and Carwile [7] pointed out that at relatively low temperatures, the difference in atomic diameters between copper and nickel is sufficient to produce strain and accompanying local residual stresses in the solvent lattice, and thereby exert a pronounced effect on the initial strength, solution hardening, and rate of work hardening of the alloys; these characteristics are also affected by temperature. As the temperature is raised, the thermal motion of the atoms is increased, and this tends to reduce the effects of the strain and local stress in the solvent lattice induced by the solute atom.

4.1. Strength

The influence of nickel content and test temperature on the yield and tensile strengths of specimens of the copper-nickel system is shown by a comparison of the results summarized in figures 4 and 5 (materials initially as annealed and as cold-drawn 40 percent, respectively). The resistance to deformation by slip or movement of dislocations in the component metals is materially increased in each by the presence of the solute atoms. This is evident even for small

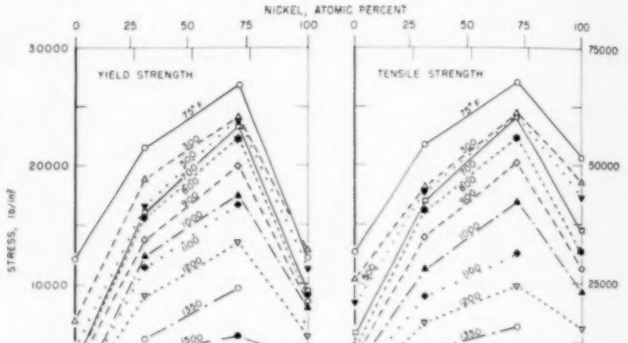

FIGURE 4. *Effect of nickel content and test temperature on the yield and tensile strengths of initially annealed specimens of the copper-nickel system.*

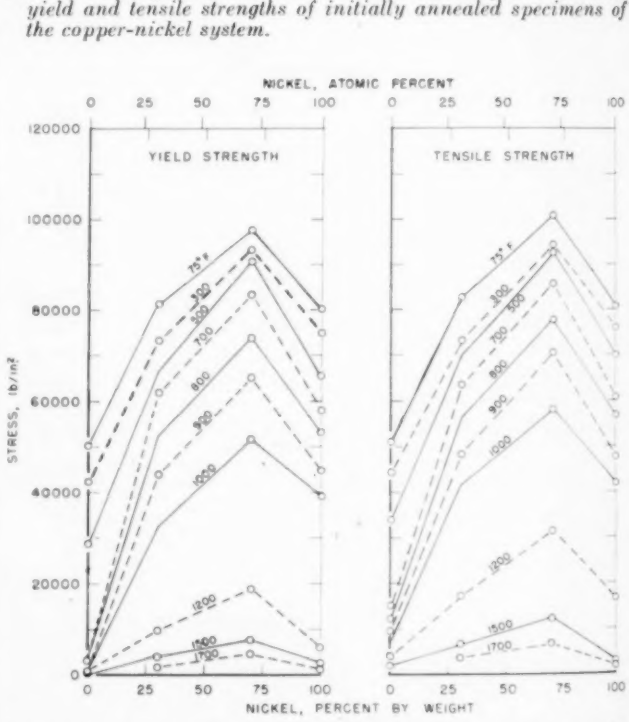

FIGURE 5. *Effect of nickel content and test temperature on the yield and tensile strengths of specimens of the copper-nickel system, initially cold-drawn 40-percent reduction in area.*

strains associated with the yield strength (0.2% offset). The strengthening effect is temperature sensitive and is affected by prior cold-working. As is shown by a comparison of the slopes of the stress-nickel-content curves, the increase in the strength properties was nonlinear as the nickel content was increased from 0 to 70 percent by weight. The latter alloy, however, was materially stronger at any temperature than its counterpart containing 30 percent of nickel.

The strengthening effect (absolute values) from the presence of a given concentration of solute atoms, in both the initially annealed and cold-drawn materials, attained a maximum at the range of about 300° to 700° F (tables 2, 3, and 4), and it is obvious that cold-drawing enhanced the strength properties. This is also the temperature range where strain-aging exerts a pronounced effect on the strength and ductility of the metals and alloys, and irregularities were observed in the stress-strain curves (fig. 3) of initially annealed specimens of the alloys.

According to Cottrell [13], aging in substitutional alloys is accelerated during plastic flow. Moreover, vacancies are created during the plastic flow, and these increase the rate of substitutional diffusion. The migrating atoms are believed, by Cottrell, to segregate to dislocations and prevent the latter from undergoing the movement that causes recovery. Hence, it would be expected that cold-drawing the present materials prior to extending in tension in the strain-aging temperature range would result in an increase in the number of vacancies, and would thus entrap the dislocations and thereby cause an increase in strength properties.

The strengthening effect of the solute atoms is also evident at the higher temperatures. At about 1,200° F, recrystallization of the initially cold-drawn materials occurred and the effects of the cold-working were diminished or removed. It is to be expected that the diffusion rate of the atoms was also increased significantly at these temperatures. The internal strains from misfit of the solute atoms in the solvent lattices and absolute values for the strength properties of the alloys were not high. However, as shown by the slope of the stress-versus-nickel-content curves, the percentage increase in the strength characteristics from the presence of the solute atoms is still appreciable.

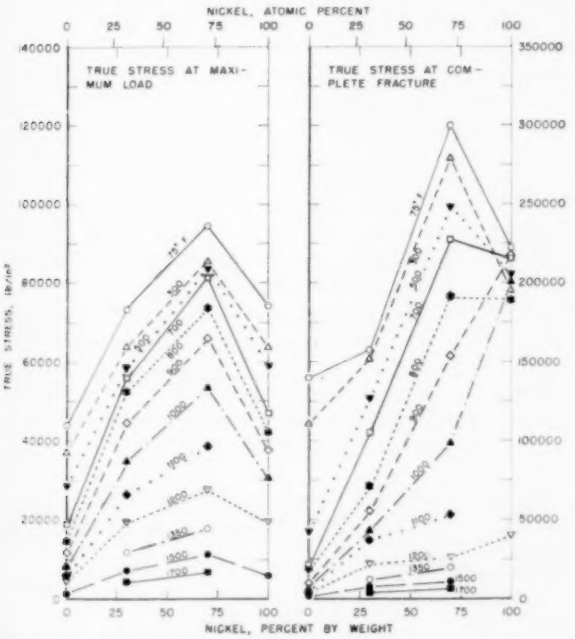
NICKEL, ATOMIC PERCENT
TRUE STRESS AT MAXIMUM LOAD
TRUE STRESS AT COMPLETE FRACTURE
TRUE STRESS, lb/in²
NICKEL, PERCENT BY WEIGHT

FIGURE 6. *Effect of nickel content and test temperature on various strength indices of initially annealed specimens of the copper-nickel system.*

The relations between nickel content of the materials and the true stress, both at maximum load and at fracture, are shown in figures 6 and 7, respectively. In general, these data conform to the described patterns of figures 4 and 5 except for the inconsistent behavior of the nickel at complete fracture. The relatively narrow spread in values of the true stress at fracture for the initially annealed nickel (fig. 6) or cold-drawn nickel (fig. 7), with temperatures ranging from 75° or 700° to 1,000° F, may be partly attributed to the necking characteristics and ductility of the nickel specimens.

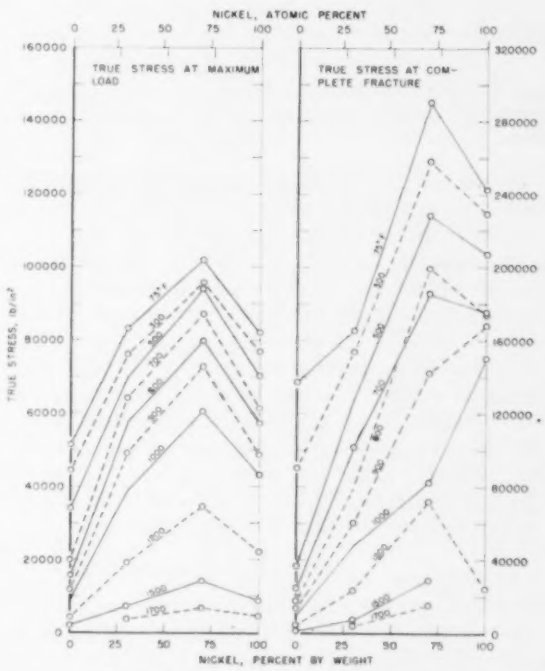
NICKEL, ATOMIC PERCENT
TRUE STRESS AT MAXIMUM LOAD
TRUE STRESS AT COMPLETE FRACTURE
TRUE STRESS, lb/in²
NICKEL, PERCENT BY WEIGHT

FIGURE 7. *Effect of nickel content and test temperature on various strength indices of specimens of the copper-nickel system, initially cold-drawn 40-percent reduction in area.*

4.2. Ductility

The influence of nickel content on the ductility at different temperatures of the materials as annealed or as cold-drawn 40 percent is shown in figures 8 and 9, respectively.

The ductility of the component metals is affected significantly by variations in the percentage of the solute atoms and temperature and by prior cold-working. The presence of 30 percent of nickel in

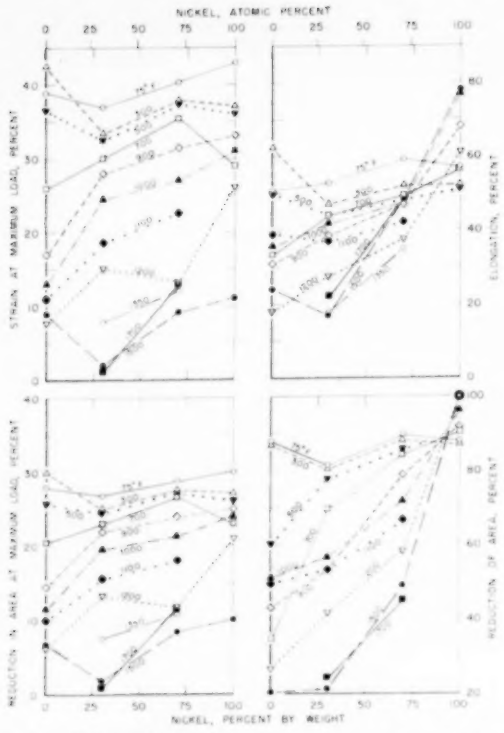
NICKEL, ATOMIC PERCENT
STRAIN AT MAXIMUM LOAD, PERCENT
ELONGATION, PERCENT
REDUCTION IN AREA AT MAXIMUM LOAD, PERCENT
REDUCTION OF AREA, PERCENT
NICKEL, PERCENT BY WEIGHT

FIGURE 8. *Effect of nickel content and test temperature on the ductility of initially annealed specimens of the copper-nickel system.*

the copper of the initially annealed materials decreased the strain at maximum load in the range 75° to 500° F, and also at 1,500° F (fig. 8). At temperatures of 700° to 1,200° F, the presence of the solute atoms resulted in an appreciable increase in the strain. Similarly, the presence of 30 percent of copper in the nickel decreased the strain at maximum load at temperatures of 75°, 900°, 1,000°, 1,200°, and 1,500° F, was without significant effect at 300° or 500° F, and increased the strain markedly at 700° F. In general, the strain at maximum load of the 70%-Ni–30%-Cu alloy at any temperature was greater than that of the 30%-Ni–70%-Cu alloy; the latter alloy had the higher value for strain at 1,200° F.

Reversals are evident in some of the curves showing the relationship between the nickel content and elongation or reduction of area. However, the slopes of these lines were altered by the nonuniform deformation (necking) that occurred after the attainment of maximum-load conditions. This was especially prominent in the pure nickel specimens, as is revealed by the relatively narrow spread and high values for reduction of area.

This pattern of behavior for the annealed material was markedly changed by cold-drawing (fig. 9). The introduction of solute atoms either in the copper or in the nickel lattice did not materially affect the strain at maximum load at temperatures below that of recrystallization of the component metals and the alloys. All the initially cold-worked materials had low values for strain at maximum load

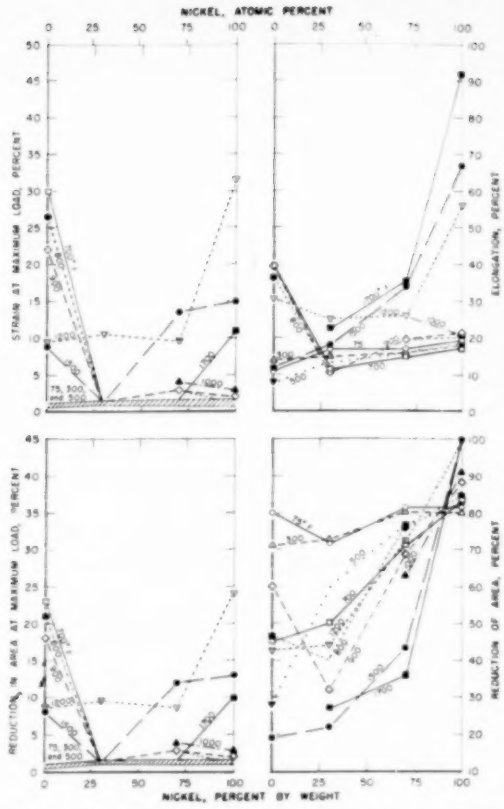
NICKEL, ATOMIC PERCENT
STRAIN AT MAXIMUM LOAD, PERCENT
ELONGATION, PERCENT
REDUCTION IN AREA AT MAXIMUM LOAD, PERCENT
REDUCTION OF AREA, PERCENT
NICKEL, PERCENT BY WEIGHT

FIGURE 9. *Effect of nickel content and test temperature on the ductility of specimens of the copper-nickel system, initially cold-drawn 40-percent reduction in area.*

at all temperatures below this range. However, at temperatures above 500° F a peak value of strain existed in each material, and its magnitude was decreased by the presence of the solute atoms. This value in each material was attained at a temperature near or above that of recrystallization and is believed to be associated with the release of the maximum amount of internal energy. The relationship between the nickel content of the materials and elongation or reduction of area also varied appreciably with test temperatures. High values for reduction of area were obtained in all the materials at 75° or 300° F; the recrystallization temperature in each material was above 75° F.

The spread in values for elongation attained a maximum in the pure nickel and was decreased by the solute atoms of copper. However, the spread in values for reduction of area was a maximum for the pure copper; this spread was decreased slightly by solute atoms of nickel.

5. Effects of Cold-Drawing and Temperature on the Tensile Properties of the 30%-Ni–70%-Cu Alloy

5.1. Strength

The influence of cold-drawing different amounts on the strength indices of the 30%-Ni–70%-Cu alloy

at various temperatures is shown by a comparison of the results summarized in figures 10 and 11. At each temperature within the range 75° to 900° F (fig. 10), the yield and tensile strengths increased nonlinearly as the amount of cold-drawing was increased. Within the range 1,200° to 1,700° F, the cold-worked alloy recrystallized in the short-time tensile tests and no significant effect of the initial cold-drawing operations was observed on the yield and tensile strengths. The values for true stress at fracture (fig. 11) were not materially altered by cold-drawing 25- or 40-percent reduction in area, but the values at 900° F or below were increased by cold-drawing 70-percent reduction in area; there was a slight increase in the fracture values at room temperature with an increase in the amount of cold-drawing, and the effect of cold-drawing 70 percent was removed at test temperatures of 1,200° to 1,700° F.

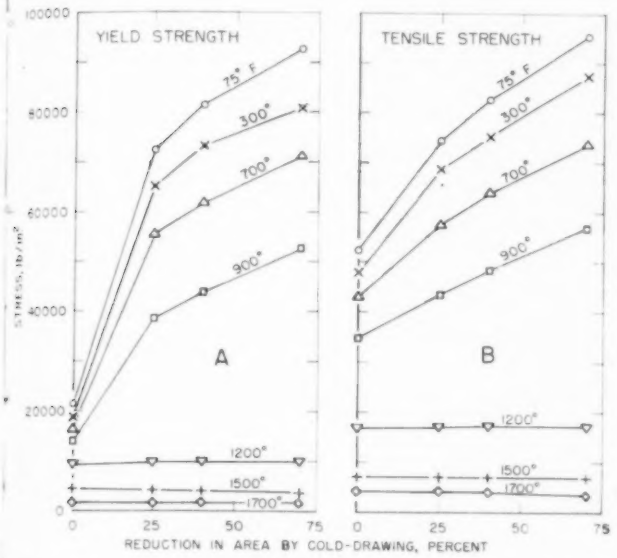

FIGURE 10. *Effect of cold-drawing and test temperature on the yield and tensile strengths of the* 30%–Ni–70%–Cu *alloy.*

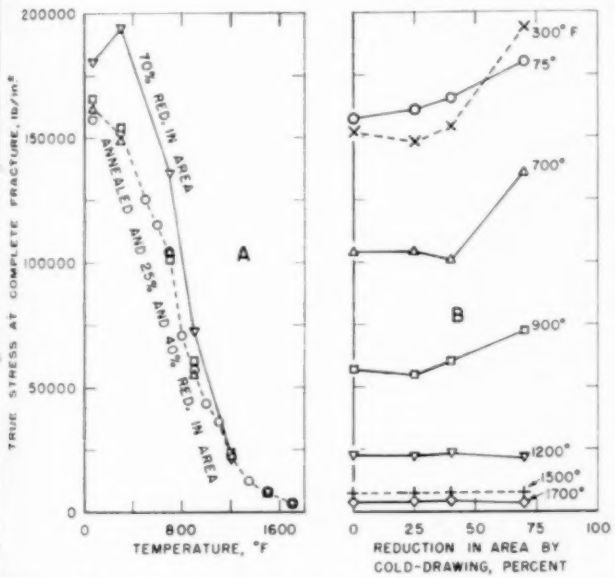

FIGURE 11. *Effect of cold-drawing and test temperature on the true stress at fracture of the* 30%–Ni–70%–Cu *alloy.*

5.2. Ductility

The values for reduction in area at maximum load, strain at maximum load and elongation of the 30%-Ni–70%-Cu alloy were decreased markedly at temperatures ranging from 75° to 900° F by cold-drawing 25-percent reduction in area, but these latter values were not changed appreciably by further cold-drawing (fig. 12, A, C, and D). The effects of cold-working on ductility of the alloy were practically eliminated at 1,200°, 1,500° or 1,700° F; the values obtained at maximum load at 1,200° F, although nearly equivalent in specimens of the initially annealed and cold-drawn alloy, were considerably higher than those obtained at 1,500° or 1,700° F.

The reduction of area was decreased slightly at 75° and 300° F by cold-drawing (fig. 12, B). The reduction of area was also decreased at 700° and 900° F by cold-drawing 25 percent or 40 percent, but with further cold-drawing the change was not so marked.

Thus, cold-drawing increased the strength of this alloy at temperatures below that of recrystallization, but this increase was accompanied by a decrease in ductility. At temperatures above that of recrystallization, the effect of cold-drawing on the strength and ductility was eliminated.

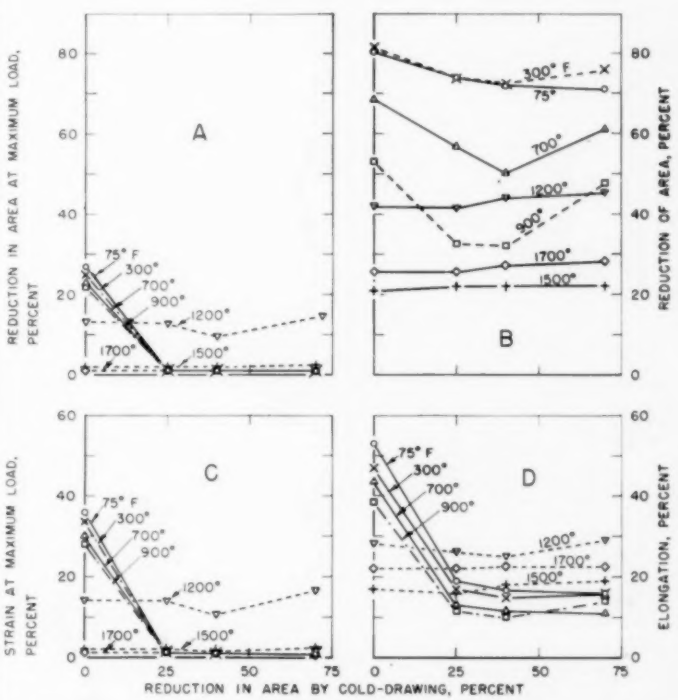

FIGURE 12. *Effect of cold-drawing and test temperature on the ductility of the* 30%–Ni–70%–Cu *alloy.*

6. Effects of Grain Size and Temperature on the Tensile Properties of Copper

The influence of grain size on the tensile properties at temperatures ranging from 75° to 1,500° F of the initially annealed high-purity copper is shown in figures 13 and 14. A change in the average grain diameter by a factor of about 5 (0.025 to 0.120 mm) had no significant effect on the tensile strength and true stress at complete fracture (fig. 13), but this increase in grain size resulted in an appreciable decrease in the yield strength at temperatures below 900° F; the grain-size effect was nil at temperatures above 1,000° F. In general, the ductility as measured by elongation and reduction of area was decreased by increasing the grain size (fig. 14). Both the fine- and the coarse-grained copper showed reversals in the curves representing the relations between reduction of area or elongation and temperature. The general trend for these values to decrease with an increase in temperature was interrupted in the ranges of about 70° to 300° F and 800° to 1,000° F; the increase in ductility with increase in temperature is especially prominent in the latter temperature range.

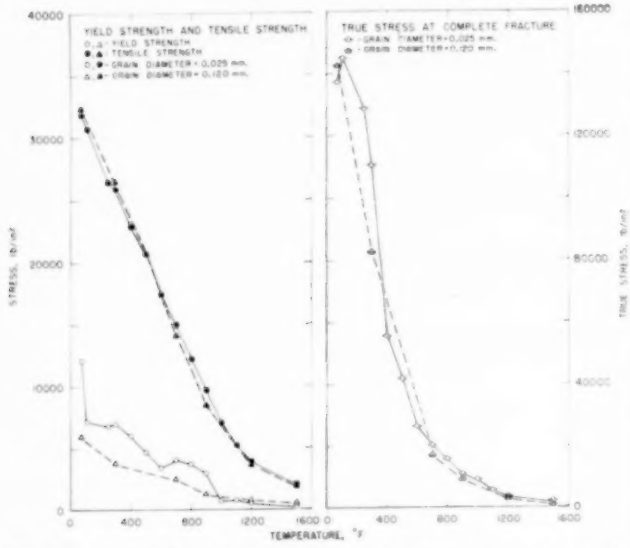

FIGURE 13. *Effect of grain size and test temperature on the strength of copper.*

A summation of these results shows that the strength and ductility of the annealed copper in tension is more dependent upon temperature than on the initial grain size.

7. Summary

The results of tests made in tension on metals of the nickel-copper system showed that the tensile properties were strongly dependent upon the percentage of solute atoms in the component lattices, temperature of test, and amount of cold-working. Although the strengthening effect due to the presence of the solute atoms attained a maximum in the temperature range where strain-aging occurred (300° to 700° F), the effect was also evident at all temperatures investigated.

The increase in yield and tensile strengths per percent of nickel was greater in the range 0- to 30-percent nickel than in the range 30 to 70 percent. The 70-percent-nickel alloy was appreciably stronger, at the same temperature, than the 30-percent-nickel alloy.

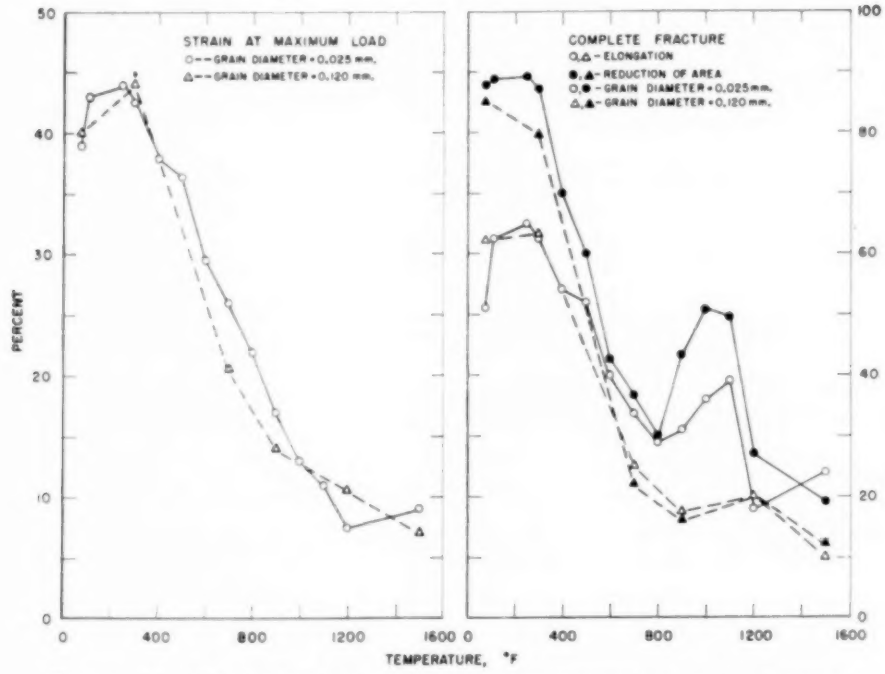

FIGURE 14. *Effect of grain size and test temperature on the ductility of copper.*

The effects of the solute atoms on ductility varied appreciably with the temperature, the amount of cold-drawing, and the index used to measure the ductility. However, at a given concentration of solute atoms, the effects of cold-drawing on both the strength and ductility were diminished or removed at temperatures above that of recrystallization.

Increasing the grain size of the high-purity copper decreased the yield strength at temperatures below that of recrystallization, and decreased the elongation and the reduction of area at certain temperatures above that of recrystallization.

8. References

[1] W. D. Jenkins and T. G. Digges, Creep of high-purity copper, J. Research NBS **45,** 153 (1950) RP2121.

[2] W. D. Jenkins and T. G. Digges, Creep of annealed and cold-drawn high-purity copper, J. Research NBS **47,** 272 (1951) RP2254.

[3] W. D. Jenkins and T. G. Digges, Effect of temperature on the tensile properties of high-purity nickel, J. Research NBS **48,** 313 (1952) RP2317.

[4] W. D. Jenkins and T. G. Digges, Influence of prior strain history on the tensile properties and structures of high-purity copper, J. Research NBS **49,** 167 (1952) RP2354.

[5] W. D. Jenkins, T. G. Digges, and C. R. Johnson, Creep of high-purity nickel, J. Research NBS **53,** 329 (1954) RP2551.

[6] W. D. Jenkins, T. G. Digges, and C. R. Johnson, Effect of temperature on the tensile properties of a commercial and a high-purity 70-percent-nickel–30-percent-copper alloy, J. Research NBS **54,** 21 (1955) RP2561.

[7] G. W. Geil and N. L. Carwile, Tensile properties of copper, nickel, and some copper-nickel alloys at low temperatures, NBS Circular 520, p. 67 (1952).

[8] A. H. Cottrell, Interactions of dislocations and solute atoms, Seminar on Relation of Properties to Microstructure, Am. Soc. Metals, p. 131 (1953).

[9] E. R. Parker and T. H. Hazlett, Principles of solution hardening, Seminar on Relation of Properties to Microstructure, Am. Soc. Metals, p. 30 (1953).

[10] A. H. Cottrell, Theory of dislocations, Progr. Metal Phys. **4,** 205 (1953).

[11] H. Suzuki, Chemical interaction of solute atoms with dislocations, Science Reports, Research Inst., Tohoku Univ. **4,** 455 (1952).

[12] J. C. Fisher, Dislocations, Seminar on Impurities and Imperfections, Am. Soc. Metals, p. 28 (1955).

[13] A. H. Cottrell, Creep and aging effects in solid solutions, Symposium on Creep and Fracture of Metals at High Temperatures, Natl. Phys. Lab., p. 141 (1956).

WASHINGTON, December 5, 1956

Journal of Research of the National Bureau of Standards Vol. 58, No. 4, April 1957 Research Paper 2754

Accuracy of the Cutler-Hammer Recording Gas Calorimeter When Used With Gases of High Heating Value

John H. Eiseman and Elwin A. Potter [1]

The accuracy of the Cutler-Hammer recording gas calorimeter, when used with gases of high heating value, is discussed. The study includes the preparation of a standard gas of high heating value, a comparison of hydrogen and methane as calibrating gases, the effect upon the instrument of changes in room and tank-water temperature, the instrument's accuracy when burning propane, the effects of bleeder burner height, and the effects of differences in inlet gas pressure. It is concluded that an accuracy of 0.25 percent, or even better, can be obtained with the Cutler-Hammer calorimeter if certain precautions are carefully followed.

1. Introduction

The tremendous increase in the distribution and use of natural gas during the past few years and the change from a cubic foot to the therm, or heating value, basis for the marketing of much of this fuel have caused many gas utility companies concern regarding the accuracy of the methods used for determining heating value.

At present, there are two general methods for determining the heating value of fuel gases. The first, and older, is by means of the manually operated water-flow calorimeter. This type of calorimeter was investigated in considerable detail at the Bureau by Waidner and Mueller [1] [2] some 40 years ago, and their publication is still a valuable reference work. A method of test for calorific value of gaseous fuels by the water-flow calorimeter has been adopted by the American Society for Testing Materials [2], and by this method an accuracy within plus or minus 0.5 percent can be obtained on gases of constant heating value. However, natural gas as delivered to consumers does not usually maintain a constant heating value and may vary over a wide range from day to day or even from hour to hour.

With a water-flow calorimeter, a trained operator requires approximately 30 min for a determination of heating value. Operation at this rate around the clock would reflect approximately 2 min of sampling time every 30 min and would leave the heating value unknown for about 94 percent of the time. Consequently, a calorimeter giving an automatic continuous record is finding more and more favor. At the present time, the only instrument of this kind on the market in this country is the Cutler-Hammer recording gas calorimeter, formerly known as the Thomas recording gas calorimeter.

The Cutler-Hammer calorimeter has received wide acceptance in the gas industry. However, in the past most of its use has been with manufactured gases of low heating value. A number of studies of the accuracy of this instrument on gases ranging from 500 to 700 Btu/cu ft have been made, among which is one by R. S. Jessup [3] of the Bureau. These studies have indicated that an accuracy well within 1 percent can be obtained, provided the calorimeter is given the necessary care, and provided also that the heating value of the gas does not vary too rapidly. Today the majority of the fuel gases used in the United States are of natural origin (predominantly methane) and have heating values that are higher and more varied than those used in the previous studies.

Because of the importance of this fundamental measurement to the gas-using public and to the gas industry, the Chemical Committee and the Promotion, Advertising, and Research Committee of the American Gas Association requested the National Bureau of Standards to undertake a study of the accuracy of the Cutler-Hammer recording gas calorimeter for testing gases of high heating value.

The Cutler-Hammer instrument has been designed to measure the total heating value of the usual commercial fuel gases. It is adapted to the use of a particular gas by making simple changes in the recorder scale and in the tank unit's gear train, orifice sizes, etc. The principle upon which the instrument operates is as follows: Gas is burned at a constant rate, and the heat developed is absorbed by a stream of air. The rates of flow of the gas, air for combustion, and air for the absorbing of heat are regulated by metering devices similar in design to the ordinary wet-gas meter. These metering devices are geared together and driven by an electric motor, so that the ratios of the rates of flow of gas, combustion air, and heat-absorbing air are constant. The gas meter is subject to independent change with respect to the tank water level in order to compensate for the wear of meter bearings and the accumulation of deposits inside the meters. The products of combustion are kept separate from the heat-absorbing air and are cooled very nearly to the initial temperature of the air. The water formed in the combustion is condensed to the liquid state. The rise in temperature of the heat-absorbing air is therefore proportional to the total heating value of the gas. This rise in temperature is measured by means of resistance thermometers of nickel and recorded graphically.

The meters are mounted in a tank of water,

[1] Mechanical Engineer, Gas Inspection Bureau of the District of Columbia.
[2] Figures in brackets indicate the literature references at the end of this paper.

adjacent to a storage compartment of smaller capacity containing a reserve supply of water. A cam-operated water pump takes water from the water-storage compartment and delivers it into the main tank, where the excess flows over a weir and returns to the reserve compartment. Thus the water level in the main tank is automatically kept constant.

A schematic diagram of the calorimeter is shown in figure 1, which was taken from the book of instructions for the care and operation of the Cutler-Hammer calorimeter [4]. Gas flows from the gas supply line through a pressure regulator and a pressure reducing orifice to the inlet chamber of the gas meter from which a part of it, approximately 85 percent, escapes through a bleeder burner and the remaining 15 percent is taken up by the gas meter. The design of this part of the calorimeter is such that the resistance to flow of gas from the inlet chamber of the gas meter to the bleeder burner is small, so that the pressure in the chamber will be nearly the same as that of the atmosphere. Practically, the differential does increase somewhat as the inlet pressure of gas to the calorimeter is increased. After leaving the gas meter the gas is mixed with air from the combustion-air meter, and this mixture then flows to the calorimeter burner. Figure 2 is a schematic diagram of the burner unit.

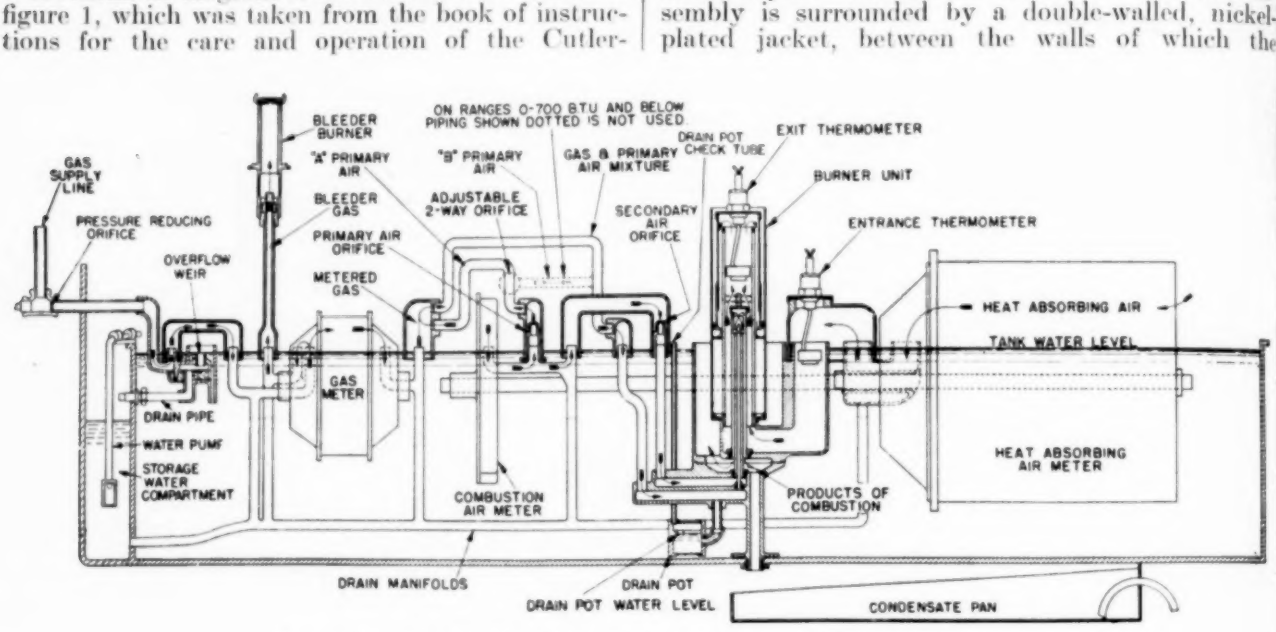

FIGURE 1. *Flow diagram of the Cutler-Hammer recording gas calorimeter.*

The air from the combustion-air meter is caused by appropriate orifices to divide into three streams, two of primary air (A and B, fig. 1), which enter the gas stream at two points between the gas meter and burner, and a third, which flows up around the burner tube and constitutes a supply of secondary air for combustion. The burner is located in a chamber that is closed at the top and open at the bottom, so that the products of combustion rising from the burner are deflected and caused to flow downward. The heat-absorbing air flows upward around the burner chamber past a system of fins attached to the outside of the burner chamber to promote heat transfer. The heat liberated in the combustion is nearly all absorbed by the heat-absorbing air, so that the products of combustion are cooled very nearly to the initial temperature of the air. The water formed in the combustion is condensed to the liquid state and drops into the condensate pan. To reduce heat loss the burner assembly is surrounded by a double-walled, nickel-plated jacket, between the walls of which the

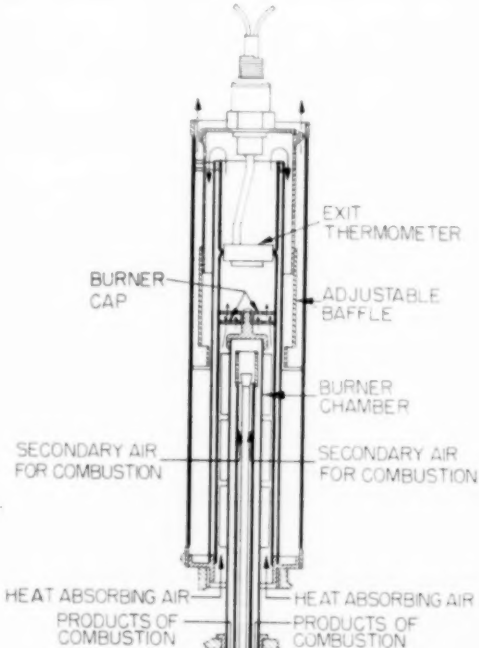

FIGURE 2. *Schematic diagram of burner unit and jacket.*

heat-absorbing air flows after passing the outlet thermometer (the inlet thermometer being in the same stream of air before it reaches the burner assembly). The distance of the flow of this air between the walls of the jacket is regulated by a baffle (fig. 2) that can be adjusted to effect an increase or decrease in the temperature rise of the heat-absorbing air and thus accomplish the desired reading of the instrument to coincide with the heating value in Btu per cubic foot of the gas used for calibration.

The temperature rise of the heat-absorbing air is measured by nickel resistance thermometers connected in adjacent arms of a Wheatstone bridge, which, with a specially calibrated slide-wire resistance S, is the measuring circuit of a Leeds & Northrup recorder. A diagram of this circuit is shown in figure 3.[3] The equal ratio arms of the bridge are

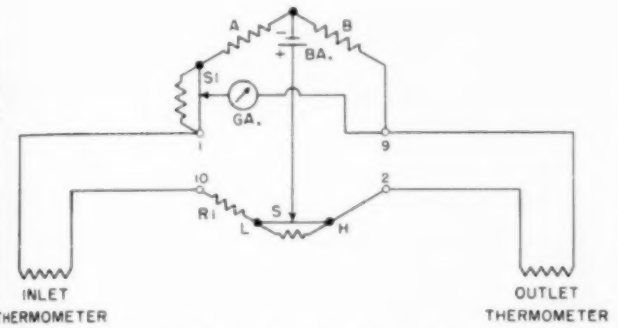

FIGURE 3. *Wiring diagram of recording system.*

shown at A and B. The adjustable resistance, S_1, is used to balance the bridge during the "cold-balance" adjustment of the recorder when the thermometers are theoretically at the same temperature. A rectifier furnishes current for the system. Any lack of balance in the bridge causes a galvanometer needle to deflect, and this actuates the recording mechanism, which moves a contact along slide-wire resistance S so as to bring the bridge back into balance. The position of this sliding contact is a direct indication of the temperature difference between the two thermometers and is recorded by means of a pen on a motor-driven paper roll, which is graduated in Btu per cubic foot, and which also accounts for time.

Some of the factors that affect the accuracy of the calorimeter to a greater or lesser degree include changes in the temperature of the water in the tank, the kind and nature of the gas used for calibration, the degree of saturation of the gas sample (see appendix A), the inlet gas pressure, the bleeder burner height, the degree of permanence of the level of the water surrounding the meters (see appendix B), and the amount of free play in meter bearings and recorder parts, etc.

The data obtained in this paper show that errors resulting from such effects may be considerably larger than might be expected from the precision attained in calibration of the calorimeter. A knowledge of the effect of such factors is essential to keeping the over-all error of measurement to a minimum.

In planning this work the theory behind the design of the calorimeter was carefully examined, but as an analysis of the theory had been published in a previous Bureau paper it was felt that only brief reference to such theory was required in this study. It was decided that the investigation should be concerned mostly with the functional accuracy of the instrument when operating under normal or field conditions. In order to save time, some of the field conditions were artificially created.

The authors conducted all of the tests made during this study under carefully controlled conditions of temperature. Most of the tests were made at the National Bureau of Standards, but some were repeated in the temperature controlled laboratory of the District of Columbia Gas Inspection Bureau, and some in the testing room at the Cutler-Hammer factory.

At the Bureau, the area containing the calorimeter and all accessory equipment was suitably enclosed and thermostatically controlled air-conditioning equipment was installed, by means of which any room temperature between 50° and 100° F could be maintained within ± 1 deg F. The relative humidity in the enclosure was controlled by means of a humidistat. Figures 4 and 5 show two views of this air-conditioned enclosure.

Devices were also installed to permit the maintenance of any desired temperature of the water in the calorimeter independently of room temperature. In the tank unit, temperatures above that of the room were maintained by conduction of heat from the auxiliary tank as its water was heated by submerged copper coils through which hot water was circulated from a thermostatically controlled source adjacent to the tank unit. Temperatures below that of the room were maintained by conduction of heat from the main tank to the auxiliary tank as its water was cooled by circulating cold water through the same

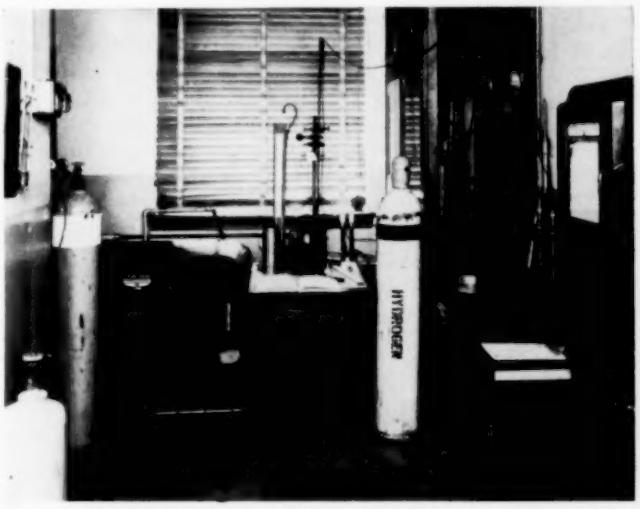

FIGURE 4. *Air-conditioned calorimeter room.*

[3] An explanation of the identifying letters or numerals shown on figure 3, but not referred to in this paper, will be found in the Cutler-Hammer Instruction Manual [4].

FIGURE 5. *Air-conditioned calorimeter room.*

submerged coils. Such changes in water temperature were effected slowly, in order that they might be accomplished uniformly. As a result, simultaneous temperature measurements at different locations in the tank unit showed no differences.

Measurements of existing temperatures were determined at appropriate locations by means of copper-constantan thermocouples, accompanied in some instances by accurate mercurial thermometers graduated in tenths of degrees. The room temperature was determined at a point adjacent to the tank unit and 53 in. above the floor by a thermocouple and by a thermometer. Temperatures relating to the tank unit were determined at five points by thermocouples: (1) the inlet thermometer, (2) the outlet thermometer, (3) the water in the main tank (which water was constantly but gently stirred by an electrically driven device, in addition to the mixing engendered by the movement of the several meters), (4) the air under the tank cover, adjacent to the heat-absorbing air meter, and (5) the products of combustion as they left the burner assembly. The cold junctions of all thermocouples were kept in an ice bath.

The procedure used in conducting tests was, first, to establish a desired equilibrium room and water temperature. Next, the condition of the calorimeter and the recorder was checked to make certain that all parts were in proper mechanical adjustment. Special care was exercised to insure such things as constant inlet gas pressure, uncontaminated room air, cleanliness of orifices and burner parts and slide wires, proper burner assembly and freedom from leaks, proper overflow of water at the weir, proper air-gas ratio, agreement of recorder scale and chart, correct mechanical balance, cold balance, etc. [4].

Temperature readings at all listed points were recorded at the beginning and end of each testing operation, with frequent observations in between, in order to evaluate the recorder reading in terms of the possible temperature factors affecting it. For example, a series of readings was taken just before the actual calibration procedures were begun, to insure that equilibrium temperature prevailed, the temperatures were then watched during the warmup period of the calorimeter until the maximum change in recorded heating value of that particular test was reached. At the conclusion of the test all temperature readings were again recorded.

Because of the over-all purpose of this study, it was agreed that it would be essential to use for calibration and testing purposes a gas with a heating value in the range of the usual natural gases, and that the heating value of such a gas should be known to a degree of accuracy at least one order of magnitude greater than that expected from the calorimeter itself. The advantages of such a gas would be: (a) its chemical and physical properties approximate those of the natural gases usually tested by the calorimeter; (b) its use would not modify the normal operation of the instrument, i. e., it could be introduced into the calorimeter without the need of changing its gears and varying the speed of rotation of the gas meter,[4] without disturbing the level of the water at the weir, with the least chance of introducing an error due to contamination of the calibrating gas with constituents of fuel gas dissolved in the water in the gas meter, and without changing the bleeder burner or influencing temperatures under the tank cover; (c) it would serve as a check on the suitability of hydrogen as a calibrating gas, because hydrogen does not have the advantages listed under (a) and (b).

2. Preparation of a Standard Gas of High Heating Value

Because methane is the chief constituent of natural gas, a pure methane would be an ideal gas for use as a standard. A supply of natural gas consisting of nearly pure methane, and containing much smaller amounts of other constituents than the usual run of natural gas, was obtained from the Southern California Gas Co. It was hoped that an analysis of this gas by means of the mass spectrometer would make possible the calculation of the heating value with the desired accuracy. Unfortunately, because the several constituents present produced overlapping spectra which introduced too much uncertainty for an accurate calculation, it was found necessary to purify this gas further even though all of the impurities totaled less than ½ of 1 percent. The analysis of the California gas as received was as follows:

	Percent
Methane (CH_4)	99. 67
Ethane (C_2H_6)	0. 15
Nitrogen (N_2)	. 04
Propane (C_3H_8)	. 07
Propylene (C_3H_6)	. 02
Butane (C_4H_{10})	. 02
Carbon dioxide (CO_2)	. 03

[4] The method of calibration of the calorimeter recommended by the manufacturer makes use of nearly pure hydrogen as the standard gas. Because the heating value of hydrogen is much lower than that of most fuel gases, the speed of the gas meter is increased in the hydrogen test by appropriate changes in the gear train connecting it with the driving motor so as to bring the recorder reading into the range of heating values normally met with in measurements on fuel gases. Calibration with hydrogen also involves other changes in the instrument (see text p. 219).

In order to calculate the heating value of this gas, with the desired accuracy, all of the ethane and carbon dioxide should be removed, and it would be desirable also to remove the propane, propylene, and butane. In short, it was hoped to remove everything except the nitrogen, which itself would not interfere with an accurate analysis.

It is well-known that activated coconut charcoal adsorbs carbon dioxide as well as ethane and higher hydrocarbons at room temperature, and that the adsorption is improved as the pressure is increased. The apparatus that was built to utilize the adsorbing power of activated coconut charcoal is shown in figure 6 and consists of the following essential parts: Four purifying towers (A), connected in series, each with a capacity of 214 cu in.; a manifold (B) with valves for connecting cylinders to either the inlet (I) or the outlet (O) of the purifiers; a condenser (C) for condensing the gas by means of liquid nitrogen contained in the Dewar flask (D), which flask can be raised or lowered around the condenser by means of an adjustable platform; a vacuum pump connected to the manifold at (F) for evacuating the entire system; and pressure gages (G) for observing

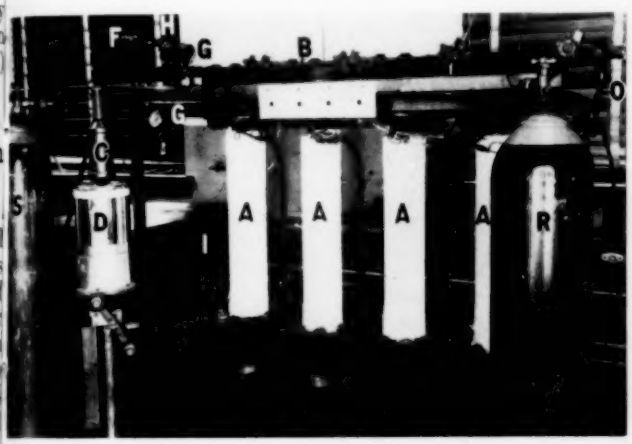

FIGURE 6. *Apparatus for adsorbing heavy hydrocarbons.*

the pressure in the system. A valve (H) is used to divide the manifold into two parts so that the supply cylinder (S), the condenser (C), and the inlet to the purifiers can be separated from the outlet from the purifiers and the one or more receiving cylinders represented by (R). The first purifying tower on the left is filled with a desiccant (silica gel) and the other three with activated coconut charcoal (6 to 8 mesh). Each tower is wrapped with a heating coil of sufficient capacity to heat the tower and its contents to a temperature of 150° C for the purpose of reactivation.

The whole apparatus was built so that it would withstand a hydrostatic pressure of 2,500 psi and was so tested.

Following the hydrostatic test, it was necessary to desiccate the entire apparatus thoroughly. A preliminary drying was accomplished by introducing room air for 2 days at a rate of approximately 180 cu ft/hr by means of the vacuum pump. Afterward, room air dried by a tower of silica gel was drawn through the system for 4 more days. The gel in the drying tower was changed each day and the used desiccant reactivated in an oven heated to 245° C. During the fourth day of purging with dry air, a drying tower was also placed on the outlet of the apparatus and the amount of water picked up in each drying tower was measured. When the tower on the outlet picked up less water than the one on the inlet, it indicated that the air within the apparatus was drier than the room air. When this condition was reached, the purging with air was discontinued and the apparatus was evacuated by means of the vacuum pump until a pressure of only a few millimeters of mercury was shown on a sensitive vacuum gage connected at one of the manifold valves. Then, with the vacuum pump still operating, dry air was admitted slowly, so that the vacuum gage remained within a few millimeters of its former reading. This dry air swept out any water vapor liberated from small cracks or recesses in the interior. After several hours of this treatment the air inlet was closed, and the pump was operated until the pressure in the entire apparatus was as low as it would go, about 1 mm of mercury. Valve (F) was then closed, the vacuum pump turned off, and the vacuum gage read. It required a week of this procedure before the apparatus would stand evacuated overnight without any change in pressure, showing that it was both dry and vacuum-tight and was ready for use. With the apparatus still evacuated, a supply cylinder (S) of the unpurified methane was connected to the manifold, and its contents were allowed to flow at a slow rate into the purifiers through valve (I) until a pressure equilibrium was reached. The inlet valve (I) was then closed and the supply cylinder (S) was connected to the condenser (C). Gas from (S) was admitted into the condenser (C) and was condensed by cooling it slowly with liquid nitrogen. This was accomplished by gradually raising the Dewar flask (D), containing the liquid nitrogen, around the condenser.

The condensing process was continued until the pressure in the supply cylinder had been reduced by 150 psi, which was the amount of change calculated to fill the condenser (C) about two-thirds full of liquid. At this point cylinder (S) was turned off and the liquid nitrogen lowered from the condenser. When, through evaporation, the pressure in the condenser had increased to the point where it at least equaled that of the gas already stored in the purifiers, the valve between the condenser and purifiers was opened and the gas from the condenser was allowed to flow into the purifiers. This continued until all of the liquid in the condenser had been vaporized, and the condenser was back up to room temperature and an equilibrium pressure prevailed.

The above process of condensing gas from the supply cylinder and transferring it to the purifiers was repeated until the pressure of gas in the purifiers had been built up to approximately 1,400 psi, which usually required three condensations. The inlet

valve (I) was then closed and the gas allowed to remain in contact with the purifying material for approximately 12 hr or overnight. A small sample of gas was then drawn from the outlet of the purifiers and analyzed by means of the mass spectrometer. If the results of this analysis indicated no impurities except nitrogen, the gas was allowed to flow from the purifiers into the evacuated receiving cylinder (R) until the pressure between the two came to equilibrium.

The cycle of purification described above was repeated a sufficient number of times to bring the pressure in the receiving cylinder (R) to at least 1,000 psi. Cylinder R was then removed from the system, its contents mixed by setting up convection currents within the cylinder, and the gas was then sampled and analyzed again. If this analysis showed no ethane or impurities other than nitrogen, the heating value of this purified gas was calculated from the analysis and the gas was ready for use as a standard.

Whenever a sample from the outlet (O) of the purifiers showed a trace of ethane, indicating inefficiency of the apparatus, the process was stopped and the gas in the purifiers was condensed and returned to the supply cylinder. The heaters surrounding the purifying towers were turned on, and the system was evacuated by means of the vacuum pump. Each heating element was controlled so that a temperature of 150° C was maintained on each of the four towers. It was found that an overnight run was sufficient to reactivate the coconut charcoal. Reactivation proved to be necessary after every 3 or 4 purification cycles.

Four 220 cu ft cylinders of purified gas were obtained by this process, each cylinder being filled to a pressure of approximately 1,000 psi. The results of the analysis of each cylinder of gas after purifica-

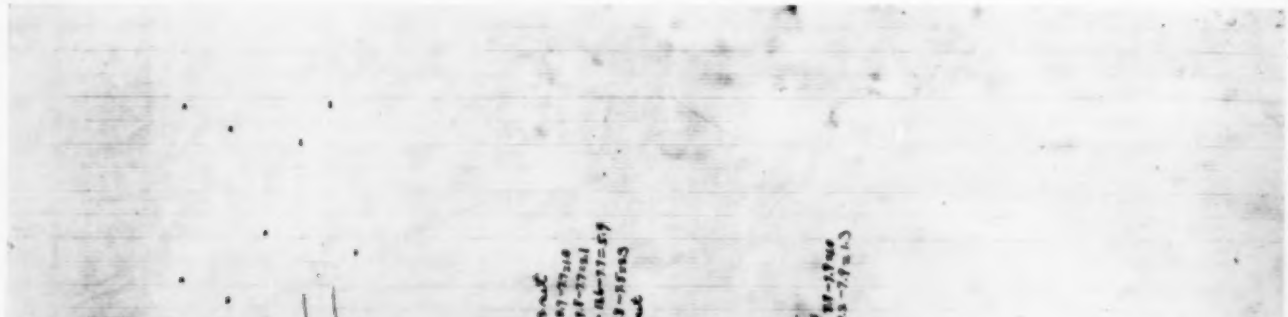

FIGURE 7. *Spectrogram of natural gas before purification.*

FIGURE 8. *Spectrogram of natural gas after purification.*

tion are shown in table 1,[5] together with the heating value calculated from these results. It will be seen from this table that the four samples are practically identical in composition and that the heating value from analysis is probably not more than ±0.1 Btu/cu ft.

TABLE 1. *Analyses of purified methane*

Cylinder	Analysis by mass spectrometer		Calculated heating value	Probable errors [a]
	Constituent	Mole percent		
			Btu/cu ft	*Btu*
127	CH_4	99.93	996.7	±0.1
	C_2H_6	0.00		
	N_2	.07		
130	CH_4	99.92	996.6	±0.1
	C_2H_6	0.00		
	N_2	.08		
133	CH_4	99.93	996.7	±0.1
	C_2H_6	0.00		
	N_2	.07		
134	CH_4	99.93	996.7	±0.1
	C_2H_6	0.00		
	N_2	.07		

[a] The probable errors given refer to the effect of errors in gas analysis only (see footnote 5 below).

The spectrograms from which the analyses of the California gas were calculated are shown in figures 7 and 8. Figure 7 shows the spectrogram of the gas before purification and indicates the presence of nitrogen, ethane, propylene, propane, butane, and carbon dioxide by the peaks at 28, 30, 42, 43, and 44. Figure 8 shows the results obtained after purification and indicates that all of the above constituents, with the exception of nitrogen, at peak 28, have been removed. This method of purification is, therefore, adequate to produce methane of sufficient purity to be analyzed with the desired precision by means of the mass spectrometer. The heating value calculated from this analysis is much more accurate than the results to be expected from the recording calorimeter. Therefore, the gas is suitable for use as a primary standard. Any stable gas of comparable heating value may be properly compared with this primary standard gas and may then be used as a secondary standard gas for testing or calibrating purposes (see appendix C).

3. Comparison of Hydrogen and Methane as Calibrating Gases

One of the questions that led to this study was the suitability of hydrogen for calibrating purposes when the calorimeter was to be used with gases having several times the heating value of the calibrating gas. The answer to this question could now be obtained by making a direct comparison between the use of hydrogen and the standard methane.

It was recognized that the use of hydrogen as a calibrating gas affects the normal operating conditions in the tank in a number of respects. For example, the use of hydrogen requires certain changes from the normal operating conditions of the instrument, including shutting off the primary air supply to the burner and the insertion of a special orifice in the gas line at the entrance to the burner. The water level surrounding the meters and the weir is disturbed when the gas meter is "blown" to refresh the water contained in the gas meter in order to facilitate a new saturation equilibrium, and when the gas meter is turning at the increased rate determined by the special hydrogen gears. Because the heat of combustion of hydrogen (approximately 319 Btu/cu ft) is much lower than that of most fuel gases, the speed of the gas meter is increased by a definite amount in order to bring the rate of heat production and consequently the reading with hydrogen into the range of the scale used during normal operation with fuel gases. Another change is caused by the purge flame burning at its temporary down-in-the-tank location, causing temperatures under the tank cover to be different.

In comparing the two gases, the calorimeter was first proved to be in normal operating condition in accordance with the manufacturer's instructions [4]. It was then calibrated with hydrogen by the method recommended in the same instruction manual, using Hydrone hydrogen. As a part of the calibration, a small change in the cold-balance rheostat was necessary in order to make the recorder show the proper reading of 1,046 Btu on its 900- to 1,200-Btu-range scale.[6] Then, making only the necessary changes from the conditions of the hydrogen test to those of normal operation, the standard gas was connected and the chart observed until the maximum change had taken place and a steady reading was obtained,

[5] The heating values in this table were calculated on the basis that the heat of combustion of pure methane is 997.4 Btu per standard cubic foot, as given in NBS Circular C417, Gas calorimeter tables (1938). A later revision of this Circular, C464 (1948), gives 996.9 Btu per standard cubic foot. The difference in these two values is due to a difference in the definition of the Btu used in the two publications. The Btu used in C464 is defined in terms of the specific heat of water at 59° F (15° C) and is the unit generally used in the gas industry [2]. The use of the older value in this paper is justified by the fact that the hydrogen used in tests of the calorimeter contained about 0.06 percent of inert impurity, so that a calorimeter calibrated with hydrogen on the assumption that it is pure would read too high by 0.06 percent in the hydrogen test.

Hence a value of 996.7 Btu on the methane of 99.93-percent purity is substantially equivalent to the manufacturers recommended reading of 1,046 Btu in a hydrogen test with hydrogen of 99.94-percent purity. It may be noted that the heat of combustion of methane in terms of the International Steam Table Btu (defined as 1,055.07 absolute joules) is 996.6 Btu/cu ft. The Term "cubic foot" as used in this paper is an abbreviation for "standard cubic foot," defined as the quantity of gas that would fill a space of 1 cu ft at 60° F if saturated with water vapor and under a total pressure of 30 in. of mercury.

The above values for the heat of combustion of methane are based on the experimental value per mole reported by Rossini [5], the value 0.5218 in. of mercury for the vapor pressure of water at 60° F, and the value $(1-(pe/RT)=0.0020)$ for the deviation of methane from the ideal gas law at 60° F and a pressure of 30 in. of mercury. Rossini assigned an uncertainty of about 0.03 percent to his result. This corresponds to 0.3 Btu/cu ft. Taking account of the uncertainty in the analysis corresponding to 0.1 Btu/cu ft, and making some allowance for the uncertainty in the deviation from the ideal gas law, an uncertainty of ±0.4 Btu is assigned to the heat of combustion of the purified methane.

[6] A table of theoretically correct readings in the hydrogen test for various ranges of the instrument is given in the manufacturer's instruction book [4] for use in the periodic testing of the instrument by the user. The values given in this table were calculated from a selected value for the heat of combustion of hydrogen together with values for the ratio of the speed of rotation of the gas meter in the hydrogen test to that in normal operation. Some allowance was also made for other effects, including the "chimney effect" discussed later in this report. The value given in the table, which is applicable for a methane range instrument, is 1,046 Btu. The final step in the calibration referred to is an adjustment of the cold-balance rheostat (S_1, fig. 2) in order to bring the reading as nearly as possible to the desired value of 1,046 Btu. This procedure, rather than additional trial and error adjustments of the baffle in the burner jacket, greatly shortens the calibration time and is very effective for giving the desired calibration reading for a known gas, even though the record will be incorrect at the lower end of the scale. However, this method of adjustment does not introduce a significant error in comparisons such as those reported in this paper, in which the calorimeter readings are well above the lower end of the scale and are fairly close together on the gases being compared (see appendix D).

as had been done for the hydrogen. The time for each evaluation averaged about 90 min. Instead of the recorder showing the expected value of 997 Btu for the standard gas, a reading of 1,000 was obtained, which was 3 Btu too high.

The procedure was then reversed. The instrument was calibrated with the methane to give a reading of 997 Btu and was then checked with the hydrogen, with a resultant reading of 1,043, or 3 Btu too low.

In order to determine whether the same results would be obtained on another calorimeter, a similar series of tests was repeated twice on a calorimeter located in the air-conditioned laboratory of the Gas Inspection Bureau of the District of Coumbia, with identical results.

It was first thought that the difference found might be caused by the type or source of the hydrogen used, but this proved not to be the case. A careful examination was made of the qualities of all of the gases involved in this problem. The composition and heating value of the methane and cylinder hydrogen used were accurately known by analysis. However, because the purity of the hydrogen generated from Hydrone had only been assumed to be sufficient not to introduce a significant error, a sample of this gas was also analyzed by means of the mass spectrometer, and the results obtained proved to be identical with the analysis obtained from the cylinder hydrogen used. The analysis is shown below:

	Mole %
Hydrogen	99.94
Oxygen	0.01
Nitrogen	.05

The question could arise as to whether all samples of hydrogen generated from different batches of Hydrone would give an analysis identical with the one listed, but it is felt that any such differences would be slight.

Additional dual tests were run, first calibrating with hydrogen and then operating with methane, with tank-water temperatures at representative equilibrium points between 60.2° and 90.5° F. In 24 such tests the results with methane differed from its known value by amounts varying from −0.3 Btu to +4.0 Btu and averaging +1.68 Btu.

These differences showed no systematic variation with temperature. It may be concluded that there is a systematic difference of the order of 0.2 percent on the average between the results of calibration with hydrogen and with methane.

It seems unlikely that errors in the accepted values for the heats of combustion of methane and hydrogen could be responsible for more than a small portion of the differences found. In view of the facts that methane has physical and chemical properties approximating those of natural gas, and that calibration with methane is carried out in exactly the same manner as measurements on natural gas, it is believed that for a calorimeter to be used for measurements on natural gas, calibration with methane of accurately known composition is preferable to calibration with hydrogen.

4. Effect of Changes in Bleeder Burner Height

One factor which affects the performance of the Cutler-Hammer calorimeter is a so-called "chimney effect", which may be explained in principle as follows: The bleeder burner of the calorimeter is located above the water level in the tank, the effective height of the burner above water level being about 8½ in. Consequently the gas pressure in the inlet chamber of the gas meter will be less in experiments with hydrogen than in experiments with methane.

This difference in pressure is too small to affect the density of the gas appreciably, but it is large enough to have a significant effect on the water level in the meter, and therefore on the quantity of gas delivered by it per revolution. The effect on the calorimeter reading is approximately equal in magnitude but opposite in sign to that (discussed in reference [3]) resulting from differences between the amounts of water vapor entering and leaving the calorimeter. Both effects, and possibly others, were considered in arriving at the table of calorimeter readings for the hydrogen test [4]. If all pertinent factors were properly considered, then calibration with hydrogen and methane should yield equivalent accuracy. In view of the differences reported in the preceding section, a few experiments were performed to confirm the existence of the chimney effect and to obtain some idea of its magnitude.

The existence of differing chimney effects was proved by exaggerating the chimney height in the following manner. Two special tubes of the same inside diameter as the bleeder outlet tube, one 15 in. and the other 30 in. in length, were successively connected to the bleeder outlet tube in place of the regular bleeder burner, first, while hydrogen was being supplied to the calorimeter and again while methane was being used. It was found with the calorimeter properly calibrated and reading 1,046 Btu with the hydrogen that with the 15-in. bleeder extension connected to the bleeder outlet tube, the chart or scale reading was 1,039.5, or 6.5 Btu low, and with the 30-in. tube the reading leveled off at 1,033, or 13 Btu low. When methane was burned under the same procedures the effects were in the same direction but of less magnitude, the drop being 2 Btu when the 15-in. tube was used, and 4 Btu when the 30-in. tube was used.

The chimney effect was further investigated by measuring the delivery rate of the gas meter through the means of a suitable laboratory wet-test meter, first with the calorimeter operating normally with the regular bleeder burner in place and then with the 30-in. extension tube replacing the regular bleeder burner, while each of the respective gases was being tested. The laboratory meter was connected to the gas burner tube or outlet of the calorimeter gas meter and read when the calorimeter meter had made 10 revolutions—which was the number causing the laboratory meter most nearly to make 1 complete revolution. The average of the 10 revolutions of the calorimeter meter in each situation is shown

in table 2. The effect on the heating value of the volumetric differences is also shown, first according to calculation and again according to the results of the "chimney-action" tests.

TABLE 2. *Effect of chimney action on gas passed by calorimeter gas meter*

Test condition	Gas used	Average volume of gas delivered per revolution of meter	Difference in heating value	
			Calculated from difference in delivery rates	Found in the "chimney action" tests
		cu ft	*Btu/cu ft*	*Btu/cu ft*
Normal use	CH_4	0.00947	------	------
30-in. bleeder extension.	CH_4	.00943	4.2	4.0
Normal use	Hydrogen from Hydrone.	.00947	------	------
30-in. bleeder extension.	Hydrogen from Hydrone.	.00934	14.3	13.0

These tests confirm the existence of the chimney effect, and show that it varies with the density of the gas and with the height of the bleeder burner (see appendix E). Figure 9 shows that the effect is a linear function of the height of the bleeder burner for both hydrogen and methane.

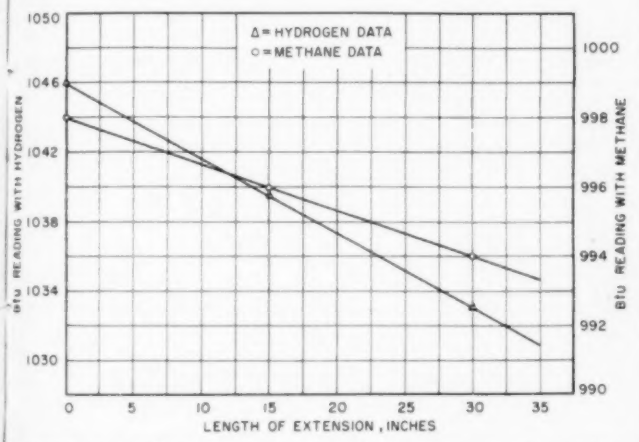

FIGURE 9. *Effect of length of bleeder burner on Btu reading.*

5. Effect of Changes in Ambient Temperature Upon the Accuracy of the Calorimeter

Before the beginning of this study complaints had been received that changes in the termperature of the calorimeter's surroundings had an effect upon the accuracy of the instrument. Preliminary test substantiated the validity of these complaints. A complete investigation of the effects of ambient temperatures upon the instrument's accuracy was made within the operating temperatures of 50° to 100° F.[7] In selecting these limitations it was felt that a leeway of 10 deg beyond the 60° to 90° limitations advocated by the manufacturer of the calorimeter was sufficient, and also well beyond the average temperature limits of operation.

After a great deal of trial and error it was found that ordinary control of room temperatures was not sufficient for our purpose. Also, that the temperature of the water in the calorimeter cannot be assumed to be the same as that of the room, no matter how closely the temperature of the room is held to a selected figure, because of the effect of the relative humidity of the room air upon the evaporation of the tank water. Therefore, it was necessary to install adequate air-conditioning equipment for the testing room.

Using the standard methane of known heating value, the instrument was calibrated under carefully controlled conditions at a predetermined basic equilibrium temperature. After the calibration was completed and after all pertinent data had been recorded, either the room temperature was changed by ± 10 deg from the current calibration or equilibrium temperature, while holding the temperature of the tank water constant, or else the room temperature was held constant and the temperature of the tank water was changed by ± 10 deg F. During tests under each of these conditions the recorded heating value was closely observed until the maximum of any changes had been reached and remained constant following the maximum change in temperature during that particular test.

In this study, this double series of tests of plus and minus changes from selected calibration temperatures was run a number of times at each of the equilibrium temperatures of 60°, 70°, 80°, and 90° F. For each temperature change the results in each respective plus and minus direction were practically identical. Tests of the effect of variation of room temperature showed no significant changes of recorded heating value if the water temperature remained constant. But because the water temperature does change with time and follows the room temperature, a special test was made to determine the time in which the tank water would change at least 10 deg with a room change of 20 deg, and it was found that this could happen in approximately 10 hr. This is illustrated by figure 10.

In table 3 are summarized the pertinent data from tests in which the tank-water temperature was changed by 10 deg F after the calibration. These figures are the average to the nearest 0.5 Btu of the results of the several tests in each respective direction at each selected temperature.

It will be seen from table 3, that with one exception, any change in the temperature of the tank water from the temperature at which the instrument was calibrated causes a change in the accuracy of the calorimeter that is reflected in the recorded heating value.

The magnitude of the effect on accuracy will depend upon two things, (1) the place in the temperature scale at which the temperature divergence takes place, and (2) the extent of such temperature change.

[7] At the factory, when calibrating the calorimeter with nearly pure hydrogen as the test gas, the manufacturer maintains the temperature of the tank water at 73° F and adjusts the baffle in the burner jacket (fig. 2), so as to obtain a specified reading at the recorder 0.4 percent higher than the 1,046 figure stated in the instruction manual for the methane-range instrument. The manufacturer's explanation is that the calorimeter would then be more nearly correct on the average if the temperature of the water in the tank should vary between the extremes of 60° to 90° F.

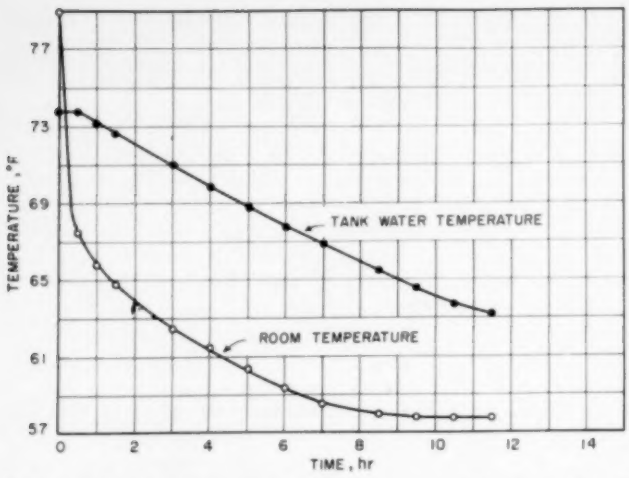

FIGURE 10. *An example of the time required for a 20-deg F change in room temperature to effect a 10-deg F change in tank-water temperature.*

TABLE 3. *Effect on calorimeter reading of changes in temperature of tank water*

Type of gas used	Equilibrium calibration temperature	Room temperature	Tank water temperature	Recorded heating value	Change in recorded heating value
	°F	°F	°F	Btu/cu ft	Btu/cu ft
Methane (997 Btu)	60.0	60.0	60.0	997.0	------
	60.0	60.0	70.0	997.0	0.0
	60.0	60.0	50.0	993.5	−3.5
	70.0	70.0	70.0	997.0	------
	70.0	70.0	80.0	995.0	−2.0
	70.0	70.0	60.0	997.0	0.0
	80.0	80.0	80.0	997.0	------
	80.0	80.0	90.0	989.5	−7.5
	80.0	80.0	70.0	999.0	+2.0
	90.0	90.0	90.0	997.0	------
	90.0	90.0	100.0	983.5	−13.5
	90.0	90.0	80.0	1004.5	+7.5

For example, if a 10-deg deviation occurs between 60° and 70° F, regardless of whether the instrument was calibrated at 60° or 70° F, no appreciable change in accuracy takes place. But if the instrument is calibrated at 60° F, and the temperature of the water subsequently decreases to 50° F, an error of 0.35 percent appears in the heating value, and it is that percentage too low. If the instrument is calibrated at 70° F and the temperature of the water subsequently increases to 80° F, an error of 0.2 percent on the low side results. In the same way, if the change is from 90° to 100° F, the instrument will read low by 1.35 percent. Conversely, if the instrument is calibrated at 90° and the temperature of the water subsequently changes to 80° F, the error is in the opposite direction and the heating value reads high by 0.75 percent.

Figures 11 and 12 illustrate the effect on the heating value recorded by the calorimeter when the temperature of the water is varied both ways from the calibration temperature.

The data of table 3 may be used to plot a curve showing the variation with temperature of the reading of a calorimeter calibrated to read correctly on methane at any given temperature of the water in the tank. The solid curve in figure 13 is such a curve for a calorimeter calibrated at 60° F (or 70° F). It will be seen that the reading will be approximately correct in the range 60° to 70° F, but will be too low at temperatures below 60° and above 70°. At 90°, for example, the error will be nearly 1 percent. A similar curve for a calorimeter calibrated at any other temperature, t, would be of the same form, but would be displaced vertically by the amount necessary to make it pass through the correct heating value (997 Btu) at the temperature t. The dotted curve in figure 13 represents the reading of a calorimeter calibrated with methane to read 0.4 percent high at 73° F (or to read correctly at about 83° F). A calorimeter thus calibrated would read high on methane by about 0.5 percent at 65° F and would read low by about the same amount at 90° F. The maximum error in the range 60° to 90° F would

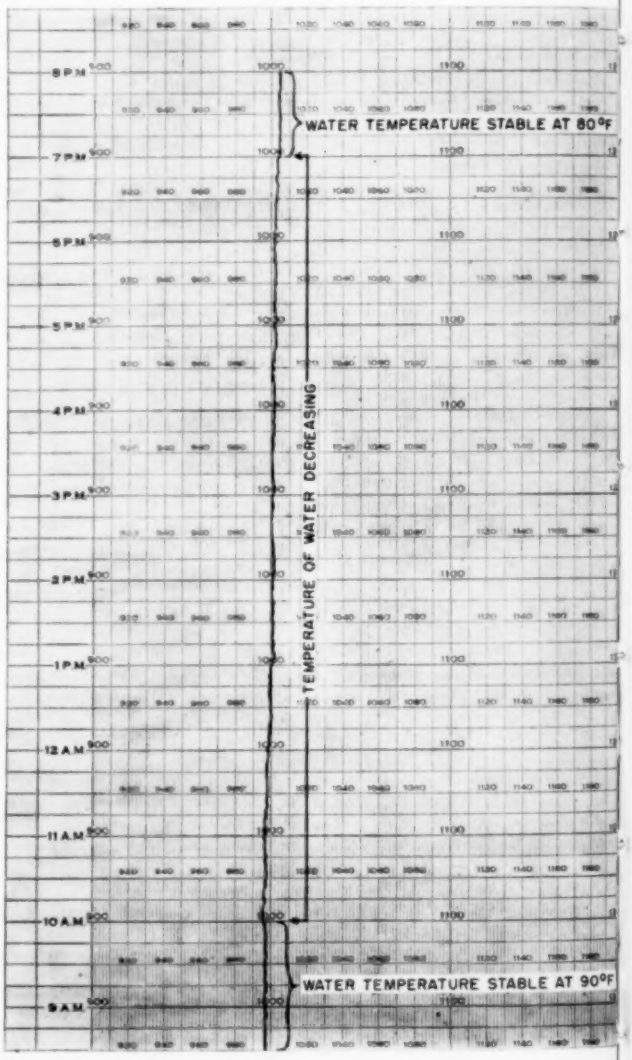

FIGURE 11. *Effect of lowering tank-water temperature on Btu reading.*

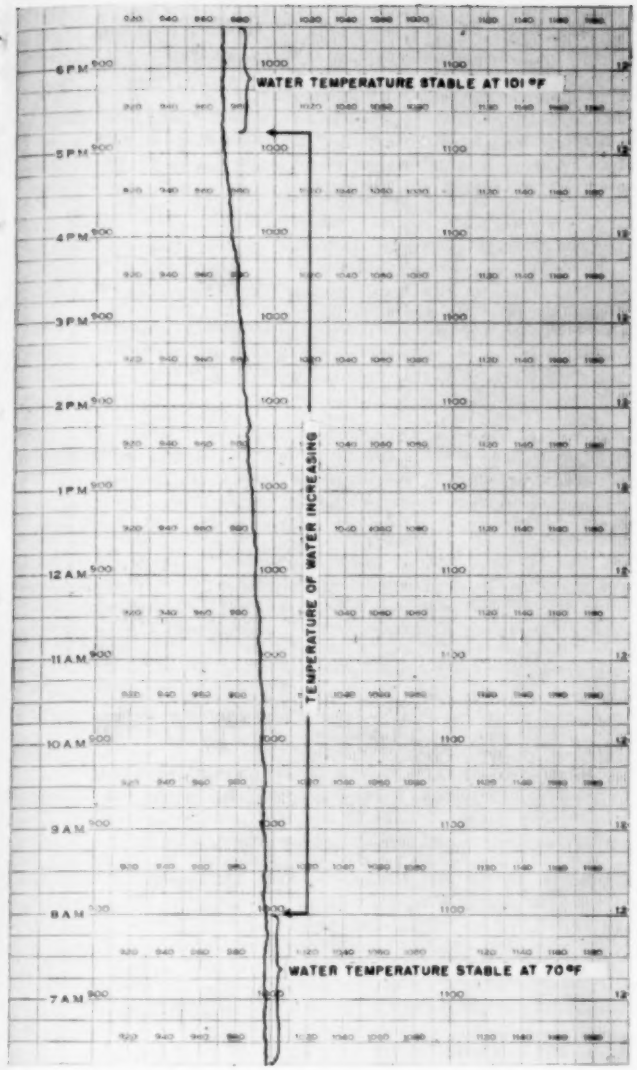

FIGURE 12. *Effect of raising tank-water temperature on Btu reading.*

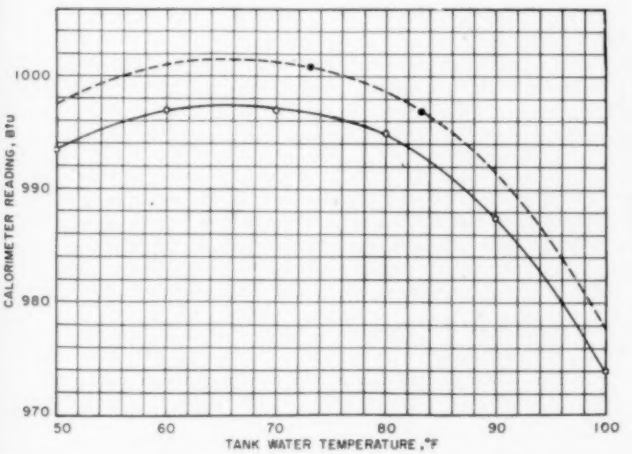

FIGURE 13. *Reading of calorimeter on methane as a function of tank-water temperature.*

then be less than if the calorimeter had been calibrated to read correctly on methane at 73° F, although the error in some parts of the range would be greater in the former case than in the latter. It is obvious from the results shown in table 3 and figure 13 that the temperature of the water in the calorimeter should not be allowed to go below 60° F or above 80° F, if errors in recorded heating value greater than 0.2 percent from this cause alone are to be avoided. For maximum accuracy the calorimeter should be calibrated to read correctly at some convenient temperature of the water in the tank, and this temperature should be maintained constant in the subsequent use of the calorimeter.

6. Accuracy of the Calorimeter on a Sample of Known Propane

Because propane is being used more and more extensively in the gas industry, it was selected as a good example of one of the higher heating value gases for the purposes of our study. Accordingly, a cylinder of "instrument-grade" propane was obtained from the Phillips Petroleum Co. After analysis by the Bureau, by a combination of mass spectrometer and infrared spectrometer determinations, its heating value was calculated and found to be 2,523 $\pm$3.5 Btu/cu ft. The results of the analysis, together with the values used for calculating the total heating value of the gas, are given in table 4.

TABLE 4. *Analysis of propane sample*

Gas	Mole %	[a]Btu/cu ft	Calculated Btu
Methane	0.15	996.9	1.5
Ethane	.01	1758.0	0.2
Nitrogen	.07	--------	--------
Carbon dioxide	.07	--------	--------
Propane	99.70	2529.0	2521.4
			2523.1

[a]The heating values were taken from NBS Circular 464.

As a part of the preparation for testing the propane, the following changes were made in the recorder: The standard scale, instead of the expanded scale, was made operative, and a new heating-value scale and chart, each graduated to 3,000 Btu were installed.

The calibration was accomplished by using the 27A–33B test gears and a cylinder of hydrogen of 99.94-percent purity at an inlet gas pressure of 0.5 in. The heating value on the recorder was adjusted for a value of 2,613, which corrected the value shown in the Cutler-Hammer Instruction Manual [4] of 2,615 for the purity of the hydrogen used.

The tank unit was then prepared for using the propane, by the installation of the proper gears, orifices, and the "bazooka" bleeder burner. The test of the propane was made by using an inlet pressure of 0.5 in., because the bleeder burner flame tended more and more to smoke as the 0.5-in. pressure was

exceeded. Sufficient time was allowed to completely saturate the water in the gas meter with propane. At the conclusion of the test the recorder scale showed a heating value of 2,517 Btu, which is approximately 0.25 percent less than the value as calculated from the analysis. Judging from these results, the Cutler-Hammer calorimeter when calibrated with hydrogen can be used with reasonable accuracy for measurements on propane.

7. Study of Effect of Inlet Gas Pressures to the Calorimeter Upon the Heating Value

A summary was made of the inlet gas pressure (inches water column) used during all of the tests. When using hydrogen generated from Hydrone the inlet pressure varied from 0.4 to 0.7 in., as compared with 0.5 in. when using cylinder hydrogen. With methane, the inlet pressure was set at 4.5 in.,—the maximum of the 2½ to 4½ in. recommended in the instruction manual [4] for general operation.

Because the measurements on methane were made with an inlet gas pressure of 4.5 in., whereas when calibrating with hydrogen the inlet pressure averaged about 0.5 in., it was decided to determine the resulting heating value effects when, with each type of gas, the instrument was calibrated at 0.5 in. and then operated at 4.5-in. inlet pressure. A part of this series of tests (calorimeter B) was repeated on one of the instruments, previously used, in the temperature-controlled laboratory of the District of Columbia Gas Inspection Bureau (see appendix F for pressure tests with propane).

The results of the series of inlet pressure tests are listed in table 5.

TABLE 5. *Heating-value change when the pressure of the gas sample to the calorimeter is increased from 0.5 to 4.5 inches, water column*

Gas	Calorimeter	
	A	B
	Btu	*Btu*
Hydrogen	+2.0	+2.0
Methane	+1.0	+0.5

8. Conclusions

In general, the Cutler-Hammer recording gas calorimeter when operated in accordance with the present instruction manual and at temperatures varying from 60° to 90° F will probably give results that are accurate to within 1.0 percent.

If under the same type of care, the calorimeter is operated under controlled conditions of temperature, so that the instrument continues to operate at very close to the same temperature at which it was last calibrated, the average accuracy will probably be within 0.5 percent. However, in all considerations of temperature, the temperature of the water in the calorimeter and not the temperature of the room is to be used as the guide.

The functional accuracy of the instrument can be further improved as follows:

(a) Gas for calibration purposes should be of the same type as the gas subsequently to be sampled. Its composition must be absolutely stable, and its heating value known to a degree of accuracy at least one order of magnitude greater than the degree of accuracy expected from the calorimeter. (b) The instrument should be calibrated weekly, as a part of the weekly care, in order to determine and correct any deviations while small. (c) When possible, the inlet pressure used should be the same for both calibration and subsequent operation.

Because the Cutler-Hammer recording gas calorimeter is a self-contained instrument, a number of concurrent conditions and effects determine the accuracy at any given moment. Some of the conditions vary with the care given to the instrument by the operator and some vary with time. The accuracy is also influenced by changes accompanying operation, for example, chemical reactions in some of the burner parts cause gradual accumulations of insulating compounds that affect the absorption of heat; dust from the air tends to accumulate in the gas and air orifices and in the fins of the fluted tube; physical particles and slime tend to accumulate in the several meters; the meter bearings wear; and the surface tension characteristics of the water at the weir can change. All of these have a deleterious effect upon the efficiency of the instrument.

In the recorder, its sensitivity or response to small heating-value changes can vary because of such things as excessive tolerances of moving parts, the fineness of adjustment of the resetting levers, the degree of tension of the suspension strips, the presence of oil film or dust on the fiber pointer, imperfect contact with the slide wires, or because of a change in efficiency of the rectifier, etc. Also, variations in the humidity of the room, as well as improper tolerances in the adjustments of the rolls, can cause differences in agreement between the scale and chart amounting to as much as 2 Btu.

For any specific summation of all such effects upon the recorded heating value, the cold-balance rheostat or the baffle in the burner jacket can be changed in a direction that will cause the pen on the properly alined chart to indicate a heating value in agreement with the heating value of the calibration gas. But, even while the calibration is in progress, or during any subsequent time interval, slight changes in some of the mentioned factors can bring about a somewhat different summation of effects. All of these effects prevent the behavior of the calorimeter from being 100-percent predictable. However, it is possible for the calorimeter to operate, under the weekly care recommended in this paper, with weekly deviations in accuracy averaging less than 0.1 per cent (see appendix G).

The authors are indebted to several organizations and to many individuals connected with these organizations for valuable advice and assistance

during the progress of this study. Acknowledgment is given to Cutler-Hammer, Inc., for furnishing a number of pieces of calorimeter equipment that were essential to this investigation, and we particularly thank E. X. Schmidt, C. W. Warner, T. M. Gilbert, and P. T. Severson of that company for helpful consultation on a number of occasions.

The Washington Gas Light Co. permitted the use of one of its calorimeters in the early part of this study and made available several pieces of test equipment, which were very useful. We express our thanks to H. L. Ketcham, Jr. who spent many hours working with us during the early part of this study, and to D. L. White for his advice and counsel.

Through the cooperation of the Rochester Gas & Electric Corp., we obtained the services of James P. Cullen, who spent a full year on this study and contributed greatly to its successful completion.

T. L. Robey, Research Coordinator of the American Gas Association, followed the progress of this investigation and was very helpful in obtaining the support of the Association.

Careful analyses of the gas samples were essential to this study, and it was through the work of the late Martin Shepherd and that of Shuford Schuhmann, Shirley Gunther, and Fred Elder of the Gas Chemistry Section, that these were obtained.

Thanks are also due to William J. Rice for his assistance while employed by NBS.

We are indebted to the Phillips Petroleum Co. for the sample of instrument-grade propane used in this study, and we thank Guy Corfield of the Southern California Gas Co. for the supply of high-purity natural gas.

Finally, we express our appreciation to E. R. Weaver, Chief of the Gas Chemistry Section, under whose general direction this work was conducted, for his continued help and understanding.

9. References

[1] C. W. Waidner and E. F. Mueller, Tech. Pap. BS **4** (1914) T36.

[2] Method of test for calorific value of gaseous fuels by the water-flow calorimeter, A. S. T. M. Designation: D900–55 (1955).

[3] R. S. Jessup, The Thomas recording gas calorimeter, BS J. Research **10,** 99 (1933) RP519.

[4] Cutler-Hammer Instruction Manual (Cutler-Hammer, Inc., Milwaukee, Wis., June 1950).

[5] F. D. Rossini, Heats of combustion of methane and carbon monoxide, BS J. Research **6,** 37 (1931) RP260; F. D. Rossini, Heat of formation of water and heats of combustion of methane and carbon monoxide. A correction, BS J. Research **7,** 329 (1931) RP343.

[6] J. H. Eiseman and Ruth F. Plapp, Weirs and the gas calorimeter, Am. Gas Assoc. Monthly **30,** No. 6, (June 1948).

10. Appendixes

10.1. Appendix A

During some of the comparison tests, using Hydrone hydrogen and cylinder hydrogen, some consistent differences in heating value seemed to appear, with the dry gas giving slightly the higher value. However, upon prolonged investigation, the apparent difference proved to be small and also questionable enough to be ignored.

10.2. Appendix B

A study entitled Weirs and the gas calorimeter, Am. Gas Assn. Monthly (June 1948) [6] had previously shown the crucial effect of the functioning of the weir in maintaining an exact level of the water in the calorimeter, and that accumulation of foreign material on the weir can easily cause errors in the instrument's accuracy of as much as 0.4 percent. It was also determined that a change of water level of 1.00 mm changes the reading by 0.7 percent. A further investigation of the effects of variations in water level was made during the current study, through the use of a slope gage 1 m in length. It was observed that such factors as speed of rotation of the meters, differences in the temperature of the water, changes in surface tension or any contamination at the weir, etc., all have an effect upon the level of the water. Experience in servicing calorimeters has indicated that the weir should not be touched, however, unless it is evident by observation that it is dirty or that the water is not flowing over it uniformly.

10.3. Appendix C

Certain precautions should be observed in using a comparison method for calibrating a gas to be employed as a secondary standard, because of the possible variations sometimes appearing in the calorimeter's results.[8] The heating value found should be double-checked by an immediate additional test of the known primary gas to determine if the primary value is duplicated. The change from the one gas to the other should be accomplished through the facility of a properly designed manifold, in order that operation of the calorimeter might be continued without cessation during the changeover.

10.4. Appendix D

When calibrating the Cutler-Hammer calorimeter, in accordance with the present instruction manual, after all phases and parts of the various operations have been checked and properly adjusted, the final change, if necessary, to accomplish a specific reading on the recorder scale, is effected by adjustment of the baffle in the burner jacket. With some calorimeters, under certain circumstances, the amount of possible normal adjustment of this baffle is not sufficient to accomplish the desired change in scale reading. However, this can only be determined by trial and error, and much time can be spent without accomplishing the desired result. The authors found and made use of the fact that a small unbalancing of the cold-balance circuit, through arbitrary adjustment of the cold-balance rheostat produces the desired scale

[8] See variations discussed on page 224.

reading in a minimum of time, and with no objectionable side effects upon the accuracy of the calorimeter. This was true because the arbitrary unbalancing affected the accuracy only toward the lower end of the scale, whereas all of the heating values in these experiments gave readings toward the upper end of the scale. The design of the instrument is such that when all adjustments are properly made, the cold-balance rheostat setting is approximately midway of its extremes. A difference of approximately 3 scale divisions in the rheostat setting corresponds to a change of 1 Btu on the recorder scale, and differences up to 3 Btu can be easily and quickly compensated in this manner. That is, the position of the pen on the scale can be adjusted to read almost exactly the true heating value of the calibrating gas. However, this procedure should not be used if the gas to be sampled has a heating value that will be recorded on the chart at a point appreciably distant from that for the gas used for calibration.

10.5. Appendix E

When hydrogen is used as the calibrating gas, the bleeder flame is under the hood and is difficult to see. As the flame must be observed in order to properly run a test when using a hydrogen generator, some operators are known to add a 10- to 15-in. extension tube to the bleeder outlet opening during calibration, in order to bring this flame above the tank cover where it can be easily observed. This practice introduces an error in the calibration and causes future recordings of the calorimeter to be high.

10.6. Appendix F

Attempts were made to test propane at different inlet pressures, but it was found that as the pressure exceeded 0.5 in. the tendency of the bleeder flame to smoke became increasingly severe. Because of this nuisance, pressure tests using the bazooka bleeder burner were discontinued. However, it may be of interest that with an improvised bleeder burner replacing the bazooka type, consisting of a straight piece of metal tubing of the same diameter as the bleeder outlet tube and of the same height as the instrument's normal bleeder burner, pressures up to 4.5 in. could be used without an objectionable bleeder flame.

With a pressure of 4.5 in. the heating value recorded was 2,522 Btu, or very close to that calculated from the analysis, whereas, with the bazooka bleeder burner and an inlet pressure of 0.5 in., the heating value recorded was 2,517 Btu. It is realized that this change of 5.0 Btu could be the result of a change in bleeder height along with the effect of the change in inlet pressure, because the position of the bleeder flame when the bazooka burner was used was 11 in. below the flame of the improvised bleeder burner.

10.7. Appendix G

An approximate 4-year record of three late model Cutler-Hammer calorimeters maintained by the Gas Inspection Bureau of the District of Columbia, operating on 1,020- to 1,200-Btu gas, shows the average weekly deviation in accuracy, as determined by weekly comparisons with a standard methane-type calibrating gas, to have been 0.93, 0.88, and 0.94 Btu, respectively (see table 6).

TABLE 6. *Approximate 4-year record of weekly deviations in accuracy of three Cutler-Hammer calorimeters, as determined by weekly checkups*

Weekly deviation in accuracy in terms of Btu	Number of times the calorimeters were found to be inaccurate by the respective Btu amounts shown in the first column		
	Calorimeter		
	A	B	C
0.0	64	85	64
.5	24	18	28
1.0	64	52	59
1.5	15	9	12
2.0	21	21	23
2.5	2	5	5
3.0	9	6	9
3.5	1	2	0
4.0	1	2	1
4.5	1	1	1
5.0	[a] 1	1	0
5.5	0	0	0
6.0	0	[a] 1	[a] 1

[a] Relates to maximum deviation found.

WASHINGTON, August 17, 1956.

U. S. GOVERNMENT PRINTING OFFICE: 1957

Recent Publications of the National Bureau of Standards

Journal of Research of the National Bureau of Standards, Volume **58**, No. 2, February 1957 (RP2735 to RP2741, incl.), 60 cents. Annual subscription $4.00.

Technical News Bulletin, Volume **41**, No. 2, February 1957. 10 cents. Annual subscription $1.00.

Basic Radio Propagation Predictions for May 1957. Three months in advance. CRPL–D 150. Issued February 1957. 10 cents. Annual subscription $1.00.

Research Papers

Journal of Research, Volume 58, No. 2, February 1957. 60 cents.

RP2735. Theory of dielectric relaxation for the three-dimensional polar rotator: lattice models leading to dimodal loss curves. John D. Hoffman and Benjamin M. Axilrod.

RP2736. Classification of perovskite and other ABO_3-type compounds. Robert S. Roth.

RP2737. Thermal expansion of some nickel alloys. Peter Hidnert.

RP2738. Intermolecular forces in air. Abraham S. Friedman.

RP2739. Matrices of spin-orbit interaction of the electron configuration $d^4\,s$. W. R. Bozman and R. E. Trees.

RP2740. A high-speed computer for predicting radioactive fallout. J. H. Wright, L. Taback, and H. K. Skramstad.

RP2741. Standard ionization-chamber requirements for 250- to 500-kilovolt X-rays. H. O. Wyckoff and F. S. Kirn.

Applied Mathematics Series

AMS47. Contributions on partially balanced incomplete block designs with two associate classes.

Publications in Other Journals

Accelerating effect of amines on polymerization of methyl methacrylate. C. M. Brauer, Ruth M. Davenport and William C. Hansen. Modern Plastics. (Modern Plastics, Inc., 575 Madison Avenue, New York 22, N. Y.) **34**, No. 3, 153 (Nov. 1956).

Adsorption of gases and vapors on glass spheres. II. Two-dimensional condensation of oxygen. J. L. Shereshefsky and C. E. Weir. J. Phys. Chem. (American Chemical Society, 1155 16th St., N. W., Washington 6, D. C.) **60**, 1162 (1956).

Bremsstrahlung polarization measurements for 1.0-Mev electrons. J. W. Motz. Phys. Rev. (American Inst. of Physics, 57 E. 55th St., New York 22, N. Y.) **104**, No. 3, 557–562 (Nov. 1956).

Compressibility of binary alkaline-earth borate glasses at high pressures. Charles E. Weir and Leo Shartsis. J. Am. Chem. Soc. (American Chemical Society, 1155 16th St., N. W., Washington 6, D. C.) **39**, No. 9, 319–322 (Sept. 1956).

Dental materials and instruments 1951–55. G. C. Paffenbarger, D. D. S. Intern. Dental J. (A. Sijthoff—Publishers, The Hague, Holland) **6**, No. 3, 299–322 (Sept. 1956).

Experimental proof for the existence of nonthermal rotational distributions of OH ($^2\Sigma^+$) in flames. Herbert P. Broida and Henry J. Kostkowski. J. Chem. Phys. (American Inst. of Physics, 57 E. 55th St., New York 22, N. Y.) **25**, No. 4, 676–680 (Oct. 1956).

Heat units and temperature scales for calorimetry. H. F. Stimson. Am. J. Phys. (American Inst. of Physics, 57 E. 55th St., New York 22, N. Y.) **23**, No. 9, 614–622 (Dec. 1955).

Measurement of W_{air} for sulfur-35 beta-rays. W. B. Mann, H. H. Seliger, and H. O. Wyckoff. Radiation Research. (Titus C. Evans, College of Madison, State Univ. of Iowa, Iowa City, Iowa.) **5**, No. 4, (Oct. 1956).

Numerical analysis. Proceedings of Symposia in Applied Mathematics, Vol. VI. John Todd. Science. (1515 Massachusetts Ave., N. W., Washington 5, D. C.) **124**, No. 3233, 1211 (Dec. 14, 1956).

Refraction and dispersion of thallium bromide iodide. William S. Rodney and Irving H. Malitson. J. Opt. Soc. Amer. (American Inst. of Physics, 57 E. 55th St., New York 22, N. Y.) **46**, No. 11, 956–961 (Nov. 1956).

Some algebraic number theory estimates based on the Dedekind eta-function. Harvey Cohn. Amer. J. Math. (The Johns Hopkins Press, Baltimore 18, Maryland.) **78**, No. 4, 791–796 (Oct. 1956).

The crystallization of flexible polymer molecules. Leo Mandelkern. Chem. Revs. (Williams & Wilkins Co., Mt. Royal and Guilford Aves., Baltimore 2, Md.) **56**, No. 5, 903–958 (Oct. 1956).

Dilworth's theorem on partially ordered sets. G. B. Dantzig and A. J. Hoffman. Annals of Mathematics Study No. 38. (Princeton Univ. Press, Princeton, N. J.) 207–214 (1956).

Integral boundary points of convex polyhedra. A. J. Hoffman and J. B. Kruskal. Annals of Mathematics Study No. 38. (Princeton Univ. Press, Princeton, N. J.) 223–246. (1956).

On systems of distinct representatives. A. J. Hoffman and H. W. Kuhn. Annals of Mathematics Study No. 38. (Princeton Univ. Press, Princeton, N. J.) 199–206. (1956).

Publications for which a price is indicated are available only from the Superintendent of Documents, U. S. Government Printing Office, Washington 25, D. C. (foreign postage, one-fourth additional, except where otherwise indicated). Reprints from outside journals and the NBS Journal of Research may often be obtained directly from the authors.

UNIVERSITY OF MICHIGAN
GENERAL LIBRARY
DOCUMENTS DIVISION
1276 ANN ARBOR MICH

UNI...
GOVERNMENT PRINTING OFFICE
DIVISION OF PUBLIC DOCUMENTS
WASHINGTON 25, D. C.

OFFICIAL BUSINESS

PENALTY FOR PRIVATE USE TO AVOID PAYMENT OF POSTAGE, $300 (GPO)

Journal of Research of the National Bureau of Standards Vol. 58, No. 4 April 1957

Contents

		Page
Comparisons of national radium standards. T. P. Loftus, W. B. Mann, L. F. Paolella, L. L. Stockmann, and W. J. Youden.	RP2749	169
Temper brittleness of boron-treated steels. Samuel J. Rosenberg.	RP2750	175
Optical and volumetric relaxation effects in glass following removal of high hydrostatic pressures. C. Weir, S. Spinner, I. Malitson, and W. Rodney.	RP2751	189
Reference wavelengths for calibrating prism spectrometers. Earle K. Plyler, L. R. Blaine, and Matthew Nowak.	RP2752	195
Tensile properties of copper, nickel, and 70-percent-copper–30-percent-nickel and 30-percent-copper–70-percent-nickel alloys at high temperatures. William D. Jenkins, Thomas G. Digges, and Carl R. Johnson.	RP2753	201
Accuracy of the Cutler-Hammer recording gas calorimeter when used with gases of high heating value. John H. Eiseman and Elwin A. Potter.	RP2754	213

[A list of recent NBS publications is given on page 3 of the cover.]

For sale by the Superintendent of Documents, U. S. Government Printing Office, Washington 25, D. C. Price 60 cents (single copy). Subscription price: $4.00 a year; $1.25 additional for foreign mailing.

UNITED STATES GOVERNMENT PRINTING OFFICE, WASHINGTON : 1957